

CHEMICAL VAPOR DEPOSITION GROWTH

QUARTERLY REPORT NO. 2

(NASA-CR-148537) : CHEMICAL VAPOR DEPOSITION
GROWTH (Rockwell International Corp.,
Anaheim, Calif.) : 93 p HC \$5.00 CSCL 07D

N76-28391

Unclassified
G3/25 47677

Contract No. 954372

"This work was performed for the Jet Propulsion Laboratory,
California Institute of Technology, under NASA Contract NAS7-100
for the U. S. Energy Research and Development Administration,
Division of Solar Energy.

The JPL Low-Cost Silicon Solar Array Project is funded by ERDA
and forms part of the ERDA Photovoltaic Conversion Program to
initiate a major effort toward the development of low-cost solar arrays."



Rockwell International



CHEMICAL VAPOR DEPOSITION GROWTH

QUARTERLY REPORT NO. 2

1 July 1976

By

**R. P. Ruth, H. M. Manasevit, J. L. Kenty,
L. A. Moudy, W. I. Simpson and J. J. Yang**

Contract No. 954372

**"This work was performed for the Jet Propulsion Laboratory,
California Institute of Technology, under NASA Contract NAS7-100
for the U. S. Energy Research and Development Administration,
Division of Solar Energy.**

**The JPL Low-Cost Silicon Solar Array Project is funded by ERDA
and forms part of the ERDA Photovoltaic Conversion Program to
initiate a major effort toward the development of low-cost solar arrays."**

**ROCKWELL INTERNATIONAL
Electronics Research Division
Anaheim, CA 92803**

"This report contains information prepared by Rockwell International under JPL subcontract. Its content is not necessarily endorsed by the Jet Propulsion Laboratory, California Institute of Technology, National Aeronautics and Space Administration or the U. S. Energy Research and Development Administration, Division of Solar Energy."

ABSTRACT

The activities of the second quarter of the contract are described. The planned modifications of the CVD reactor system have been completed. Additional samples of special substrate materials have been received from several vendors.

Results with CVD Si sheet growth in He atmospheres on glasses have been encouraging; deposition on Corning Code 1715 glass has resulted in polycrystalline films with {100} and/or {110} preferred orientations, depending upon the deposition temperature in the 850-1000°C range..

Fired polycrystalline alumina with enlarged grains resulting from supplementary high-temperature firing procedures beyond the normal commercial processing has been found very promising for growth of Si sheet with enhanced grain sizes. Films with grain dimensions as large as 200 µm have been prepared.

Preparation of p-type doped Si sheet material has begun, and both epitaxial baseline material and polycrystalline material on various substrates have been B doped throughout the concentration range from 10^{15} - 10^{20} cm $^{-3}$. Experiments to establish Si layer growth rates by SiH₄ pyrolysis in the presence of HCl in a range of concentrations have begun, as the first requirement for establishing a two-step Si deposition process for formation of enhanced grain sizes.

Various film characterization procedures--including SEM analyses, x-ray diffraction analyses, surface profilometry, and electrical measurements (resistivity, carrier concentration, mobility, spreading resistance profiles)--have been used to correlate Si sheet properties with CVD parameters and substrate properties.

Additional Si sheet samples have been submitted to OCLI for solar cell processing and measurement of photovoltaic performance, and the most recent results are summarized.

Conclusions and recommendations based on the work to date are outlined, and plans for the third quarter are given. Manpower and funding expenditures are summarized, and the updated technical program plan is included.

CONTENTS

	<u>Page</u>
1. Introduction	1
2. Technical Discussion	3
2.1 Task 1. Modification and Test of Existing CVD Reactor System	3
2.2 Task 2. Identification/Development of Suitable Substrate Materials	9
2.2.1 Rationale and Procedure for Material Selection	9
2.2.2 Evaluation and Preparation of Candidate Substrate Materials	11
2.3 Task 3. Experimental Investigation of Si CVD Process Parameters	28
2.3.1 Si CVD on Selected Substrates	29
2.3.2 Experiments Involving SiH ₄ -HCl Mixtures	38
2.3.3 Studies of Effects of B Doping Using B ₂ H ₆ Source	40
2.3.4 Determination of Background Impurity Doping Level in Reactor System	41
2.4 Task 4. Preparation of Si Sheet Samples	43
2.5 Task 5. Evaluation of Si Sheet Material Properties	43
2.5.1 Properties of CVD Si Films on Glass Substrates	44
2.5.2 Properties of CVD Si Films on Polycrystalline Alumina Substrates	51
2.5.3 Comparison of Methods for Measuring Electrical Properties of CVD Si Films	64
2.6 Task 6. Fabrication and Evaluation of Solar Cell Structures	68
3. Conclusions and Recommendations	75
4. Plans For The Third Quarter	77
5. New Technology	79
6. References	81
Appendix A. Manpower and Funding Expenditures	A-1
Appendix B. Updated Technical Program Plan	B-1

PRECEDING PAGE BLANK NOT FILMED

ILLUSTRATIONS

<u>Figure</u>		<u>Page</u>
2-1.	Simplified Schematic Diagram of Vertical-Chamber CVD Apparatus for Si Sheet Growth	3
2-2.	Schematic Diagram of Modified Si CVD Reactor System	6
2-3.	Overall View of Modified Si CVD Reactor System, Showing Control Center in Separate Cabinet, Bank of Mass Flow Controllers in Lower Center, and Vertical Reactor Chamber at Right	8
2-4.	Close-Up View of Bank of 13 Mass Flow Controllers	8
2-5.	Linear Thermal Expansion Coefficients as a Function of Temperature for Si and Various Other Materials	10
2-6.	Dektak Profilometer Traces of Surfaces of Vistal Polycrystalline Alumina Substrates at Three Stages of Preparation	17
2-7.	Dektak Profilometer Traces of Surfaces of Vistal Polycrystalline Alumina Substrates at Three Stages of Preparation	18
2-8.	SEM Photographs of Vistal Alumina Substrates in As-fired Condition	19
2-9.	SEM Photographs of Vistal 4 (four consecutive firings) Alumina Substrate Surface in As-fired Condition	20
2-10.	Nomarski Interference-contrast Photomicrographs of Surfaces of Polished Vistal Alumina Substrates of Four Different Firing Histories	22
2-11.	Nomarski Interference-contrast Photomicrographs of Surface of Same Region of Vistal 2 (two consecutive firings at >1800°C for 6 hr) Polycrystalline Alumina Substrate under Different Optical Conditions	23
2-12.	Nomarski Interference-contrast Photomicrographs of Surface of Same Region of Vistal 3 (three consecutive firings at >1800°C for 6 hr) Polycrystalline Alumina Substrate under Different Optical Conditions	24
2-13.	SEM Photographs of Surface of MRC Superstrate Polycrystalline Alumina Substrate, Viewed at 30 deg Angle with Sample Surface	26
2-14.	SEM Photograph of CVD Si Deposit on OI Glass GS211 at ~850°C in H ₂ Atmosphere	30
2-15.	Optical Photomicrographs of CVD Si Film on Polished Vistal 4 Polycrystalline Alumina Substrate, at Two Different Magnifications	34
2-16.	SEM Photographs of CVD Si Film of Figure 2-15, at Two Different Magnifications	35
2-17.	SEM Photographs of CVD Si Film on As-fired Vistal 4 Polycrystalline Alumina Substrate, at Two Different Magnifications	36
2-18.	Dektak Profilometer Traces of Surfaces of CVD Si Films Deposited by SiH ₄ Pyrolysis	37
2-19.	SEM Photograph of Whisker-like Deposit of Si on Zircon	39
2-20.	Changes in Si Growth Rate at 1025°C Caused by Additions of HCl to SiH ₄	40

ILLUSTRATIONS (Cont)

<u>Figure</u>		<u>Page</u>
2-21.	Measured Carrier Concentrations in Epitaxial CVD Si Films as a Function of B ₂ H ₆ -in-He (46 ppm) Additions	42
2-22.	SEM Photographs of Surface of CVD Si Film Grown on Corning Code 1715 Glass by SiH ₄ Pyrolysis in He at ~860°C	46
2-23.	SEM Photographs of Surface of CVD Si Deposited on Corning Code 1715 Glass by SiH ₄ Pyrolysis at 1000°C in He	48
2-24.	SEM Photographs of Surface of Si Film Deposited on Owens-Illinois GS211 Glass by SiH ₄ Pyrolysis at ~860°C in He.	50
2-25.	SEM Photographs of CVD Si Film on Refired ASM805.	52
2-26.	SEM Photographs of Film in Figure 2-25 after Extensive Etching in Modified Sirtl Etch	53
2-27.	Hole Concentration (arbitrary scale factor) as Function of Depth in Si CVD Film of Figures 2-25 and 2-26.	55
2-28.	SEM Photographs of Surface of B-doped CVD Si Film Deposited by SiH ₄ Pyrolysis in H ₂ at 1025°C on As-fired Superstrate Alumina Substrate	58
2-29.	SEM Photographs of Surface of B-doped CVD Si Film Deposited by SiH ₄ Pyrolysis in H ₂ at 1025°C on Polished Superstrate Alumina Substrate	59
2-30.	SEM Photographs of 25 μm-thick B-doped (~10 ²⁰ cm ⁻³) Si Film on As-fired ASM805	62
2-31.	SEM Photographs of 25 μm-thick B-doped (~10 ²⁰ cm ⁻³) Si Film on Polished MRC Superstrate.	63
2-32.	Dektak Profilometer Traces for Surfaces of B-doped CVD Si Films Grown at ~1030°C in H ₂ by SiH ₄ Pyrolysis, on Two Polycrystalline Alumina Substrates	65
2-33.	Comparison of Electrical Properties of CVD Si Films on Various Substrates as Determined by Hall Bridge and van der Pauw Methods	67
2-34.	SEM Photographs of Channel Produced in Si Film by Pulsed Laser Scribing	69

TABLES

Table		Page
2-1.	Candidate Substrate Materials Received during First Quarter from Various Suppliers	12
2-2.	Candidate Substrate Materials Received during Second Quarter from Various Suppliers	14
2-3.	Average Surface Roughness of Polycrystalline Ceramic Substrates (3M Co.) Measured by Surface Profilometer (Sloan Dektak)	15
2-4.	Average Apparent Grain Size of Several Polycrystalline Alumina Substrate Materials as Measured on Sample Surface.	25
2-5.	Properties of Selected Glasses Used as Substrates for Si CVD Sheet Growth.	29
2-6.	Properties of CVD Si Films Grown by SiH ₄ Pyrolysis in He on Corning Code 1715 Glass.	44
2-7.	Electrical Properties of CVD Si Films Grown by SiH ₄ Pyrolysis on Glass Substrates in He Carrier Gas.	49
2-8.	Electrical Properties of Undoped CVD Si Films Grown by SiH ₄ Pyrolysis in H ₂ at 1031°C on Large-grain Vistal 4 Alumina and (0112) Sapphire Substrates.	57
2-9.	Electrical Properties of B-doped CVD Si Films Deposited by SiH ₄ Pyrolysis on Single-crystal and Polycrystalline Substrates of α Alumina (Al ₂ O ₃)	61
2-10.	CVD Si Sheet Samples* Submitted to OCLI during First Quarter for Solar Cell Processing	71
2-11.	B-doped CVD Si Sheet Samples Submitted to OCLI during Second Quarter for Solar Cell Processing and Measurement	73

1. INTRODUCTION

This contract began December 29, 1975, and is of 18-month duration. This second quarterly report covers the second three months of the program - April, May, and June, 1976.

The purpose of the contract is to explore the chemical vapor deposition (CVD) method for the growth of Si sheet on inexpensive substrate materials. The work is carried out at the Rockwell Electronics Research Division in Anaheim, but also involves some experimental solar cell fabrication and evaluation by the Photoelectronics Group of Optical Coating Laboratory, Inc. (OCLI), in City of Industry, California.

The formal objective of the contract is development of CVD techniques for producing large areas of Si sheet on inexpensive substrate materials, with sheet properties suitable for fabricating solar cells meeting the technical goals of the Low Cost Silicon Solar Array Project (LCSSAP). The techniques developed are to be directed toward (1) minimum-cost processing, (2) production of sheet having properties adequate to result in cells with terrestrial array efficiency of 10 percent or more, and (3) eventual scale-up to large-quantity production.

The CVD method as applied to Si sheet growth involves pyrolysis or reduction of a suitable Si compound at elevated temperature and (approximately) atmospheric pressure in a flow-through (open-tube) system. A carrier gas is used to transport the reactants to the deposition chamber, in which the substrate is mounted on a SiC-coated carbon pedestal heated by rf from outside the chamber. The properties of the Si sheet are determined by deposition temperature, reactant concentrations, the nature of the carrier gas, the Si source compound used, growth rate, doping impurities (added by introduction of appropriate compounds into the carrier gas stream), and the properties of the substrate.

The specific technical goals established for the contract include the following:

Si sheet area (per sample)	30 cm ²
Si sheet deposition rate	5 µm per min
Si sheet thickness	20 to 100 µm
Si sheet crystal structure	100 µm average grain size
Intragrid dislocation density	<10 ⁴ per cm ²

The principal technical problems to be solved are (1) establishing preferred CVD process parameters (temperature, reactant concentrations, carrier gas composition, doping impurities, growth rate) for optimized intragrid properties for the Si sheet grown on various substrate materials; (2) identifying suitable substrate materials that will survive the environment of the CVD process and be potentially inexpensive and available in large areas, yet be as favorable as possible to Si grain growth; and (3) achieving adequate grain size in the Si sheet to provide satisfactory solar cell properties.

Many characteristics of the CVD method indicate that it has considerable promise for achieving the 1985 technical and cost goals of the LCSSAP: (1) it produces only that amount of Si that is actually required for the photovoltaic effect, without the requirement of additional Si for purely structural reasons; (2) it is a relatively low-temperature process and thus is energy-conservative, not requiring melting of Si at any stage;

(3) it does not require refined/purified polycrystalline Si starting material, using instead a high-purity compound of Si that is actually a product of one of the early steps in the preparation of polycrystalline semiconductor-grade Si; (4) it is inherently a large-area process, capable of potential scale-up to areas that are practical for large array fabrication in the LCSSAP; (5) impurity doping for junction formation can be carried out during CVD growth of the Si sheet; (6) thicknesses are closely controllable by reactant flow-rate adjustments; and (7) it has the capability for eventual development of a continuous fabrication process, in which the Si material, the junction or barrier, and the required contacts are all fabricated in a single integrated series of operations in one apparatus.

Si sheet growth by CVD on inexpensive substrates will almost certainly be polycrystalline, because such substrates will be either amorphous or microcrystalline and will thus provide little or no ordering influence on the growth mechanism. However, the prospects of at least closely approaching the project goal of 10 percent terrestrial array efficiency are considered good. The chances of obtaining sufficient cost reduction per unit area of active cell surface appear strong enough that a cost-per-watt figure within the project goals should be achievable with this process.

The contract program is composed of six main technical tasks, as follows: (1) modification and test of an existing CVD reactor system; (2) identification and/or development of suitable inexpensive substrate materials; (3) experimental investigation of CVD process parameters using various candidate substrate materials; (4) preparation of Si sheet samples for various special studies, including solar cell fabrication; (5) evaluation of the properties of the Si sheet material produced by the CVD process; and (6) fabrication and evaluation of experimental solar cell structures by OCLI, using standard and near-standard processing techniques.

The progress achieved during the second quarter is described by task in the following section, followed by a summary of conclusions and recommendations and an outline of the work planned for the third quarter. This is followed by the New Technology statement and a listing of references used in this report.

The manpower and funding expenditures are summarized in Appendix A, and the Updated Technical Program Plan is included as Appendix B.

2. TECHNICAL DISCUSSION

This section contains a summary of the results obtained during the second quarter in performance of the Statement of Work of this contract, and interpretation of the results where appropriate. This discussion is arranged by task, although the interlocking of the tasks is such that this distinction is not always easily made.

2.1 TASK 1. MODIFICATION AND TEST OF EXISTING CVD REACTOR SYSTEM

The apparatus required for the chemical vapor deposition of Si films has been highly developed in recent years. It consists of six main components: (1) deposition chamber (reactor), with provision for supporting the heated substrates on which Si is deposited; (2) reactant gas manifold and distribution line system, with appropriate metering, valving, and controls; (3) reservoirs or tanks of the required reactant and carrier gases, with associated purifiers and/or filters; (4) vacuum system for evacuating selected portions of the reactor and gas manifold, as needed; (5) provision for burning, reprocessing, or otherwise discharging the exhaust gases existing from the reactor system; and (6) power supply for heating the substrates in the reactor chamber - usually an rf generator with an external coil which couples to a susceptor, which also serves as the substrate support.

Throughout the first quarter of this program an existing laboratory-type CVD reactor system with a vertical deposition chamber was used. This system is similar to that used extensively at Rockwell in previous studies of semiconductor epitaxial growth by CVD, and is shown schematically in simplified form in Figure 2-1.

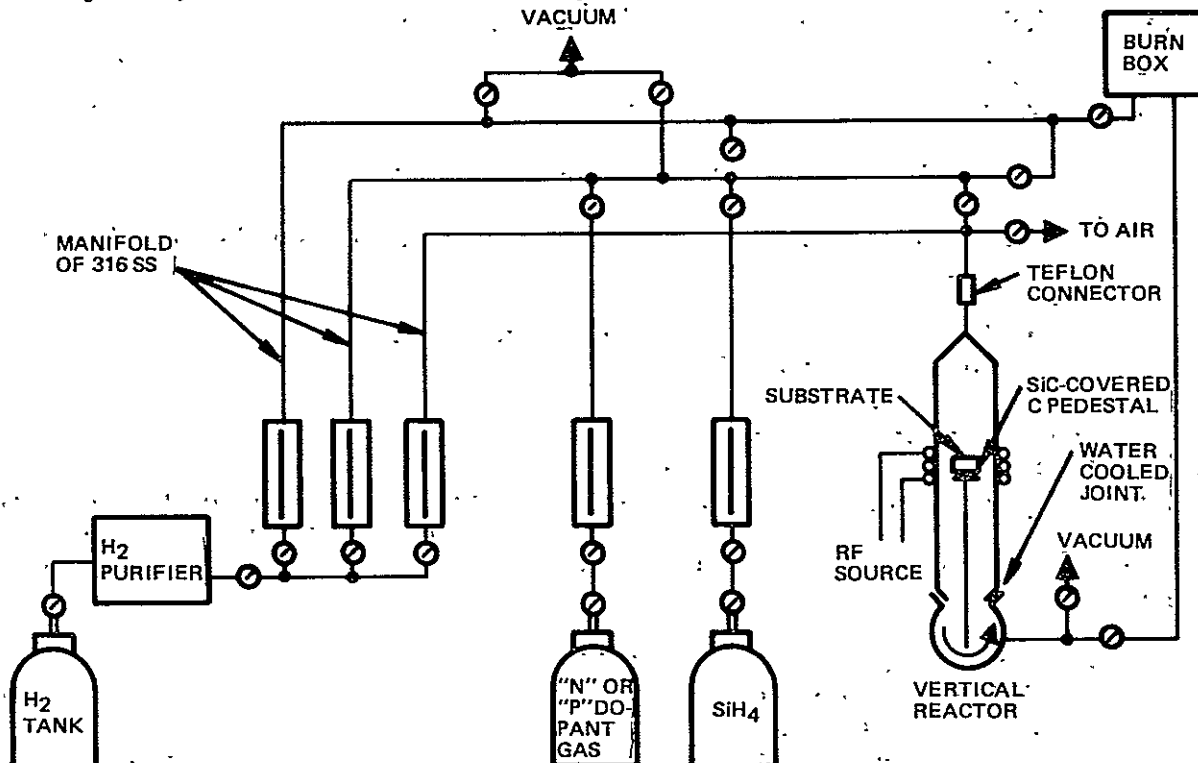


Figure 2-1. Simplified Schematic Diagram of Vertical-Chamber CVD Apparatus for Si Sheet Growth

Even in its simplest form a system of this type provides the following capabilities:

1. Growth of undoped or doped Si films on any substrate that will withstand the growth temperature, using several different sources of Si, including SiH_4 or a Si halide or mixtures of SiH_4 and HCl
2. Etching of Si on the substrate or removing solid reaction products from the walls between deposition experiments, using HCl
3. Use of one or more carrier gases to establish a desired growth atmosphere.
4. Evacuation of sections of the apparatus, including the reactor chamber, while gas flows are continued in other sections
5. "Homogenization" of gas flows prior to introduction of the gases into the reactor
6. Trapping of moisture and other condensables that are probably typical of the impurities present in "electronic grade" gases.

To improve the control of the Si CVD process for this program a number of modifications were planned for the reactor system shown in Figure 2-1. These changes were intended to provide a more versatile system that would offer greater reproducibility and reliability than previously available.

The modifications were originally scheduled for completion by March 1, but because of vendor delays in delivery of some of the key components to be used in the modifications it was necessary to reschedule the completion of the system modifications to April.

As a result, at the end of the first quarter the plans for this task for the second quarter, as delineated in Quarterly Report No. 1 (March 31, 1976), included the following activities:

1. Complete installation of new reactor system components and controls
2. Test modified reactor system upon completion
3. Prepare written Standard Operation Procedure for modified reactor system, as required by contract
4. Conduct Design and Performance Review of reactor system for JPL personnel, as required by contract.

Modifications in the Si CVD reactor system were completed in mid-April and the contractually-required Design and Performance Review of the modified system was conducted for JPL personnel on April 15, 1976, as scheduled (see Updated Technical Program Plan, Appendix B). The Standard Operation Procedure for the modified reactor system was also completed and delivered to JPL personnel at the time of the Review.

The necessity for delaying the initially-planned completion of the reactor modifications and for rescheduling the design review was caused by delays in delivery of the mass flow controllers and the control and readout units which control the valves and flow meters in the reactor system. The last of these units was received late in March; thus, there was barely enough time to complete the planned modifications prior to the scheduled review date, but this was accomplished through expenditure of considerably more manpower than had originally been allotted to this task.

A schematic diagram of the reactor system incorporating the modifications is given in Figure 2-2. The modifications include the following main items:

1. Thirteen Tylan Model FC-260 Mass Flow Controllers. All gas lines involved directly in the CVD process are controlled by this means. The only lines not so controlled are the carrier gas bypass and reactant "dump-out" line leading to the burn-box at the top of the reactor-system hood enclosure, and a separate H₂ line to admit that gas to the chamber for pre-deposition "etching" when carrier gases other than H₂ are being used. The controller locations are as follows:
 - 2 in parallel main gas flow lines, one leading into the reactor chamber and the other provided for mixing reactants in desired proportions and at constant total flow prior to introduction into the chamber
 - 3 in Si source compound supply lines (SiH₄, SiH₂Cl₂, and a bubbler for SiHCl₃ and SiCl₄)
 - 1 in bubbler-source carrier gas line
 - 1 in HCl line
 - 2 in dopant lines (n- and p-type impurity source compounds)
 - 2 in gas lines for dilution of doping compounds
 - 2 in diluted dopant lines (n and p type)
2. One Tylan Model GPT-104 Automatic Sequence Timer associated with the controllers. The timer is capable of providing automatically-timed control of flow intervals in 10 different lines (i. e., 10 signal channels), with up to four different events (such as on and off) per channel programmable in each cycle of the sequencer.
3. Four Tylan Model RO-14 Control and Readout Units. These are included in the centralized control panel to handle the outputs of the 13 mass flow controllers. Each readout unit has a maximum capacity of four input channels.
4. Two Model 5150A Hewlett-Packard Thermal Printers. Each of these is capable of sequential printing of 20 channels of digital information per cycle of the printer (printing time ~1/3 sec per line, data input acceptance interval adjustable down to one second). These are used to provide permanent records of experimental parameters when desired. These printers each include a timer, so that all data are related to printed digital time recordings.
5. Ten Nupro Model 4BK air-operated valves. These are triggered by switch-activated solenoids, and are installed on the reactor system to improve control over film thickness, nucleation phenomena, and impurity concentration and distribution. Two of these valves are Nupro Model SS-4BK-S2 zero-dead-space valves, to further reduce the amount of uncontrolled and/or unwanted reactant flow in the system.

**H₂ PURGE
TO SOURCE TANK**

NOTES:

- **ALL TUBING**
1/4" **SS**
EXCEPT AS NOTED
 - **V = MANUAL BELLows
VALVE (VACUUM)**
 - **F = MANUAL BELLows
VALVE (GAS FLOW)**
 - **M = MANUAL BELLows
VALVE (MASS FLOW)**
 - **A = AIR-OPERATED
BELLows VALVE
(GAS FLOW)**
 - **B = BACK-PRESSURE
REGULATOR**
 - **ALL GASES TRAPPED
WITH COLD TRAPS**
 - **SiH₄, DICHLOROSILANE,
N AND P DOPANTS,
AND HCl PIPED IN
FROM SEPARATE
FUME HOOD TO
APPROPRIATE MFC**
 - **MFC = MASS FLOW
CONTROLLER**

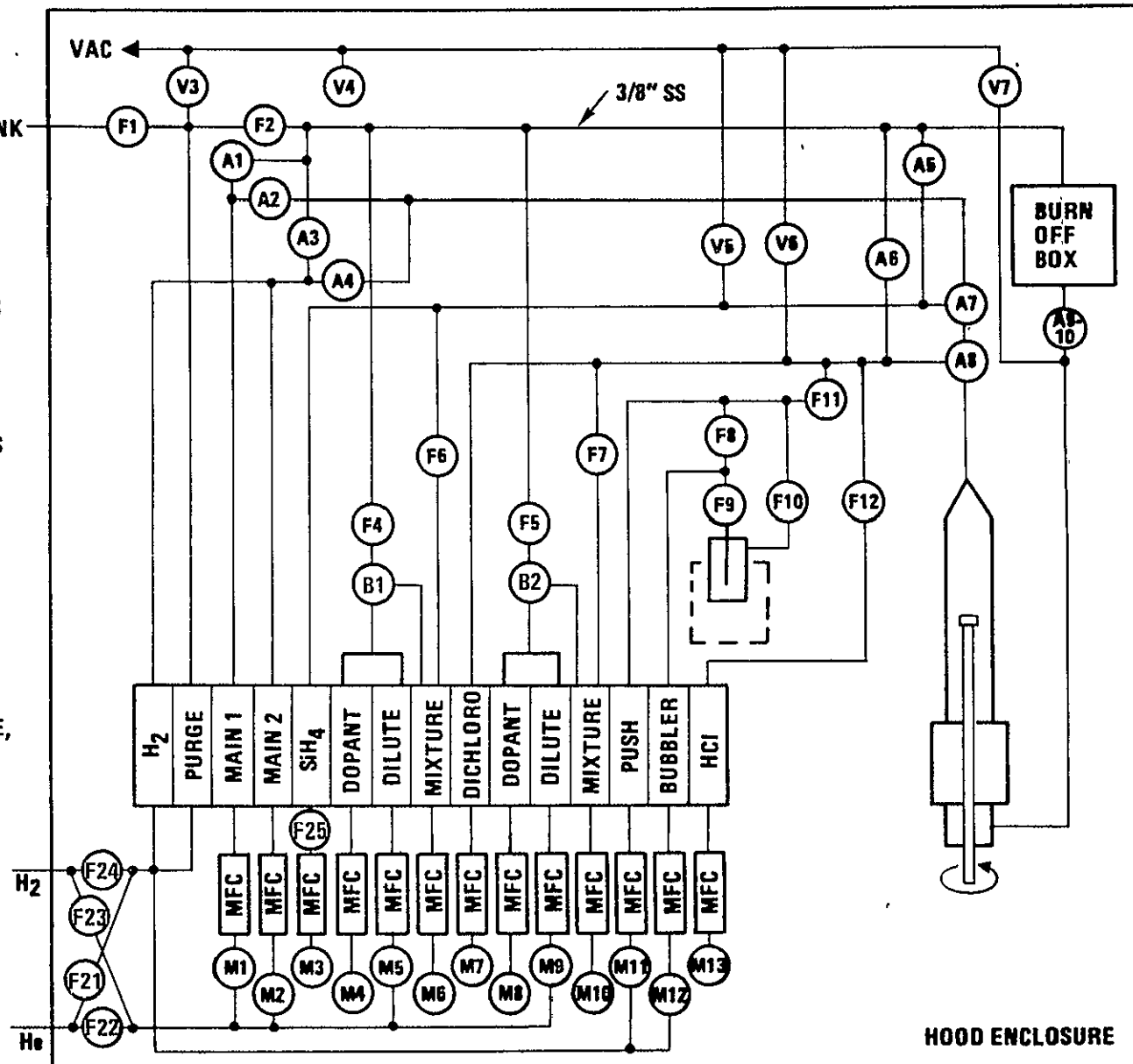


Figure 2-2. Schematic Diagram of Modified Si CVD Reactor System

6. One Alcatel Model ZM2012C Vacuum Pump. This pump serves both as the forepump for the trapped mercury-vapor diffusion pump and as the roughing pump for the reactor system. This type of pump has improved pumping speed over conventional oil-immersed mechanical vane pumps, provides essentially zero backstreaming of hydrocarbon vapors because of its "dry" construction, and is relatively quiet in operation.

In addition to the reactor system itself, which is enclosed in a separate high-flow-rate fume hood, an external control center is housed in a separate floor-mounted cabinet at the side of the hood. This cabinet accommodates the sequence timer, the four readout units, two recorder-printers, and the master valve control panel.

The entire CVD reactor system is shown in the photograph in Figure 2-3; the external control cabinet can be seen at the left, the bank of mass flow controllers in the lower center, and the vertical reactor chamber at the right. A close-up view of the mass flow controllers is shown in Figure 2-4. The conventional rotameters can be seen above the mass flow controllers; these were left in the system to provide convenient visual indication of gas flow and, incidentally, a continuing check on the functioning of the controllers.

Following completion of the reactor modifications in mid-April, and after two deposition experiments were carried out with the modified system, it was observed that there were significant discrepancies between the reactant gas flow rates as read (and controlled) by the mass flow controllers and the rates indicated by the conventional rotameters that had been left in the lines in series with the mass flow controllers. Upon careful investigation of the problem, in collaboration with the manufacturer (Tylan Corporation, Torrance, CA), it was determined that faulty temperature sensors had inadvertently been used in the mass flow control units, rendering their calibrations inaccurate and/or unstable. Each of the units was returned to the manufacturer for replacement of the sensor, after which proper performance of the devices appeared to be obtained on the Si CVD system. However, further problems of inaccurate and/or unstable performance of several of the mass flow controllers appeared, and it was subsequently determined by the manufacturer that faulty insulating cement had been used in assembling the temperature sensors into the units. This problem was also corrected by the manufacturer very promptly. These problems and the relatively quick solutions obtained demonstrated the importance of the fortuitous fact that the manufacturer of these components is located nearby and is willing and able to send a representative to Anaheim on very short notice to assist in finding and correcting problems.

Several other minor difficulties were encountered during the quarter in achieving full operational capability of the reactor system, and a few minor changes have been made in the system since the Design and Performance Review in April. For example, a four-way ball valve was found to allow He from the input gas line to leak into the input H₂ line. In its place, separate stainless steel lines for each gas and connecting manual bellows-sealed valves were installed. In addition, a manual bellows-sealed valve has been added between the SiH₄ mass flow controller and the glass rotameter to help minimize some recently observed problems with possible contamination of the SiH₄ mass flow controller.

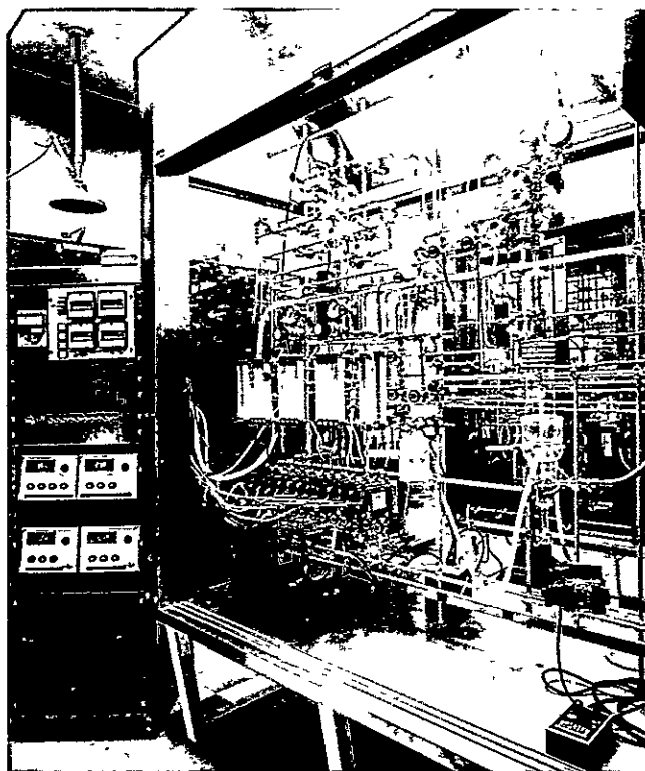


Figure 2-3. Overall View of Modified Si CVD Reactor System, Showing Control Center in Separate Cabinet, Bank of Mass Flow Controllers in Lower Center, and Vertical Reactor Chamber at Right

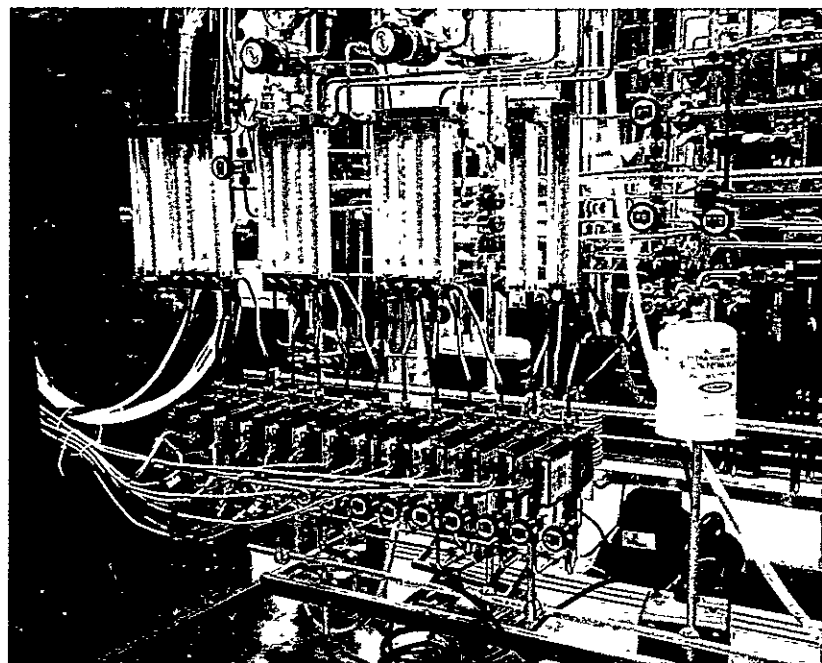


Figure 2-4. Close-Up View of Bank of 13 Mass Flow Controllers

Except for minor modifications that will be made from time to time throughout the remainder of the contract work and for routine maintenance and repairs that will occur on a continuing basis, it is anticipated that no further activity concerned with modification and test of the CVD reactor system will take place. Thus, this is the last report in which Task 1 work will be explicitly discussed as such. In the future, any required work with the reactor system will be described as part of the Task 3 activities; this is consistent with the Updated Technical Program Plan.

2.2 TASK 2. IDENTIFICATION/DEVELOPMENT OF SUITABLE SUBSTRATE MATERIALS

The 1985 cost goals of the LCSSAP are such that it now seems almost certain that no single-crystal material (other than perhaps Si itself) could be used as the substrate for low-cost large-area Si solar arrays meeting the technical performance goals of the project. Future developments, of course, could alter this outlook, but for the requirements of this contract other materials far less favorable to Si crystal growth must be considered and evaluated. This is the starting premise in the search for candidate substrate materials.

2.2.1 Rationale and Procedure for Material Selection

In attempting to identify candidate substrate materials for CVD growth of Si sheet which will meet the technical goals of this contract, several considerations are necessary. First of all, the material must be potentially inexpensive. This means that as an absolute upper limit, in today's market as well as in 1985, it must be less expensive than Si itself for comparable sizes and shapes.

Next, it must be available, or potentially available, in relatively large areas. Present technology probably should already have produced similar material in sizes larger than those in which commercially available Si is produced.

In addition, the properties of the substrate material should be compatible with those of Si. Its linear thermal expansion behavior should parallel that of Si as closely as possible, from at least the Si sheet deposition temperature down to room temperature. The Si film must also be chemically stable with respect to the substrate surface, so that the transition layer at the interface does not cause separation or other interaction of the two components. Also, the substrate surface must be stable relative to the carrier gas and the products of Si formation, notably H₂ when SiH₄ is the source of Si and HCl when the Si-containing halides are used to produce the Si.

Only a few classes of materials now available commercially could be considered initially as candidate substrate materials, based on cost, availability, and reported properties. These include the amorphous glasses, glass-ceramics, and polycrystalline ceramics. Many glasses are available in very large sheet form, and others are potentially susceptible to fabrication into large sheets. Some glass-ceramics are also produced in large sheets (the order of square meters), and many of the polycrystalline ceramic materials are now available in areas up to about 300 cm².

Figure 2-5 gives the linear thermal expansion coefficient (TEC) as a function of temperature for several possible substrate materials, as well as for some other familiar materials for comparison, throughout the range from below room temperature up to Si CVD temperatures. These data provide guidance in the selection of candidate materials for further experimental evaluation.

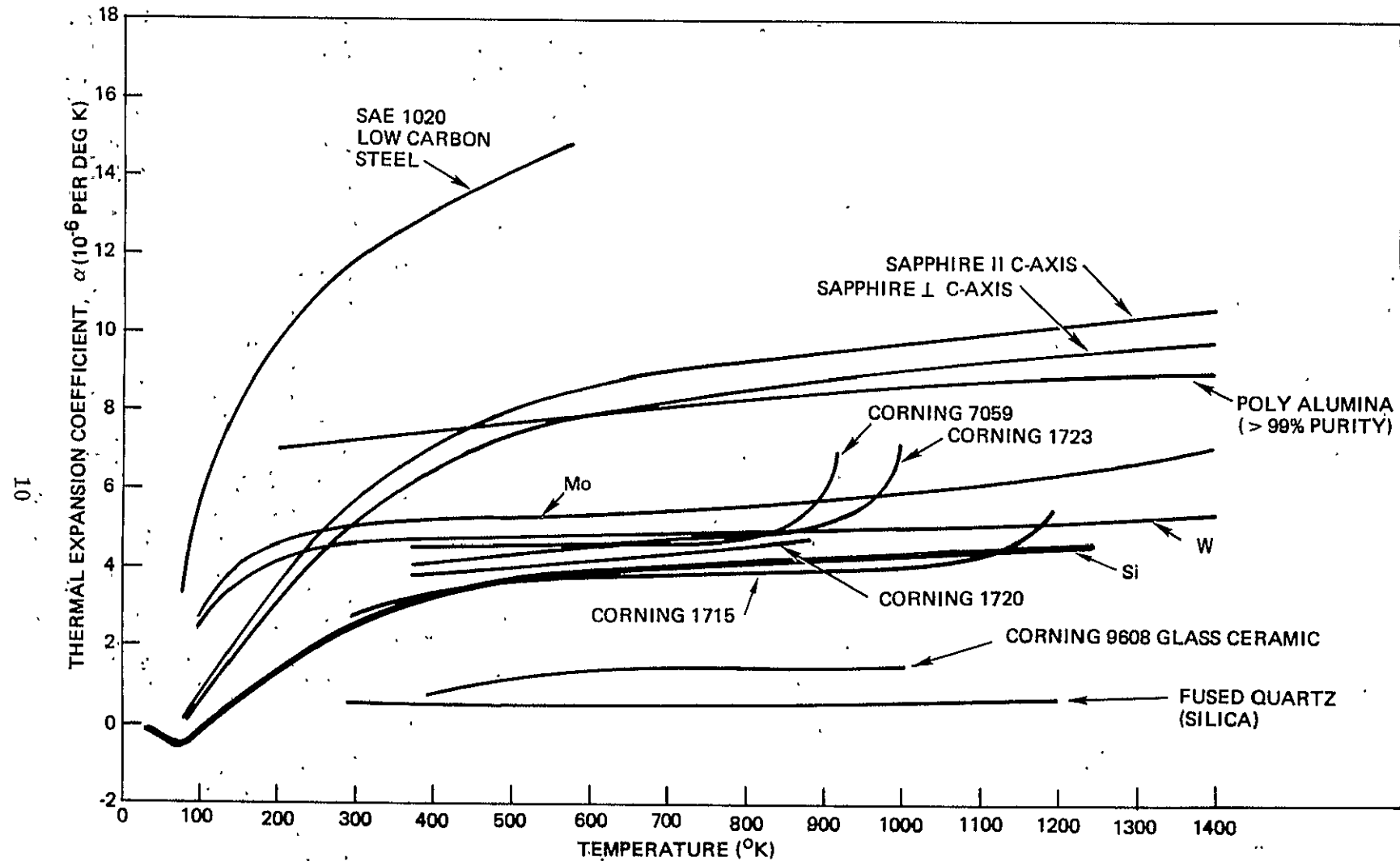


Figure 2-5. Linear Thermal Expansion Coefficients as a Function of Temperature
for Si and Various Other Materials

Before a potential substrate material is used for Si growth, the following characteristics, determined on representative samples, are established: physical appearance (unaided eye); thickness; surface roughness; general appearance at 100X and/or 450X magnification; and (optional) structural properties determined by such procedures as X-ray, reflection electron diffraction (RED), and SEM examination of the surface.

Substrates of interest are then subjected to exploratory Si CVD growth in both H₂ and He atmospheres at temperatures consistent with the reported properties of the material. For example, for free-standing glasses temperatures below the softening point are used; for glazes on ceramics, higher than softening temperatures may also be used; for the high-temperature stable ceramics, temperatures up to about 1200°C can be considered, depending upon the properties of the Si-containing compounds in the carrier gas atmosphere.

A thick ($\geq 20 \mu\text{m}$) Si film usually is grown on the substrate, in the presence of a small wafer of sapphire; the latter helps in monitoring the test substrate material stability in the carrier gas and growth atmosphere, as revealed by any obvious contamination pattern in the Si growth on at least the part of the sapphire nearest the substrate. The thick Si film also helps to determine if the difference in TEC between the Si and the substrate leads to detectable bowing of the composite due to the differential stresses developed upon cooling to room temperature. The Si film also helps reveal certain nonuniformities in some of the substrates.

2.2.2 Evaluation and Preparation of Candidate Substrate Materials

Table 2-1 lists all of the substrate materials of which samples were received from various vendors during the first quarter of the program.

The response of most of the glass and ceramic manufacturers contacted for assistance in solving the substrate problem has been excellent. Both commercially-available and specially-prepared materials have been supplied for evaluation as potential low-cost substrates.

During the first quarter, using the existing reactor system (prior to modifications), preliminary deposition experiments with two of the available glasses were discouraging because of adverse physical and/or chemical effects on the glass in the CVD process, even at relatively low temperatures. Both Corning Code 7059 and Corning Code 1723 glasses were found to be inadequate for the growth of acceptable quality Si by CVD. Code 7059 glass bowed too much when Si was deposited on it in He at 700°C for it to be a useful substrate for solar cell fabrication, and Code 1723 glass failed in both H₂ and He atmospheres; amorphous structural features were found on the film surface grown in H₂ at 850°C, and contamination of the companion sapphire substrate occurred during Si deposition in He at 850°C. Moderately encouraging results, however, were obtained with fired polycrystalline alumina substrates, which were used for Si deposition at temperatures above 1000°C. These materials exhibit some preferred orientation in their polycrystalline structures, and the films grown on these were also preferentially oriented. The alumina substrates used were those of the highest purity: MRC Superstrate, Coors ADS995, and 3M ASM805. The latter was found to have the best as-fired surface of the alumina substrates obtained in the first quarter.

Table 2-1. Candidate Substrate Materials Received during First Quarter from Various Suppliers

SUBSTRATE IDENTIFICATION		MATERIAL/TYPE	THERMAL EXPANSION COEFF (TEMP RANGE) (10 ⁻⁶ PER DEG C)	SURFACE ROUGHNESS OR FINISH	THICKNESS (mm)	NOMINAL PURITY (%)
Corning	0221*	Lime Borosilicate	7.4 (0-300°C)	<0.5 Microinch	0.25	-
	0317*	Alumina Soda Lime	8.7 (0-300°C)		1.52	-
	1723*	Aluminosilicate	5.4 (25-670°C)		0.76, 1.27	-
	7059*	Barium Alumino-borosilicate	4.6 (0-300°C)		0.81	-
Owens-Illinois* GS-186	GS-186	Proprietary High-temperature Glass	4.7 (0-300°C)	Mechanically Polished; Prob <1 Microinch	0.76, 1.02	-
	GS-210	"	3.8 (0-300°C)		1.02	-
	GS-211	"	3.6 (0-300°C)		1.02	-
	GS-213	"	2.6 (0-300°C)		1.07	-
Coors	ADS 96F	Alumina	8.1 (25-1000°C)	As Fired	0.63	96
	ADS 995	Alumina	7.7 (25-1000°C)		0.69	99.5
	Refrined Large-grain Al ₂ O ₃ *	Alumina	~7.3 (25-800°C)		0.56	99.3 (Before Firing)
	Vistal	Alumina	8.3 (25-1200°C)		0.97	99.9
MRC	Superstrate	Alumina	7.3 (25-800°C)		0.63	99.6
Kyocera	F1330	Forsterite	10.5 (40-400°C)		1.32	-
Union Carbide		Graphite	2.8(c) (300-1100°K)		0.97, 1.52	-
Oriented Pyrolytic						-
Pemco-Glidden-Durkee	P2P36	Lithium Aluminosilicate Glaze on Cordierite	~3		0.20 - 0.25	-
	P3T235	Boron Aluminosilicate Glaze on 94% Alumina	~5.5		0.13 - 0.15	-
3M	ASM475*	Zircon (ZrO ₂ ·SiO ₂)	4.9 (25-900°C)	2µm (CLA)**	3.18	-
	ASM614	Alumina	7.9 (25-900°C)		0.63, 0.79	96
	ASM614, W/743 Glaze*	Lead Borosilicate on Alumina	~6.5 (40-540°C)	< 1 Microinch	0.89, 1.09	-
	ASM701*	Cordierite (2MgO·2Al ₂ O ₃ ·5 SiO ₂)	3.7 (25-900°C)	~4.5µm (CLA)**	0.71 (Total)	-
	ASM772	Alumina	7.7 (25-900°C)		3.18	-
	ASM805*	Alumina	7.7 (25-900°)	<1-2 Microinch	0.25, 1.02	99.5
	ASM838	Alumina	7.7 (25-900°)		1.08	-
					0.63	99.9
					0.13, 0.71	99.5

* Some samples of these materials were received prior to start of contract

**CLA = center line average

Based on these results, the plans for this task for the second quarter, as listed in Quarterly Report No. 1, included the following activities:

1. Continue experimental evaluation of candidate substrate materials by Si CVD experiments as suitable samples become available, and continue and/or complete screening of materials received during first quarter
2. Continue interactions with potential suppliers of substrate materials
3. Compare properties of as-fired and mechanically-polished alumina substrates from several suppliers, and compare Si film properties grown on both types
4. Continue to investigate the effects of various substrate surface treatments on the resulting Si film properties.

During the second quarter efforts were continued for identifying and obtaining candidate substrate materials, additional screening experiments were carried out with substrates already obtained--including some specially prepared materials supplied by vendors as a result of contacts made earlier in the program, and the preparation of the surfaces of some substrate materials by mechanical polishing techniques was undertaken. These activities are summarized in the following sections.

2.2.2.1 New Substrate Materials Obtained

Additional suppliers of candidate substrate materials were contacted. Discussions were held with Saxonburg Ceramics, Inc. (Saxonburg, PA); Alberox Corporation (New Bedford, MA); National Beryllia Corp. (Haskel, NJ); Morganite, Inc. (Dunn, NC); McDanel Refractories Corp. (Beaver Falls, PA); Honeywell Ceramic Center (Golden Valley, MN); Ferro Corp. (Independence, OH); Wisconsin Procelain Co. (Sun Prairie, WI); and Du-Co Ceramics (Saxonburg, PA).

Table 2-2 lists the additional substrate materials, beyond those shown in Table 2-1, that were received during the second quarter, with some of the pertinent properties given.

2.2.2.2 Substrate Surface Characterization and Preparation

The surface roughness of a group of as-fired polycrystalline substrates obtained from the 3M Co. was measured by surface profilometry (Sloan Dektak), and the results of these measurements are given in Table 2-3. The surface roughness is expressed as an average peak-to-valley dimension determined by measurement on the profilometer trace. The probe stylus has a radius of 12.5 μm , and a tracking force equivalent to 50 mg is used. Many of these substrate materials are to be used in planned Si CVD experiments, in both the as-fired and the polished condition.

Because of the rough surfaces on the as-fired aluminas and on some of the other ceramic materials (Tables 2-1 and 2-2) obtained from various manufacturers, several groups of substrates from among those listed have been selected for mechanical polishing. The first materials so processed were the aluminas Superstrate (MRC) and Vistal (Coors), the latter a material that has been subjected to several consecutive additional firings by the manufacturer in order to increase the average grain size.

The purpose of this polishing procedure is twofold. First, polishing will generate smooth surfaces on the substrates and thus result in smoother film surfaces, and yet retain benefits to the Si sheet nucleation and growth process that accrue from the presence of the substrate crystal grains that intersect the mechanically generated surface.

Table 2-2. Candidate Substrate Materials Received during Second Quarter from Various Suppliers

SUBSTRATE IDENTIFICATION	MATERIAL/TYPE	THERMAL EXPANSION COEFF (TEMP RANGE) (10 ⁻⁶ PER DEG C)	SURFACE ROUGHNESS OR FINISH	THICKNESS (mm)	NOMINAL PURITY (%)
Corning 1715	Calcium alumino-silicate	~3.5 (0-300°C) (Ann. pt. 866°C) (Soft. pt. 1066°C) (Work. pt. 1399°C)	As mfd	0.76	
Saxonburg	Alumina	—	As fired	1.27	97.5
Honeywell	Mullite (3Al ₂ O ₃ ·2SiO ₂)	~5.0	As fired	1.65 - 1.78	
Atomics Intl. (AI)	Proprietary glass on ASM805 alumina	— (Soft. pt. 830°C)	As mfd	0.063 - 0.076	
Morganite	Recrystallized alumina	~8	As mfd	3.12	
Kyocera	Zircon (Z360)	~4.7 (40-800°C)	As mfd	1.02	
3M Co	Zircon (ASM475)	4.9 (25 - 900°C)	As fired	0.56	
Chi-Vit Corp	Alumino-silicate glass on nickel steel	~4.5	As mfd	0.15 0.30	

Table 2-3. Average Surface Roughness of Polycrystalline Ceramic Substrates
(3M Co.) Measured by Surface Profilometer (Sloan Dektak)

MATERIAL DESIGNATION	MATERIAL	MATERIAL PREPARATION PROCESS	THICKNESS (mm)	AVERAGE VERTICAL PEAK-TO-VALLEY DIMENSION (μm)	
				SIDE A	SIDE B
ASM614	Alumina	AlSiBase*	0.63	1.2	1.2
ASM614	Alumina	AlSiBase*	0.89	1.3	1.5
ASM614	Alumina	Dry press	0.79	2.5	2.5
ASM614	Alumina	Dry press	1.08	3.0	3.5
ASM772	Alumina	AlSiBase*	1.02	0.5	0.75
ASM772	Alumina	AlSiBase*	1.08	1.8	0.75
ASM838	Alumina	AlSiBase*	0.13	0.6	0.50
ASM838	Alumina	AlSiBase*	0.71	0.6	0.40
ASM805	Alumina	AlSiBase*	0.63	0.08	0.2
ASM743 glaze on ASM614	Lead Borosilicate on alumina	-	0.71	0.003	1.5
ASM614	Alumina	Refired	0.63	3.2	2.5
ASM805	Alumina	Refired	0.63	<0.1	0.27
ASM772	Alumina	Refired	0.25	1.2	1.0
ASM838	Alumina	Refired	0.69	0.4	0.75
ASM832	Alumina	AlSiBase*	0.71	3.0	1.0
ASM777	Alumina	AlSiBase*	0.48	2.0	1.6
ASM701	Cordierite	Dry Press	1.02	15.0	6.5
ASM475	Zircon	Dry Press	3.18	5.0	4.5
ASM701	Cordierite	Dry Press	3.18	5.0	7.5
ASM475	Zircon	Dry Press	0.56	4.0	4.0

*Process trademark of 3M Co.

ORIGINAL PAGE IS
OF POOR QUALITY

Second, simultaneous Si growth experiments on polished and as-fired substrates are especially important. The actual growth facets of an as-fired polycrystalline substrate are not--on the average--in the same crystallographic orientations as those that are delineated in x-ray analyses for preferred orientation in the substrate materials. This is because the crystal planes so identified are referenced to the nominal surface plane of the substrate wafer as it is mounted for x-ray analysis; that is, the planes identified as preferred orientations in the alumina are parallel to the nominal wafer surface, but the growth facets are nearly all at appreciable angles to this plane. Thus, to establish correlations between substrate preferred orientations and the observed Si film habit it is necessary to grow Si on a polished surface coinciding with the nominal substrate surface.

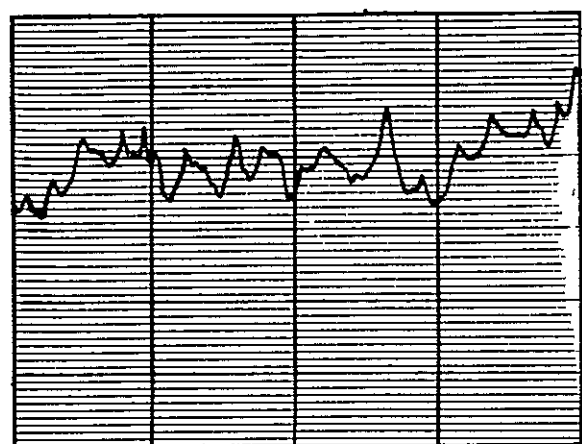
In addition to the two aluminas mentioned above, other aluminas of different (lower) purity, zircon, mullite, and cordierite are now being polished for subsequent Si film growth experiments to be done early in the third quarter. Results of the sheet growth experiments on polished substrates will be used in the attempt to determine a reasonable balance between the increased cost of preparing substrates by this additional processing step and the expected improvement in the surface characteristics (and perhaps the internal structure) of the resulting polycrystalline Si films.

Vistal is a large-grained high purity alumina (99.9 percent) manufactured by Coors Porcelain Company. There are four groups of Vistal substrates, each of which has a different firing history; these substrates have been fired beyond the normal alumina processing by virtue of one, two, three, and four consecutive firings at $>1800^{\circ}\text{C}$ for six hours each. As a result, four different average grain sizes have been achieved. One batch of Vistal substrates, including several samples of each of the four different firing histories, was lapped for 10 hours with a slurry of $5\ \mu\text{m}$ SiC particles to produce a flat fine-lapped finish. Prominent irregular crevices intersecting the lapped surfaces on the four samples clearly delineated the range of grain sizes that resulted from the consecutive firings, even without any chemical etching. Surface photomicrographs of each of the four lapped surfaces were shown in Figure 2-12 of Quarterly Report No. 1, and profilometer traces of the surfaces of as-fired and lapped specimens of each of the four groups were also shown (Figure 2-26) in that report.

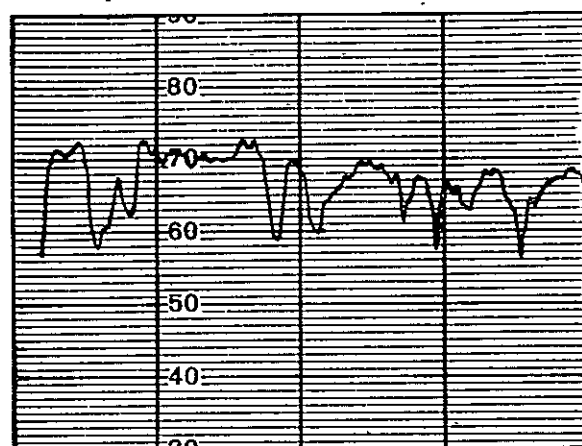
A comparison of profilometer traces for Vistal substrates in the as-fired, lapped, and polished conditions is shown in Figure 2-6 for material with one and two firings and in Figure 2-7 for material with three and four firings. In each case the horizontal scale is such that one major chart division corresponds to a distance of 0.2 mm along the sample surface. These figures show the obvious (and expected) improvement in surface smoothness resulting from lapping and polishing, but also clearly show the deep crevices between neighboring crystal grains in the lapped condition and the shallow but finite steps between grains in the polished condition.

The SEM photographs in Figure 2-8, which show representative areas of samples of each of the four Vistal groups in the as-fired condition, illustrate the wide range of grain sizes present in each group; grains from $5\ \mu\text{m}$ to over $200\ \mu\text{m}$ across can be seen. (The apparent debris on the surface--especially prominent in Figure 2-8c--is caused by incomplete cleaning of the substrate prior to examination in the SEM.)

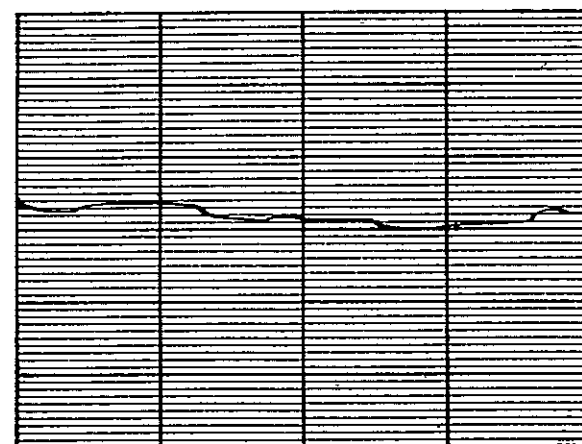
All as-fired substrates exhibited a three-dimensional surface with gently rounded grains projecting less than $\sim 10\ \mu\text{m}$ in a vertical direction, as shown in Figure 2-9 for a Vistal 4 (four consecutive firings) substrate. Figure 2-9a is with the sample oriented for the standard viewing angle of 45 deg, while Figure 2-9b shows the same sample (at approximately the same magnification) viewed at a low angle of 25 deg with the sample surface, showing more clearly the height of the individual projecting crystals.



AS FIRED



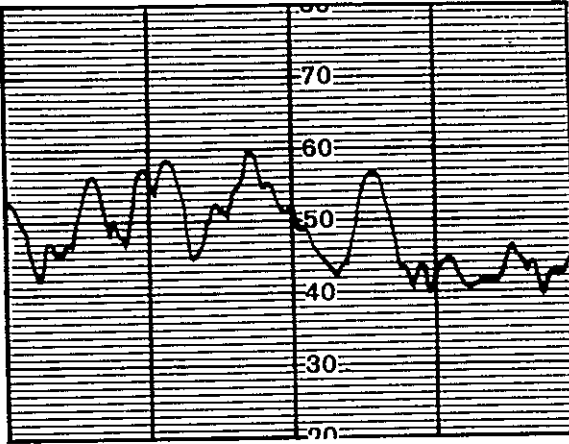
LAPPED



POLISHED
(a)

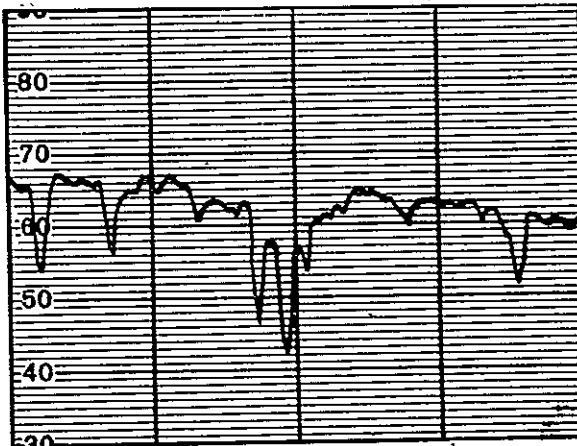
VISTAL 1

VERT
SCALE
0.5μm/div

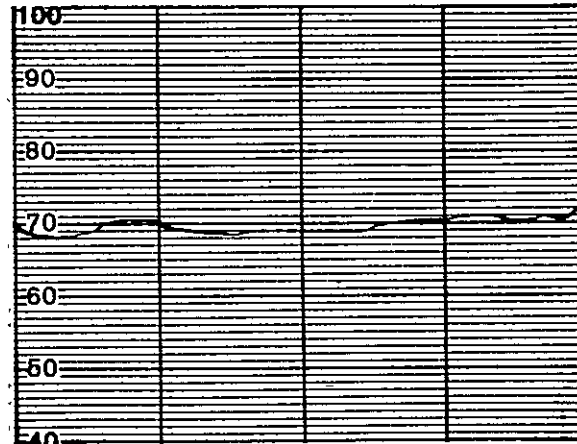


AS-FIRED

VERT
SCALE
0.1μm/div



LAPPED

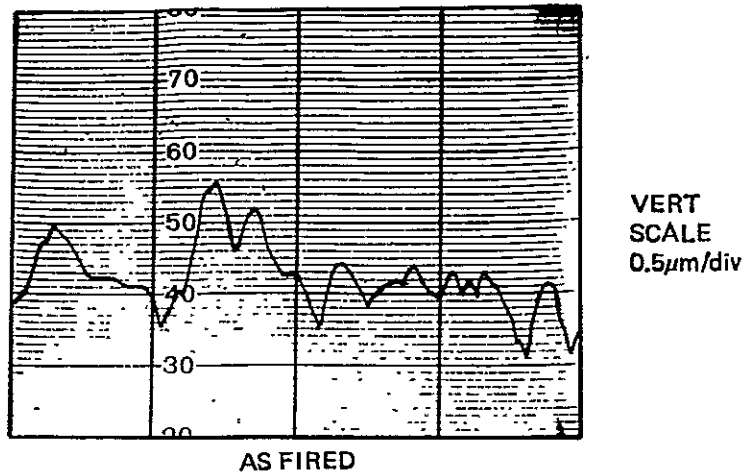


POLISHED
(b)

VISTAL 2

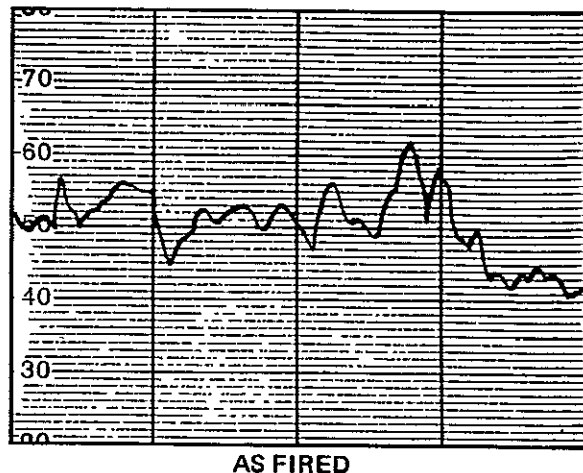
ALL HORIZONTAL SCALES 0.2 mm/div

Figure 2-6. Dektak Profilometer Traces of Surfaces of Vistal Polycrystalline Alumina Substrates at Three Stages of Preparation: (a) Vistal 1 (one firing at $>1800^{\circ}\text{C}$ for 6 hr); (b) Vistal 2 (two consecutive firings).



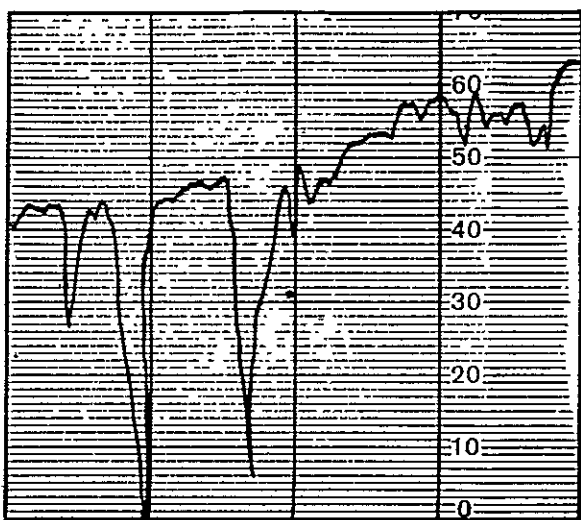
AS FIRED

VERT
SCALE
0.5 μm/div

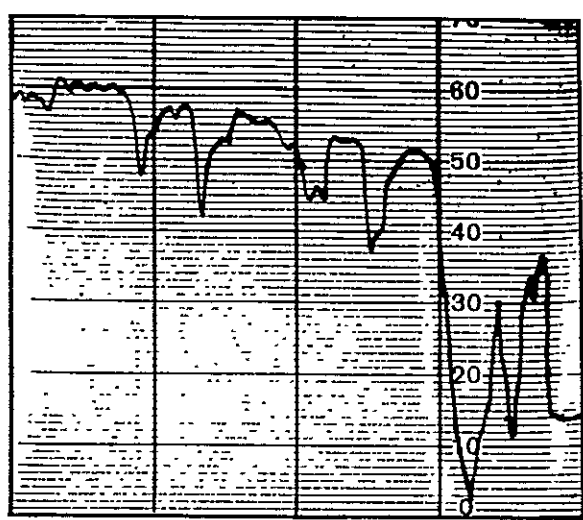


AS FIRED

VERT
SCALE
0.1 μm/div

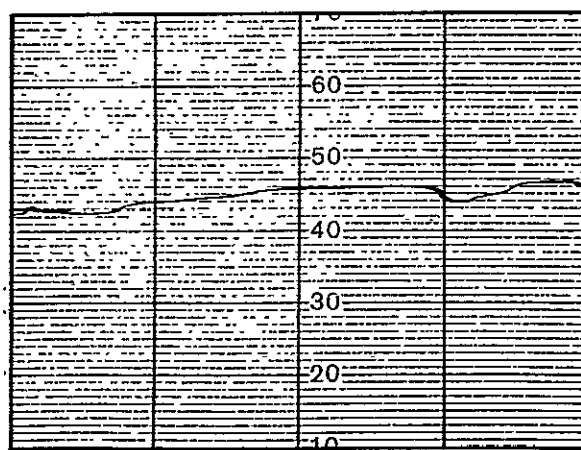


LAPPED



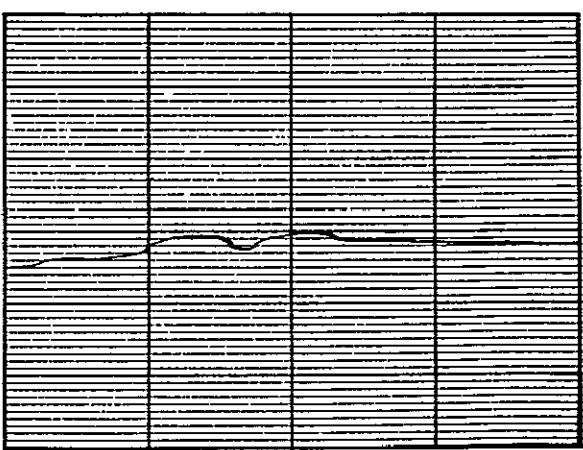
LAPPED

VERT
SCALE
0.1 μm/div



POLISHED

(a) VISTAL 3



POLISHED

(b) VISTAL 4

ALL HORIZONTAL SCALES 0.2 mm/div

Figure 2-7. Dektak Profilometer Traces of Surfaces of Vistal Polycrystalline Alumina Substrates at Three Stages of Preparation. (a) Vistal 3 (three consecutive firings at $>1800^{\circ}\text{C}$ for 6 hr); (b) Vistal 4 (four consecutive firings).

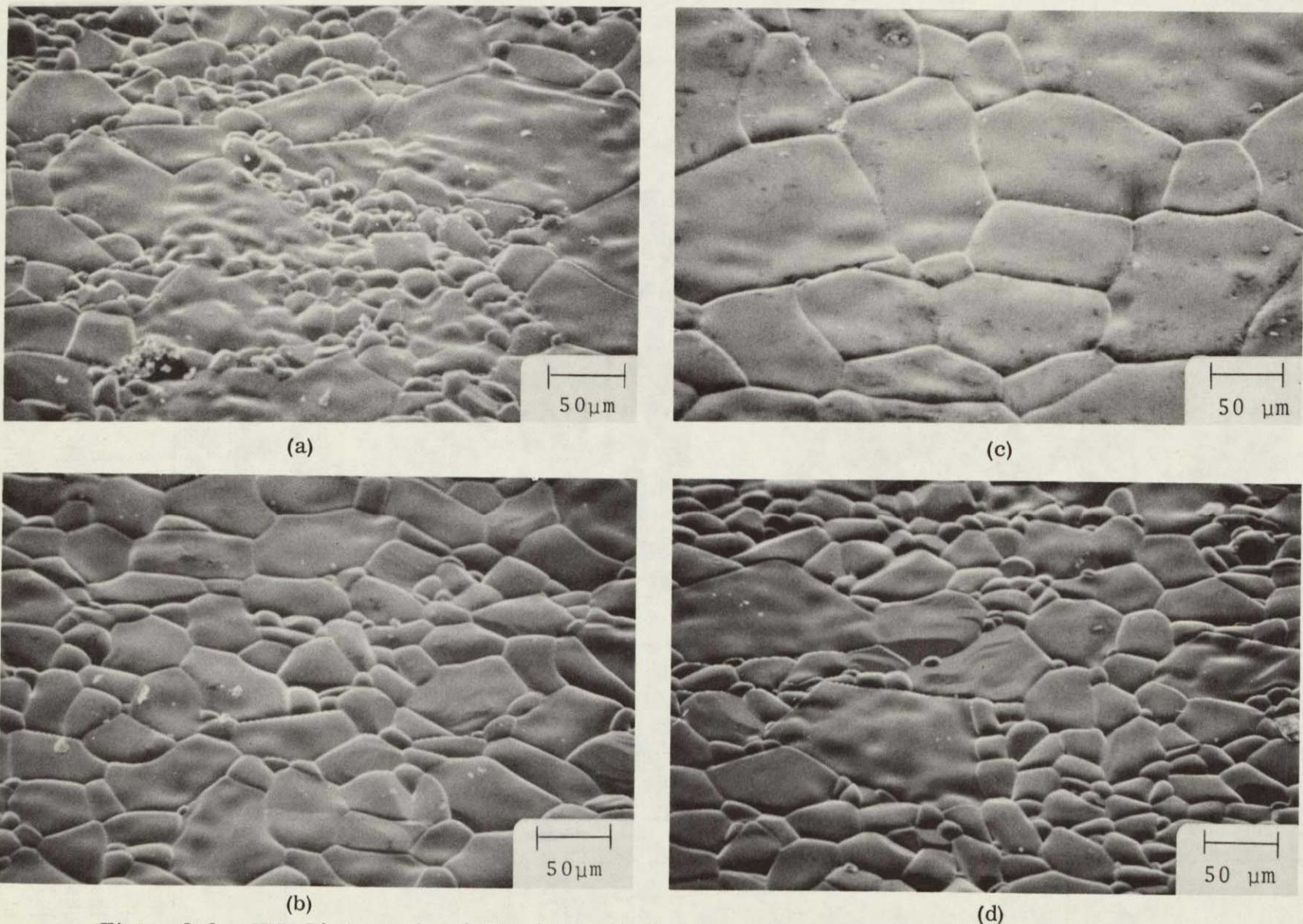
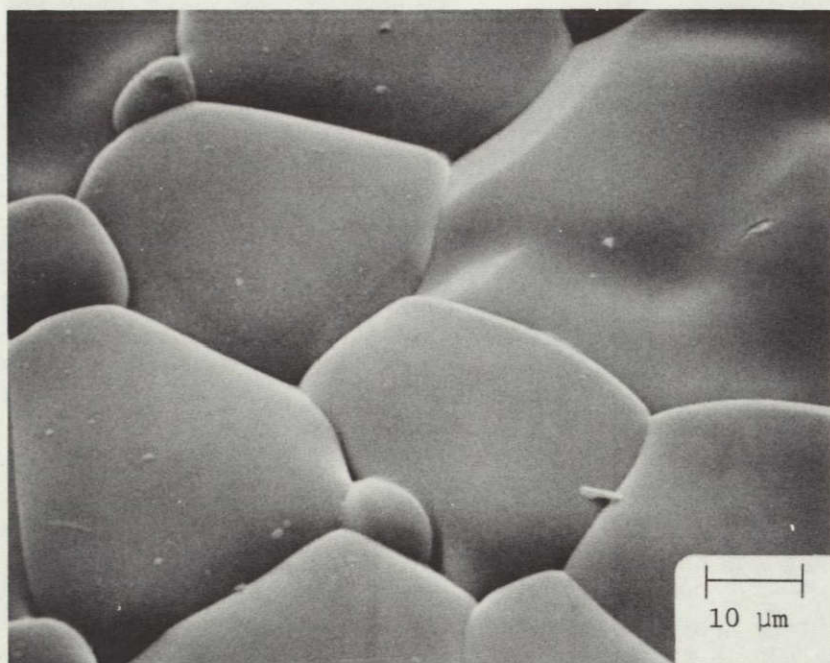
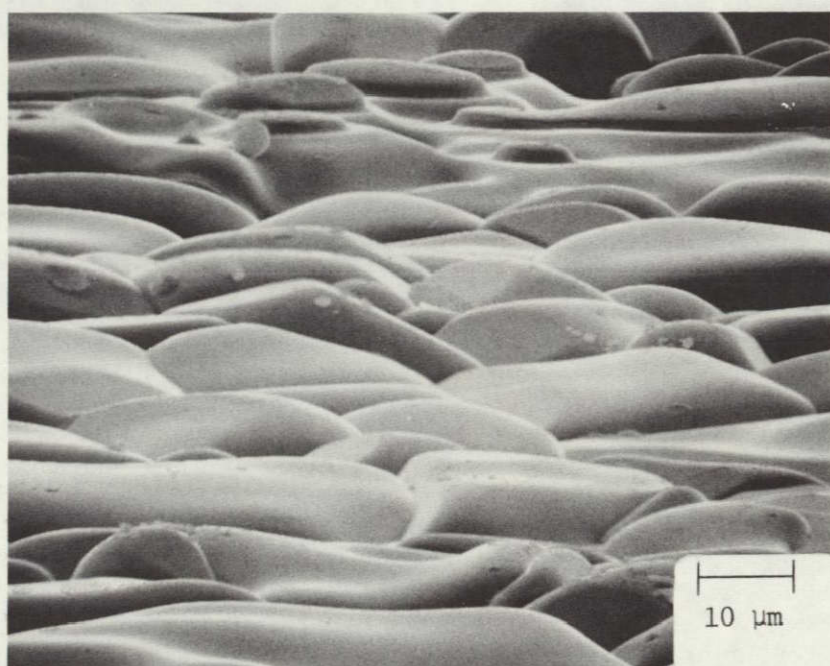


Figure 2-8. SEM Photographs of Vistal Alumina Substrates in As-fired Condition. (a) Vistal 1 (one firing at $>1800^{\circ}\text{C}$ for 6 hr); (b) Vistal 2 (two consecutive firings); (c) Vistal 3 (three consecutive firings); (d) Vistal 4 (four consecutive firings). (All photographs taken at 45 deg viewing angle with sample surface.)



(a)



(b)

Figure 2-9. SEM Photographs of Vistal 4 (four consecutive firings) Alumina Substrate Surface in As-fired Condition. (a) Viewing Angle 45 deg; (b) Viewing Angle 25 deg with Sample Surface.

The surfaces of polished Vistal substrates of each of the four groups are shown in the optical photomicrographs of Figure 2-10, made with the Nomarski interference-contrast objective on the microscope. These photographs show in strong relief the individual crystal grains in each of the four groups and illustrate clearly a progression in grain size from Vistal 1 to Vistal 4 (Figure 2-10a to 2-10d). The polished Vistal 4 substrate shows the largest average grain size and generally more uniform distribution of large grains.

Additional characteristics of the Vistal substrates are shown in the optical photomicrographs in Figures 2-11 and 2-12. The former shows the surface of a polished Vistal 2 (two consecutive firings) and the latter a polished Vistal 3 (three consecutive firings), in each case exactly the same region of the surface shown at the same magnification but with three different optical conditions. Some transmitted illumination through the substrate was used in order to show interior features. In (a) of each figure the substrate surface is in focus with the Nomarski interference-contrast objective set for maximum visibility of surface features. In (b) of each figure the color-contrast lever of the objective is shifted to use a different wavelength region of the illumination and thus bring out subsurface features, although the initial focus was not changed. Finally, in (c) of each figure the camera was focused on a plane just below the sample surface to delineate additional features. The procedure emphasizes the three-dimensional characteristics of even an optically-polished surface, and clearly illustrates the incidence of various voids and inclusions in this polycrystalline alumina material. (The other two Vistal groups exhibited similar characteristics.)

During the early stages of preparation of the polished substrates at Rockwell--specifically, during the lapping stage--it was noted that Vistal samples from the third and fourth groups appeared to have similar grain sizes, in terms of the areas between prominent grain boundaries and/or crevices in the lapped surfaces. In some regions the grains in the third group actually appeared larger. When polishing was completed, the photomicrographs of the surfaces of the polished Vistal substrates made with the Nomarski interference-contrast objective clearly delineated the apparent grain boundaries at the surface. At this stage, the examined sample of the fourth group appeared to contain larger individual grains than that of the third group (cf Figure 2-10). However, in the set of four as-fired substrates examined in the SEM, the Vistal 3 had larger grains than the Vistal 4 (Figures 2-8c, d).

Although the question is not yet completely resolved, representative substrates from the four groups were examined to determine an average grain size for each group, and the apparent individual grain sizes listed in Table 2-4 are believed to be representative.

If the average grain size in Vistal 3 is actually larger than that in Vistal 4, it would be an unexpected result and would suggest the possibility that the containers in which the substrates were supplied to Rockwell may have been improperly marked. This possibility is now being investigated. If this is not the explanation, then the details of the high-temperature firing cycles employed by Coors in preparing these substrates will be of major importance, since it would then appear that competing mechanisms are involved in the recrystallization process and an optimum firing procedure might be found.

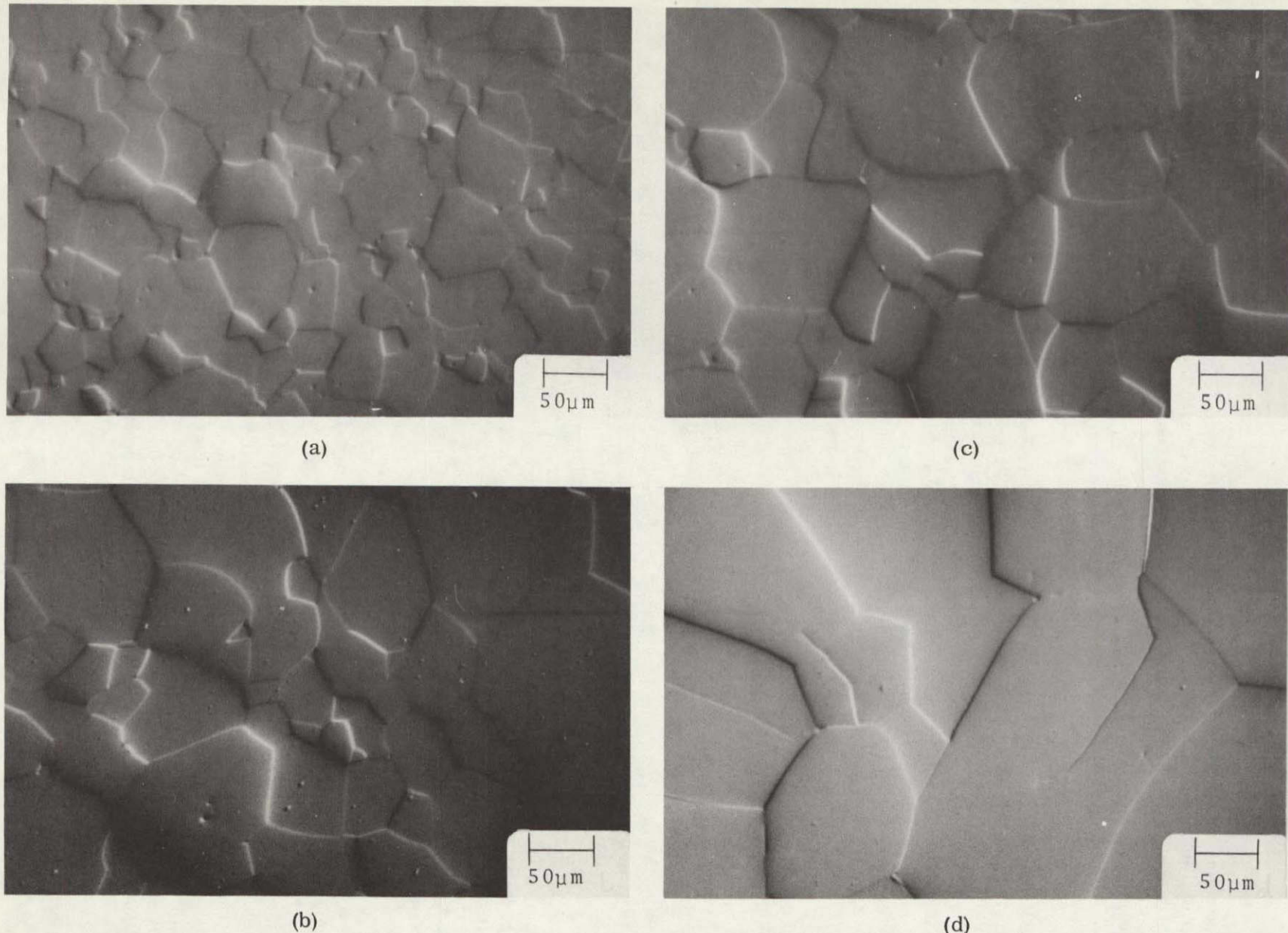


Figure 2-10. Nomarski Interference-contrast Photomicrographs of Surfaces of Polished Vistal Alumina Substrates of Four Different Firing Histories. (a) Vistal 1 (one firing at $>1800^{\circ}\text{C}$ for 6 hr); (b) Vistal 2 (two consecutive firings); (c) Vistal 3 (three consecutive firings); (d) Vistal 4 (four consecutive firings). (All photographs at normal incidence.)



(a)

(b)

(c)

Figure 2-11. Nomarski Interference-contrast Photomicrographs of Surface of Same Region of Vistal 2 (two consecutive firings at $>1800^{\circ}\text{C}$ for 6 hr) Polycrystalline Alumina Substrate under Different Optical Conditions. (a) Surface Focus, Optimized Color Contrast; (b) Surface Focus, Changed Wavelength; (c) Subsurface Focus.

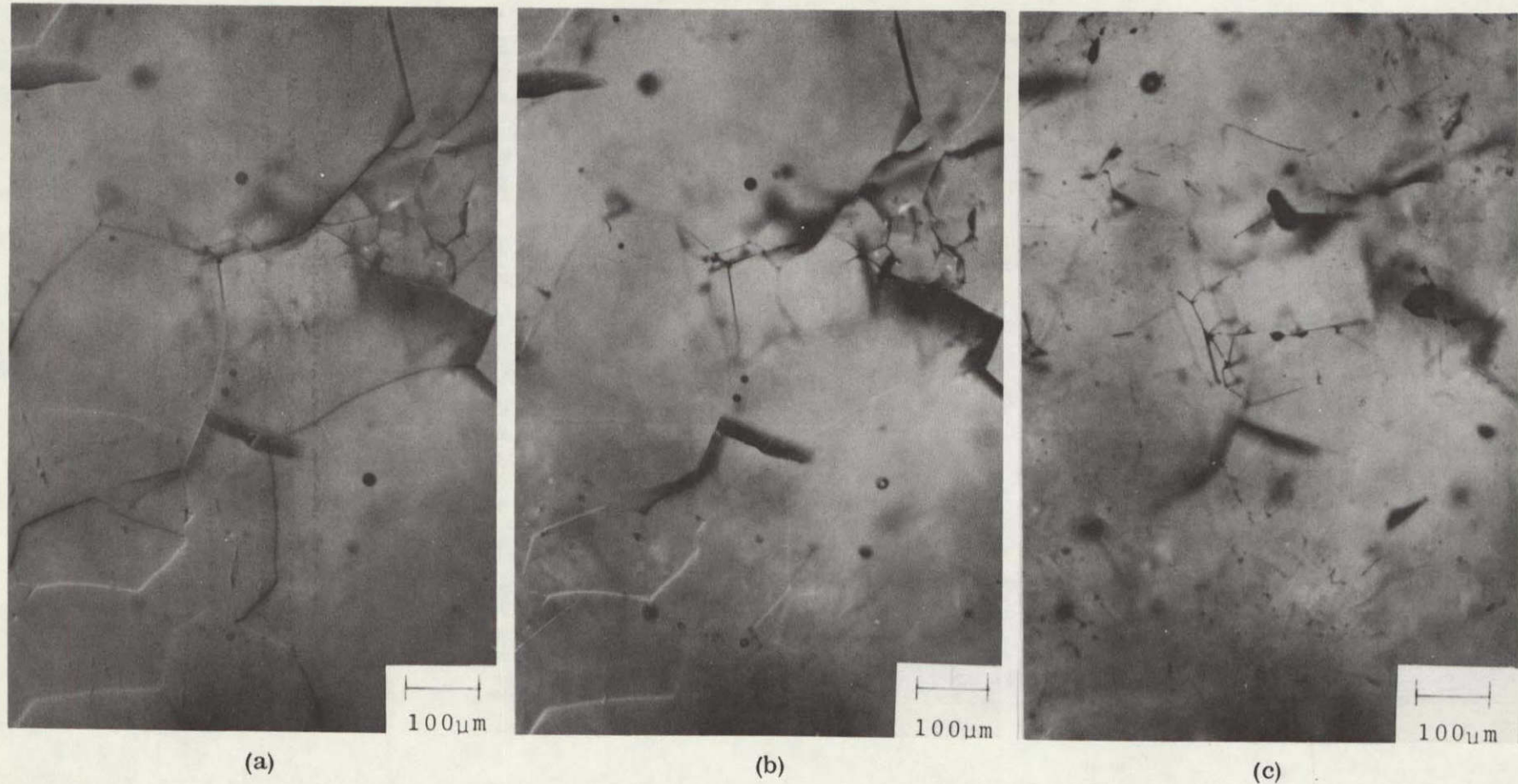


Figure 2-12. Nomarski Interference-contrast Photomicrographs of Surface of Same Region of Vistal 3 (three consecutive firings at $>1800^{\circ}\text{C}$ for 6 hr) Polycrystalline Alumina Substrate under Different Optical Conditions. (a) Surface Focus, Optimized Color Contrast; (b) Surface Focus, Changed Wavelength; (c) Subsurface Focus.

Table 2-4. Average Apparent Grain Size of Several Polycrystalline Alumina Substrate Materials as Measured on Sample Surface

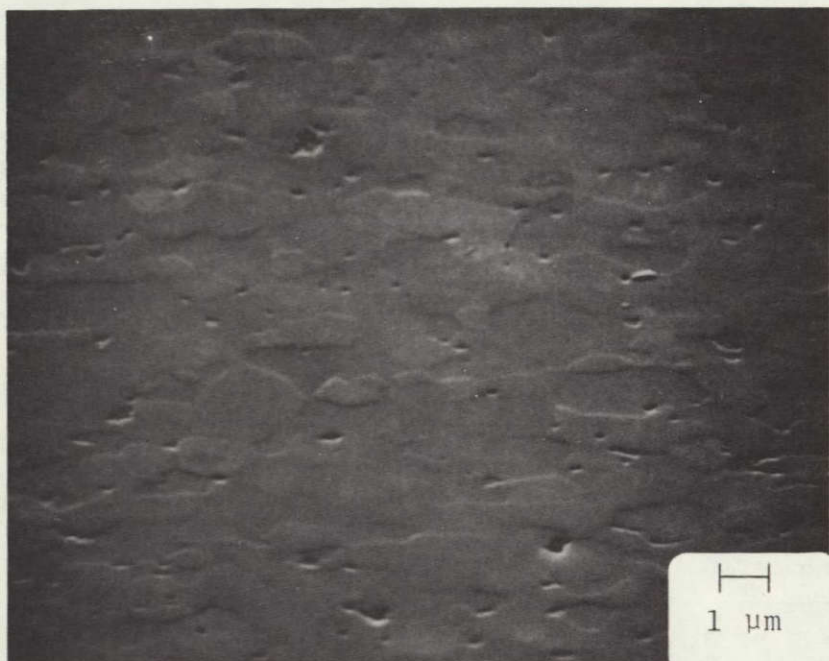
Substrate Material	Ave Grain Size at Surface of As-fired Material (μm)	Ave Grain Size at Surface of Polished Material (μm)
Vistal 1 (Coors)	20	35
Vistal 2 (Coors)	36	74
Vistal 3 (Coors)	80 - 100	70
Vistal 4 (Coors)	28	>120
Superstrate (MRC)	~ 0.8	~ 1.5

Superstrate is an alumina of 99.6 percent purity manufactured by Materials Research Corporation (MRC), and has been used in the as-fired condition in earlier Si CVD experiments in this program (see Quarterly Report No. 1). Samples of this material have also been polished during this quarter, and the results are indicated in the SEM photographs in Figure 2-13.

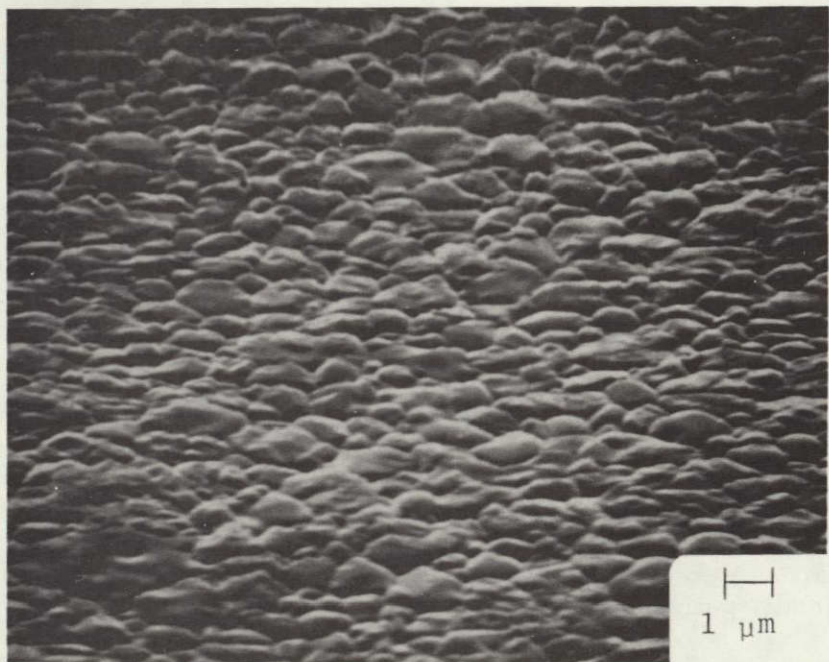
The surface of this material, both in the as-fired condition (Figure 2-13a) and in the polished condition (Figure 2-13b), is very different from that of the Vistal alumina. First, the apparent average grain size is considerably smaller than that of Vistal 1 (the smallest-grained of the Vistal series), averaging about $1 \mu\text{m}$. Second, the Superstrate exhibits numerous grain boundary voids that show up especially in the polished surface (Figure 2-13b). Apart from the grain size itself, the presence of such voids could make it difficult to achieve adequate cleaning (and drying) of these substrates prior to use in deposition experiments. The average value for grain size in this material also is given in Table 2-4.

Relatively thin samples of zircon ($\text{ZrO}_2 \cdot \text{SiO}_2$) were received from two manufacturers late in the quarter, for possible use as substrates for Si films. These materials--ASM475 from 3M and Z360 from Kyocera--are listed in Table 2-2. The ASM475 zircon was found by profilometry to have an average peak-to-valley surface roughness of $4 \mu\text{m}$ (see Table 2-3); the Z360 has not yet been characterized. As mentioned above, these two materials are among the polycrystalline ceramics now being mechanically polished for use as substrates in forthcoming experiments.

A preliminary evaluation of these materials as possible substrates was accomplished by using them in a Si CVD experiment involving parameters known to be satisfactory for deposition of Si on the polycrystalline aluminas that have been used to date. The zircon wafers were used with only chemical cleaning and a H_2 etch at 1250°C in the reactor prior to Si deposition. The results of the CVD experiment are described under Task 3, in Section 2.3.1.2.



(a)



(b)

Figure 2-13. SEM Photographs of Surface of MRC Superstrate Polycrystalline Alumina Substrate, Viewed at 30 deg Angle with Sample Surface. (a) As-fired; (b) Polished.

Finally, just before the end of the quarter, experiments were begun to investigate the effects of thin metal layers on the growth and properties of the CVD Si films. Initial experiments involve metal layers previously deposited by sputtering techniques on substrates of several different glasses. Because of its almost negligible solubility in Si at temperatures used for Si CVD on glasses, Ti metal is being used first. Results will be discussed in a later report.

Based on the data obtained to date for films grown by conventional Si CVD growth techniques on the materials supplied for this program (see Tasks 3 and 5), the most promising substrates are the Corning Code 1715 glass and the large-grained Vistal aluminas from Coors. Requests have been made to Corning and Coors for additional substrates of these and other similar materials considered important to the continuing experiments planned for this program.

2.3 TASK 3. EXPERIMENTAL INVESTIGATION OF Si CVD PROCESS PARAMETERS

Si deposition experiments performed in the period prior to the contract start date indicated that some of the substrates received from various glass and ceramic manufacturers were reactive in a H₂ atmosphere at the high growth temperatures used--up to 950°C for a special high-temperature glass supplied by Owens-Illinois and ~850°C for a glazed alumina (ASM743) obtained from 3M. Major contamination was in evidence in films grown on companion pieces of single-crystal sapphire used as control wafers in those experiments. The use of an inert carrier gas such as He was thus regarded as necessary for studying Si growth phenomena on substrate materials reactive to H₂.

During the first quarter a variety of CVD experiments was carried out to establish baseline performance data for the reactor system, including temperature distributions on the sample pedestal, effects of carrier gas flow rate on temperature, effects of carrier gas flow rate on film thickness uniformity in H₂ and in He (with H₂ producing more uniform results), and Si film growth rates by SiH₄ pyrolysis as a function of temperature for H₂ and for He. An activation energy for the deposition process in the temperature range up to 850-900°C of ~1.8 eV was found for either carrier gas. Above that temperature range the growth rate was found still to increase with temperature in H₂ but with a much lower activation energy (~0.14 eV). For He the rate passes through a maximum at 850-900°C, decreasing rapidly for further increases in temperature, indicating a difference in the deposition process at high temperature (>850°C) in the two gases.

The observed difference in Si deposition rate by SiH₄ pyrolysis at temperatures above 850-900°C in H₂ and in He tends to discourage the use of He at higher temperatures because of the increased time required to obtain a given Si film thickness. Further, the film thickness uniformity across the pedestal was observed to be much better for Si deposited in H₂ than in He, particularly at higher temperatures. In addition, generally better looking Si films have been achieved--on substrates other than glasses--by deposition in H₂ than in He; the latter has been found to be the preferred carrier gas for Si deposition on glasses.

At the end of the first quarter the status of the work of this task was such that the following activities were proposed for the second quarter:

1. Continue experiments to identify preferred CVD parameters as well as candidate substrate materials for Si film growth
2. Continue experiments with two-step deposition process on selected substrate materials
3. Pursue investigation of effects of doping impurities on Si film growth phenomena and on Si film properties
4. Initiate study of the effects of in situ and post-growth annealing on final properties of the Si film.

When the extensive CVD reactor system modifications were completed and the system tested early in the second quarter, CVD experiments were resumed in the above areas.

2.3.1 Si CVD on Selected Substrates

Experiments to identify suitable CVD parameters for Si deposition on several substrate materials either not yet tested or previously tested and found promising have been carried out during the quarter. These are described in the following sections.

2.3.1.1 Experiments with Glass Substrates

A series of Si deposition experiments was undertaken to evaluate Corning Code 1715 glass and two proprietary glasses from Owens-Illinois (OI); GS211 and GS213. The properties of these three glasses are summarized in Table 2-5. Most of the studies to date have been with Corning Code 1715, which is especially interesting because of the close match between its TEC and that of Si (see Figure 2-5).

Table 2-5. Properties of Selected Glasses Used as Substrates for Si CVD Sheet Growth

Glass Identification	Type of Glass	Thermal Expansion Coeff. (10 ⁻⁶ per deg C)	Strain Point (°C)	Annealing Point (°C)	Softening Point (°C)
Corning 1715	Calcium alumino-silicate	~3.5**	834	866	1060
OI*GS211	Proprietary	~3.6(0-300°C)	-	-	1075
OI*GS213	Proprietary	~2.6(0-300°C)	-	-	1135

*Owens-Illinois

**See Figure 2-5

All three substrates failed the SiH₄-in-H₂ growth tests at ~850°C, evidenced by whisker type growth on the substrate surfaces and/or major contamination of the Si film grown on the companion sapphire substrate. As an example, Figure 2-14 is an SEM photograph of the surface of the Si deposit grown on glass GS211 at ~850°C in H₂ (4 lpm flow rate), with a SiH₄ flow rate of 25 ccpm. In addition to the obviously defective deposit on the glass, the Si growth on the neighboring sapphire was seriously damaged by some contaminant, presumably resulting from the glass reaction with the CVD environment.

However, in a SiH₄-in-He environment at about the same temperature the Si films deposited on the three glasses appeared to be quite normal; contamination of the companion sapphire substrate did not appear to occur in any of the three cases.

A series of Si deposition experiments was subsequently carried out in He with Corning Code 1715 glass over a temperature range from ~860 to ~1000°C. The He flow rate was 6 lpm and the SiH₄ flow rate 25 ccpm in each of the experiments. The Si film grew at a rate of ~0.6 μm/min to a thickness of ~6 μm in the experiment at ~860°C; ~1.4 μm/min to a thickness of ~14 μm at 914°C; ~1.0 μm/min to a thickness of ~16 μm at 955°C; and ~1.0 μm/min to a thickness of ~20 μm at 1000°C.

The films grown at the three higher temperatures each had a dull finish at the conclusion of the experiment. The film surface was heavily textured on all four samples, but the nature of the surface features was quite different in the four cases,

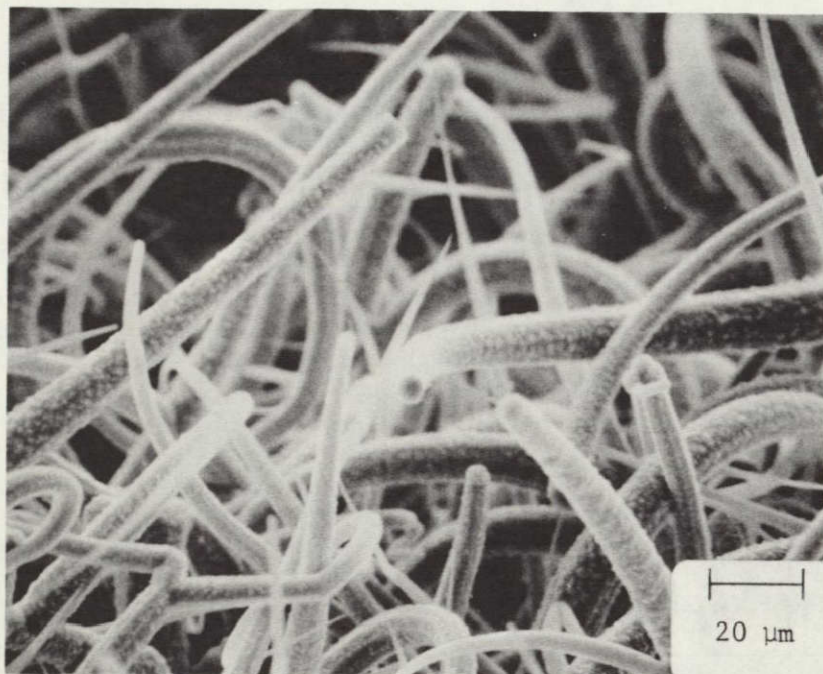


Figure 2-14. SEM Photograph of CVD Si Deposit on OI Glass GS211 at $\sim 850^{\circ}\text{C}$ in H_2 Atmosphere

as shown by optical microscope and SEM examination. The SEM photographs, obtained as part of the Task 5 activities, show a film surface with well-ordered crystallographically-faceted features producing good reflectivity at certain viewing angles to the normal for the $6 \mu\text{m}$ deposit prepared at a low growth rate at $\sim 860^{\circ}\text{C}$ (see Figure 2-22, Task 5). The surface texture in this case bears a resemblance to those observed on Si films grown on some of the relatively fine-grained polycrystalline aluminas.

As the deposition temperature was increased, the surface texture of the deposited film was observed to change toward a coarser, more three-dimensional appearance, with numerous bulbous projections. The Si film deposited on Corning Code 1715 glass at 1000°C , for example, grew at almost a 50 percent faster growth rate than the one grown at $\sim 860^{\circ}\text{C}$ and was $\sim 20 \mu\text{m}$ thick, rather than $\sim 6 \mu\text{m}$. SEM examination showed a much different surface texture, with little obvious faceting on the relatively tall surface features (see Figure 2-23), which accounts for the dull appearance of this film. These films are further described under Task 5 (see Section 2.5.1).

The films deposited on glass at the three higher temperatures in He may have been formed by a somewhat different growth mechanism than the one deposited at $\sim 860^{\circ}\text{C}$, related to the presence of a maximum in the growth rate vs temperature curve for Si deposition by SiH_4 pyrolysis in He (Figure 2-15 in Quarterly Report No. 1). This possibility will be considered further in interpreting the results of additional experiments with Si deposition on this glass using other CVD parameters.

Further evidence of systematic structural differences as a function of growth temperature in the films deposited on Corning Code 1715 glass in this temperature range is provided by x-ray diffraction analyses of these samples. These measurements

are discussed in more detail under Task 5. The structural changes observed could be consistent with a change in the dominant layer growth mechanism in this temperature range, as mentioned above.

The experiments with Si deposition on Owens-Illinois glasses GS211 and GS213 were done in He carrier gas (6 lpm) with a SiH₄ flow rate of 25 ccpm. The film on GS211 was deposited at ~850°C at a rate of ~1.7 μm/min to a thickness of ~35 μm, while that on GS213 was deposited at 860°C at a rate of ~2 μm/min to a thickness of ~50 μm. In both cases deeply textured surfaces resulted on the Si deposit, producing a very dull appearing finish.

SEM examination of the film on GS211 indicated somewhat irregular pyramidal growth features, averaging about 4 μm across with moderate faceting (see Figure 2-24b, Task 5). There were also what appeared to be large clusters or "chunks" of Si distributed about the surface, indicating a less orderly growth process than was observed at the same deposition temperature on Corning Code 1715 glass.

Electrical measurements on the undoped Si film on GS211 glass, reported along with the results of measurements on the Si-on-1715 samples in the Task 5 discussion, indicate a much higher conductivity than for the other (undoped) Si-on-glass films. A higher p-type carrier concentration ($\geq 10^{15} \text{ cm}^{-3}$) is also indicative of a high density of imperfections of some type - possibly some impurity from the glass.

Analyses of the Si film deposited on GS213 glass were not completed prior to preparation of this report. However, studies with these and other similar glasses will be continued to determine their suitability as substrate materials for this program. Thicker Si films doped to appropriate impurity levels will be prepared on these glasses in the coming quarter, to permit subsequent fabrication of solar cell structures under the Task 6 work at OCLL.

A single growth experiment was done with a glazed nickel-steel supplied by Chi-Vit Corp. (Chicago, IL). The coating is an alkaline-earth aluminosilicate glass. In order to avoid contamination of the SiC-covered carbon pedestal used in the experiments with the aluminas, a pedestal of old vintage was used in direct contact with the steel base. During the heating of the pedestal and substrate, however, a part of the SiC layer separated from the carbon pedestal and sprayed the substrate with debris. Rather than abort the experiment, a Si film was grown on the glaze at ~850°C in a He atmosphere in spite of the contamination. Adherence of the film to the glaze was observed, and further experiments with this composite substrate are therefore planned.

2.3.1.2 Experiments with Alumina and Zircon Substrates

Si sheet growth experiments with polycrystalline alumina substrates during the second quarter involved the following materials: 1) ASM805 (3M), standard-fired and refired; 2) Vistal 4 (Coors), polished and as-fired; 3) Vistal 3 (Coors), polished and as-fired; 4) Vistal 2 (Coors), polished and as-fired; 5) Vistal 1 (Coors), polished and as-fired; and 6) Superstrate (MRC), polished and as-fired. In addition, two different zircon substrates — ASM475 from 3M and Z360 from Kyocera—were used in the as-manufactured condition in one deposition experiment. Most of these materials have been characterized as to surface roughness, preferred crystallographic orientation, size and shape of surface features, average internal grain size, and stability in H₂ and in He atmospheres, in addition to the properties known from information supplied by the manufacturers.

Because of the very large crystal grains in the Vistal substrates, major interest centered on deposition experiments with those materials in both the as-fired and the mechanically polished condition. As indicated earlier in the Task 2 discussion, simultaneous deposition on polished and as-fired substrates should not only allow establishing correlations between substrate preferred orientations and the observed Si film growth habit but also establish the effects on the topography of the upper Si film surface of growth on a smooth polished polycrystalline surface as opposed to a rough faceted polycrystalline surface. The added variant of having four different substrate grain sizes for the Vistal alumina should also provide further valuable information about the Si growth habit.

The large α -alumina grains of the Vistal substrates (Figures 2-8, 2-9, 2-10)—both polished and as-fired—provide individual "single crystals of sapphire" for the growth of Si deposited by the pyrolysis of SiH₄. For the as-fired substrates these individual sapphire grains have exposed facets—presumably natural crystallographic planes—that serve as the growth surfaces for the deposited Si. The spatial (not crystallographic) orientation of these facets with respect to the plane of the nominal substrate surface will be largely a consequence of the process used to form the ceramic and of any subsequent firing (annealing) procedure. Whether some of these partially-randomly oriented growth surfaces will be crystallographic planes of α -alumina that are favorable to epitaxial growth of CVD Si is a matter of chance.

For the case of the polished substrates, the surface generated by the mechanical polishing process will intersect all individual α -alumina single-crystal grains lying in the surface of the substrate wafer. The plane so defined in each surface grain will have a definite crystallographic orientation in that individual α -alumina crystal; whether some of those arbitrarily-defined (by the polishing process) crystal planes will happen to be planes of sapphire that are favorable to the epitaxial growth of CVD Si is again a matter of chance, and is influenced by the spatial orientation of the surface crystals resulting from the ceramic forming process and any subsequent firing. The main distinction in the case of the polished substrate is that the polished surface can be correlated with crystallographic planes found to be preferred orientations in the polycrystalline ceramic material.

The deposition experiments with the Vistal aluminas were all done at a temperature of $\sim 1025^{\circ}\text{C}$. This temperature was selected to be favorable to epitaxial growth of Si on α -alumina while keeping any autodoping effects to a minimum. H_2 was the carrier gas (4 lpm) and the SiH_4 flow rate was 25 CCPM. In each case, the substrates were exposed to a 15 min predeposition treatment in H_2 (4 l pm) at 1250°C . A growth rate of $3.0 \mu\text{m}/\text{min}$ was used.

The Si films grown in these experiments exhibited discrete regions of high reflectivity as viewed by the unaided eye, for both the polished and the as-fired samples. Closer inspection indicated that epitaxial (i.e., single-crystal) Si growth had undoubtedly occurred on many of the large individual crystal grains. Those which were oriented properly to control the growth of single-crystal Si produced the highly reflective grains or islands in a sea of otherwise polycrystalline-appearing smaller grains.

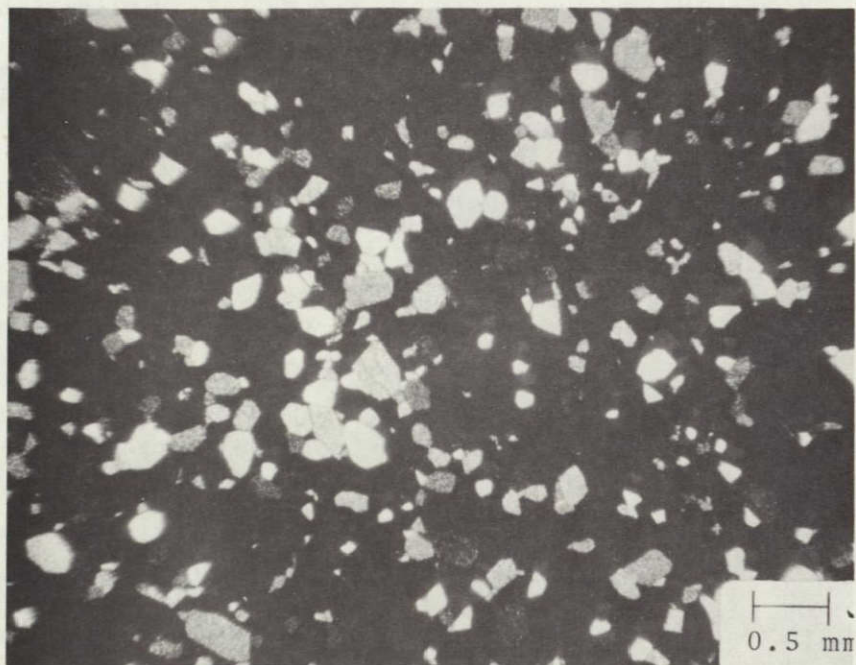
The large grains with Si deposits that were non-reflective either are exposed single-crystal Si with non-reflecting planes or non-single-crystal Si which was formed because the deposition conditions (probably temperature) were not consistent with single-crystal growth on that orientation of α -alumina (Al_2O_3). For example, single-crystal Si growth on $(11\bar{2}0)$ Al_2O_3 is better at $1075-1100^{\circ}\text{C}$; on (0001) Al_2O_3 , at 1200°C ; on $(01\bar{1}2)\text{Al}_2\text{O}_3$, at $1025-1100^{\circ}\text{C}$, in the type of reactor used here.

Optical photomicrographs of a Si film $18 \mu\text{m}$ thick deposited on a polished Vistal 4 substrate are shown in Figure 2-15. They show the highly reflective epitaxial regions immersed in less favorably oriented Si, as discussed above. Figure 2-15a is at low magnification, to give an indication of the fraction of the total area of Si that consists of growth that is epitaxial or at least highly oriented. Figure 2-15b shows the cluster of islands seen near the center of Figure 2-15a but at higher magnification, to illustrate the variety of oriented Si growth found in this film.

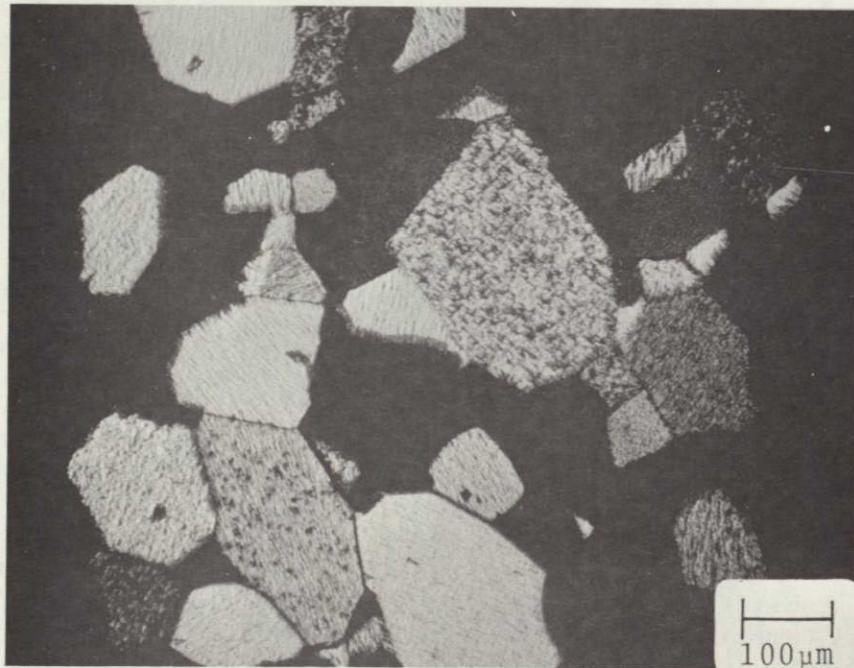
SEM photographs of the same film deposited on polished Vistal 4 are shown in Figure 2-16. Figure 2-16a shows a region of the film surface at relatively low magnification. Several very large grains are visible in the field, although most of the film surface appears fine-grained. The large grain in the center is nearly $200 \mu\text{m}$ long in its largest dimension. Figure 2-16b shows at higher magnification the intersection of that grain with another more obviously epitaxial grain. The film appears to replicate the large grain structure of the substrate, although the surface boundaries between grains—except for the prominent epitaxial grains—are subtle and difficult to detect in these figures.

The surface of the Si film grown simultaneously on an as-fired Vistal 4 substrate is shown in the SEM photographs in Figure 2-17, both of which were made at normal incidence. The film again appears to replicate the grain boundary structure of the substrate; this is more readily visible in the case of the unpolished substrate involved here. Some very large grains are evident in this film, as in the film on the polished substrate. However, many of the areas outlined by what appear to be grain boundaries propagated through the film from the substrate are merely regions of relatively fine-grained polycrystalline Si growth such as has been seen on other alumina substrates. This is evident in Figure 2-17b, which shows a region that appears to be epitaxial and other areas exhibiting typical polycrystalline surface features.

The results obtained with the other three groups of Vistal substrates—both polished and as-fired—were similar to those described above for Vistal 4, but with correspondingly different grain sizes.



(a)

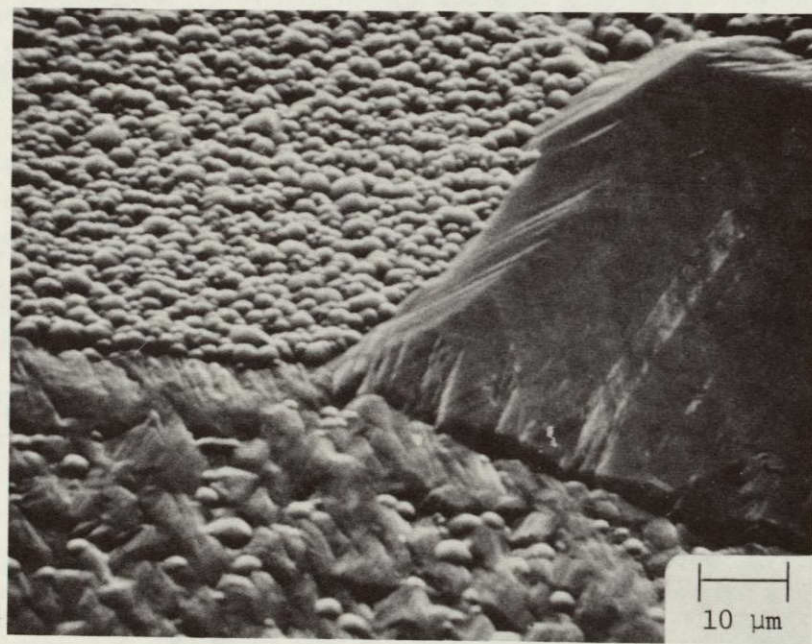


(b)

Figure 2-15. Optical Photomicrographs of CVD Si Film on Polished Vistal 4 Polycrystalline Alumina Substrate, at Two Different Magnifications



(a)

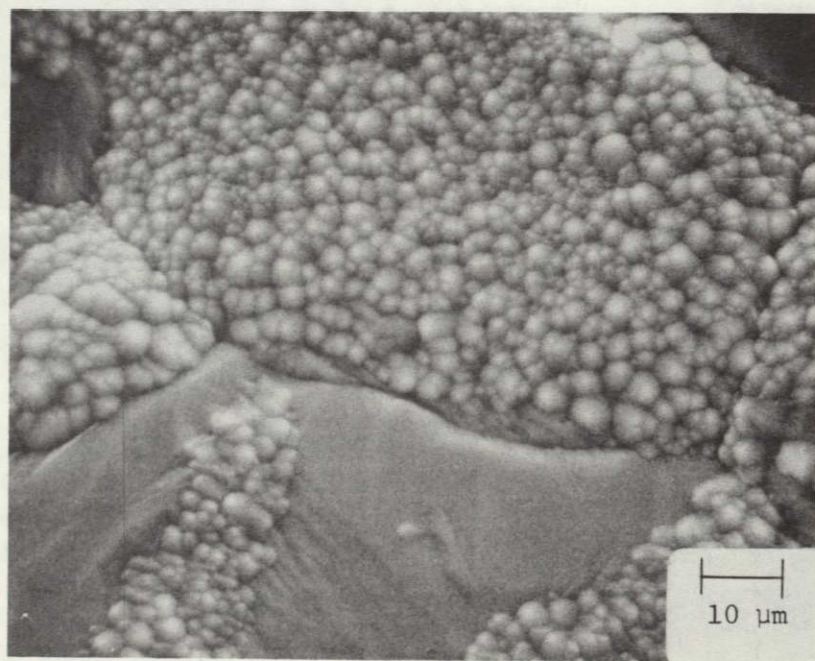


(b)

Figure 2-16. SEM Photographs of CVD Si Film of Figure 2-15, at Two Different Magnifications. (Viewing angle 45 deg with sample surface)



(a)



(b)

Figure 2-17. SEM Photographs of CVD Si Film on As-fired Vistal 4 Polycrystalline Alumina Substrate, at Two Different Magnifications.
(Viewing at normal incidence.)

The surface roughness of the Si deposits on the Vistals was found to be considerably better on the films grown on the polished surfaces than on the unpolished surfaces. Dektak profilometer traces, shown in Figure 2-18, reveal at least a factor of 5 improvement in surface roughness for these 18 μm -thick films.

Two Si CVD experiments using established procedures were performed early in the quarter with ASM805 alumina substrates to compare as-fired with refired material supplied by the 3M Co. The first films were grown on substrates which were cleaned only with organic solvents and H_2O rinses; the films were covered with growth whiskers, consistent with the presence of some surface contamination. Another film grown on a refired alumina substrate which was acid-cleaned was found to be essentially free of whiskers, but the growth on the sapphire companion wafer appeared partially contaminated, indicating either the purity of the refired alumina was adversely affected by the firing process or the technique used in preparing the refired material for deposition needed improvement.

It was subsequently determined that there may have been an impurity contamination introduced into the alumina during the refiring process by the manufacturer. The refired substrates were stacked in a furnace with a support and cover of lower purity than the ASM805, and contamination could have occurred from the support and/or cover. Although the refired ASM805 appeared to contain larger grain sizes (as shown in Figure 2-11, Quarterly Report No. 1), the average appearance of the Si overgrowth on the refired surface resembled that of films grown on the as-fired ASM805 (cf Figure 2-19b, Quarterly Report No. 1, with Figure 2-25a, of this report).

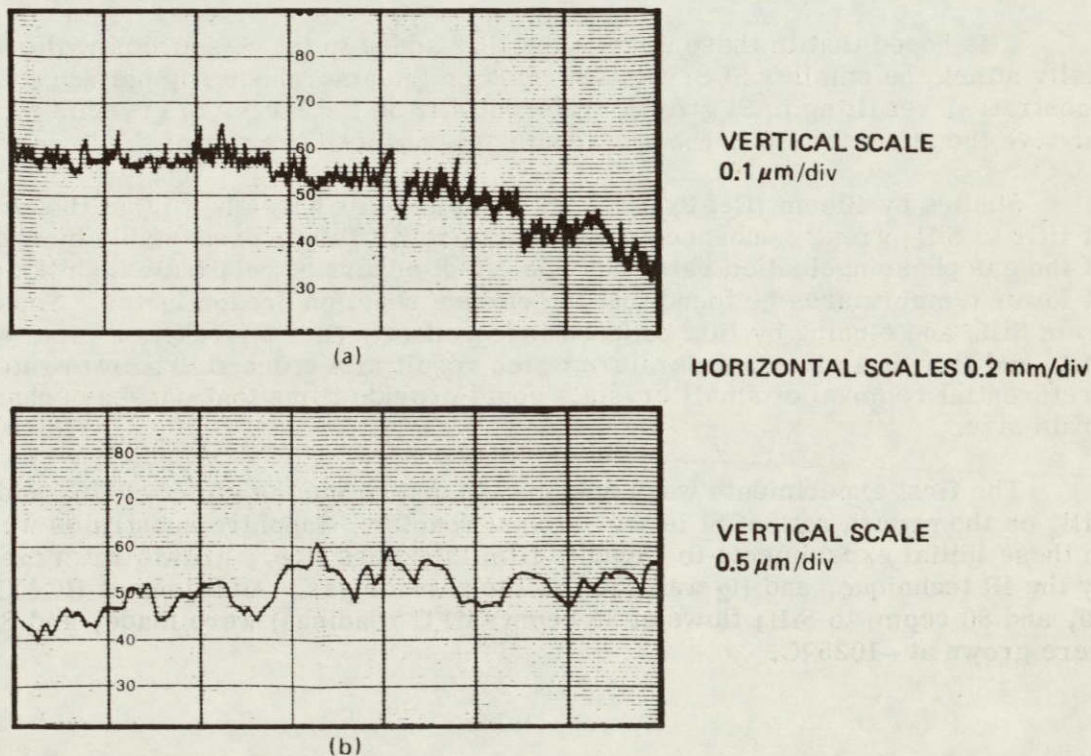


Figure 2-18. Dektak Profilometer Traces of Surfaces of CVD Si Films Deposited by SiH_4 Pyrolysis on (a) Polished Vistal 4 (four consecutive firings at $>1800^\circ\text{C}$ for 6 hr) and (b) As-fired Vistal 4. (Horizontal scale 0.2 mm/div)

Undoped and doped films were also grown on as-fired and polished MRC Superstrate alumina under growth conditions previously found favorable for the high-purity aluminas: ~1025°C in H₂ at growth rates of ~1.3 and ~3.5 μm/min. The results are discussed in Section 2.5.2.

The receipt of relatively thin zircon substrates from 3M (ASM475) and Kyocera (Z360) toward the end of this quarter (see Section 2.2.2.2) prompted as a first test an evaluation of these materials for film growth under conditions found sufficient for growth of Si on the aluminas. The substrates were solvent- and acid-cleaned and subjected to a H₂ etch at 1250°C before film deposition at 1025°C. The whisker-like growth shown in the SEM photograph of Figure 2-19 indicates that zircon is not as hardy as alumina toward this type of processing. Further studies with zircon are planned during the next quarter, when polished zircon substrates will be available for direct comparative growth studies with the unpolished, as-manufactured material.

2.3.2 Experiments Involving SiH₄-HCl Mixtures

An investigation was begun to determine if SiH₄-HCl mixtures could be used to enhance grain growth in polycrystalline Si films grown on low-cost substrates. Previous studies at Rockwell demonstrated that by adding HCl to SiCl₄ it was possible to encapsulate an amorphous SiO₂ region between two patches of bare Si with a highly twinned Si deposit, x-ray diffraction examination of which gave no evidence of polycrystalline structure (Ref 1). The HCl added was largely responsible for inhibiting the growth of Si directly on the oxide layer while, at the same time, the Si growth extended from the two bare Si regions and joined to form a "bridge" over the SiO₂.

It is hoped that in these studies the HCl added to the Si sources will preferentially attack the smaller Si crystals formed on the amorphous and polycrystalline substrates, resulting in Si growth preferentially on the larger Si crystals which survive the attack by HCl, thereby leading to enhanced grain growth.

Studies by Bloem (Ref 2) in a horizontal reactor have shown that the addition of HCl to SiH₄ greatly enhances epitaxial Si growth rates, presumably by reduction of the gas phase nucleation rate, but this effect occurs at relatively high temperatures; at lower temperatures he found that the etching reaction predominates. Since growth from SiH₄ and etching by HCl proceed independently (Ref 2), reactant mixtures of SiH₄ and HCl at a given temperature which result in a reduced Si growth rate and preferential removal of small crystals could provide films that possess enhanced grain size.

The first experiments were designed to determine the effect of HCl additions to SiH₄ on the growth rate of Si in the vertical reactor. Sapphire substrates were used in these initial experiments to expedite film thickness (i.e., growth rate) measurements by the IR technique, and H₂ was used as the carrier gas. Additions of HCl (10, 20, 40, and 80 CCPM) to SiH₄ flows of 25 CCPM (MFC readings) were made, and Si films were grown at ~1025°C.

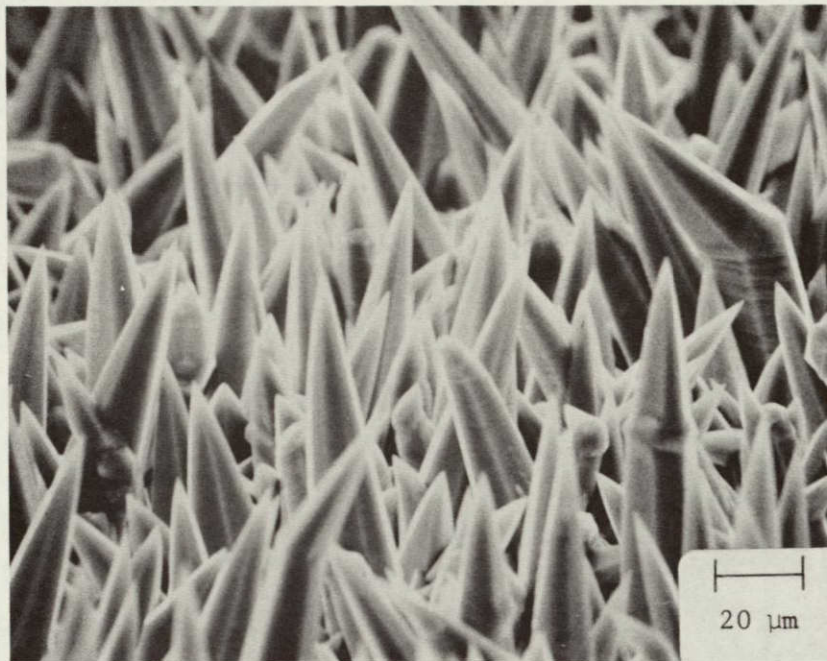


Figure 2-19. SEM Photograph of Whisker-like Deposit of Si on Zircon.
Growth by SiH₄ Pyrolysis at 1025°C in H₂ Atmosphere.

At the first HCl flow rate of 10 CCPM a slight increase in growth rate was observed, but with progressive additions of HCl the growth rate gradually decreased. At a flow of 80 CCPM of HCl, the Si growth rate was only 43 percent of its original value. But then it was noted that the SiH₄ readings on the MFC readouts were not consistent with the readings from run-to-run on the glass rotameters in series with the MFC calibrated in SiH₄. Several deposits with MFC readouts at the same number (25 CCPM) indicated quite large growth rate variations (as great as 1 μm/min); subsequent experiments on glass and alumina substrates had to rely on rotameter readings rather than MFC readings. When the SiH₄ MFC was disassembled, a white coating (presumably SiO₂) was observed, indicative of air and/or moisture contamination of the SiH₄. As indicated in Section 2.1, a valve was added to the deposition apparatus to separate the MFC from the rotameter and to isolate it from the rest of the system.

When these and other apparatus problems were corrected, the set of HCl-in-SiH₄ experiments was repeated. From Figure 2-20 it can be seen that an increased growth rate at 10 CCPM HCl flow was not observed, and that on the average the Si growth rate decreased more gradually with HCl additions than was previously observed. Additional experiments at higher HCl-to-SiH₄ concentration ratios are planned for the next quarter.

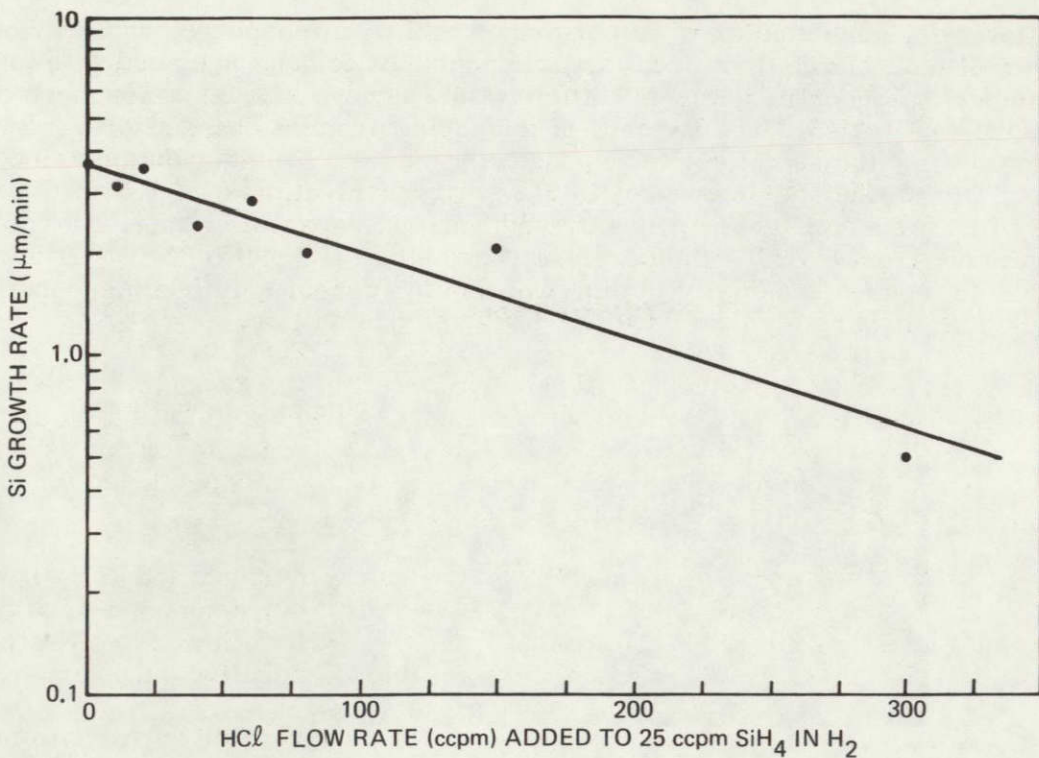


Figure 2-20. Changes in Si Growth Rate at 1025°C Caused by Additions of HCl to SiH₄

2.3.3 Studies of Effects of B Doping Using B₂H₆ Source

Si layers grown by CVD can be readily doped during growth by introduction of an appropriate compound containing the doping impurity into the carrier gas stream along with the Si compound being used. In some ways the method is almost ideal for producing either n- or p-type Si sheet on a substrate, since the dopant gases are homogeneously mixed with the Si compound external to the reactor and prior to film deposition. Such n-type sources as AsH₃ and PH₃ and the p-type source B₂H₆ have been almost universally applied for doping epitaxial Si films.

However, the crystallographic properties of polycrystalline films grown in different atmospheres and under different growth conditions can be expected to vary considerably with the dopant source and to affect the electrical properties of the films. For example, it has been reported that B atoms enhance the growth rate and the grain size of polycrystalline Si films, especially at higher concentrations ($>10^{18} \text{ cm}^{-3}$), whereas As tends to have the reverse effect. This favors the growth of p-type Si films for the thicker base region of a solar-cell structure, and the formation of the thin n-type front layer either by subsequent post-growth counterdoping (diffusion or ion implantation) with As or P or by sequential CVD growth of an As-doped or P-doped film.

However, such studies were performed in a H₂ atmosphere, and previous studies at Rockwell have shown that much larger amounts of dopants are needed to produce a given impurity concentration in SOS films (Ref 3) grown in a He atmosphere than in a H₂ atmosphere. Also, the efficiency of the doping process changed with growth temperature and the specific growth process used. Preliminary data obtained in earlier research (Ref 3) indicate decreases in carrier concentration at high growth temperature in SOS films for a constant growth rate and constant dopant flow rate, but no definite trend was apparent over the temperature range studied (1040–1080°C). If low temperatures are to be used eventually in this program for deposition in halide-containing atmospheres, it is not evident what the doping trends will be.

It would also be expected that higher concentrations of dopants must be added in the gas phase to achieve a given effective impurity concentration in the Si as the layer becomes more polycrystalline, especially if the defects in the layer act as sinks for the impurities. The results of electrical measurements on films doped for various nominal concentrations should indicate any such effects.

For at least the above reasons, p-type doping experiments using B₂H₆ as the dopant source were initiated, first on high-resistivity (100)-oriented n-type Si single-crystal substrates to test the quality of the dopant source, followed by growth on sapphire and polycrystalline alumina substrates for comparative purposes.

The B source was nominally 46 ppm B₂H₆ in a He carrier in order to minimize the presence of H₂ in experiments involving an inert atmosphere. Different concentrations of B₂H₆ were introduced into the growth atmosphere, either by injecting the dopant source directly from the tank into the carrier gas stream containing SiH₄ or by using a gas proportioner, which dilutes the tank source of B₂H₆ with the carrier gas before injection into the main gas stream containing the SiH₄.

By varying the amount of proportional gas injected, it was possible to demonstrate the growth of B-doped Si films on sapphire over a large carrier concentration range, as shown in Figure 2-21. Doping levels as high as 10²⁰ cm⁻³ have been measured by the van der Pauw technique in Si films grown on sapphire and on polycrystalline aluminas. The electrical properties of the B-doped films grown to date are summarized in Section 2.5.2.

2.3.4 Determination of Background Impurity Doping Level in Reactor System

For the purpose of establishing the background impurity doping level of the modified CVD reactor system and reactant gases and source compound in use at the time, measurements were undertaken on several undoped Si-on-sapphire samples grown in H₂ and in He carrier gas, at ~1000°C and at ~1100°C. The two films grown in H₂ were deposited at nearly the same rate (3.3 μm/min and 3.7 μm/min), while the films grown in He were deposited at different rates (1.2 μm/min and 0.72 μm/min).

The films grown in H₂ were more uniform in thickness, consistent with earlier observations of film uniformity obtained with H₂ and with He carrier gases. However, nearly an order of magnitude difference in net carrier concentration was observed between the deposit near the center of the pedestal and that approximately halfway out toward the pedestal periphery, for either carrier gas.

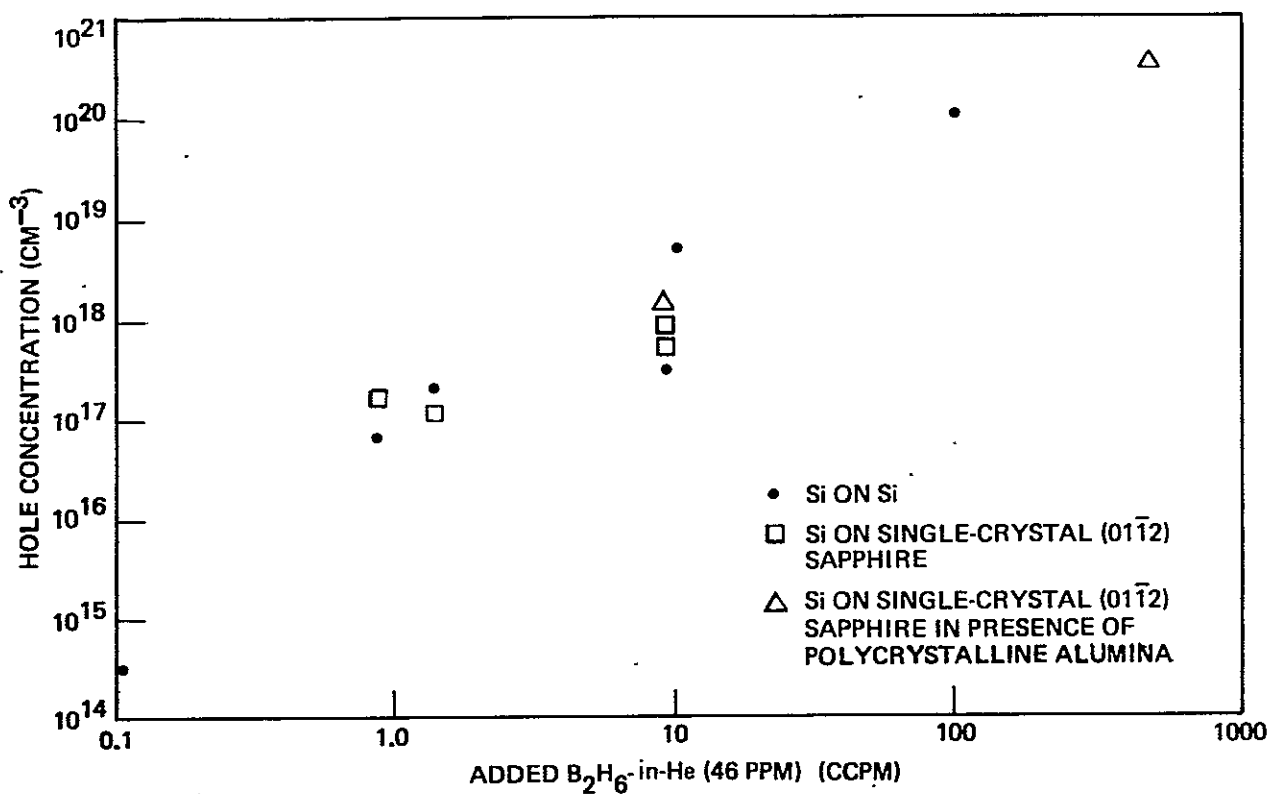


Figure 2-21. Measured Carrier Concentrations in Epitaxial CVD Si Films as a Function of B_2H_6 -in-He (46 ppm) Additions.

The apparent background impurity doping level of $\sim 4 \times 10^{14} \text{ cm}^{-3}$ indicated by these measurements (even though made on films grown on sapphire rather than on single-crystal Si substrates) is a more acceptable value than the $\sim 2 \times 10^{15} \text{ cm}^{-3}$ previously obtained and reported in the first quarterly report. It is not known at this time if the lower value is associated with a real reduction in the unintentional acceptor doping level in the films relative to those measured earlier or if the difference is in some way attributable to a measuring apparatus problem that was found and corrected early in the second quarter.

2.4 TASK 4. PREPARATION OF Si SHEET SAMPLES

The work of Task 4 is entirely in support of the activities of Tasks 3, 5, and 6. It consists primarily of the preparation of individual samples or groups of samples of CVD Si on various substrates, utilizing established deposition procedures. These samples are mainly for use in film characterization studies (Task 5) to examine the variation in Si properties with systematic deposition parameter variations or for use in fabrication of exploratory solar cell structures at OCLI (Task 6). Occasionally, special samples of a non-routine nature are prepared which still do not require extensive exploratory evaluation of the interdependence of CVD parameters on the resulting properties of the films; such work is also a part of this task. Any samples prepared strictly for demonstration purposes are also considered part of this task.

Of over 50 Si CVD experiments carried out during the second quarter only about 10 utilized established procedures to prepare samples for routine analysis, processing, or demonstration.

Ten samples, representative of various Si CVD experiments carried out on the contract prior to mid-April, were delivered to JPL on April 16, 1976, at the request of the JPL Technical Manager.

2.5 TASK 5. EVALUATION OF Si SHEET MATERIAL PROPERTIES

During the first quarter several procedures were developed and/or applied to the characterization of Si sheet material produced by CVD on various substrates under investigation.

Thus, the surfaces of the films were characterized by x-ray diffraction, reflection electron diffraction, scanning electron microscope, optical microscopy, and surface profilometric techniques. X-ray diffraction methods were used to obtain preliminary information on the amount of preferred orientation and the grain size in films deposited on polycrystalline alumina at several different temperatures. Methods of SEM analysis and classical metallography combined with etching procedures were used to provide some evidence of vertical or columnar growth in Si films on alumina. Only limited electrical measurements were made, primarily because of the emphasis on structural properties of the films and the fact that only undoped films had been prepared.

At the end of the first quarter the following specific activities were planned for this task, as suggested in Quarterly Report No. 1:

1. Continue to use x-ray line broadening techniques for grain-size determination, provided film properties still fall in useful range of the method; employ new angle-mode programmer system for automated acquisition of linewidth data
2. Continue to evaluate preferred orientation in polycrystalline substrates and in Si films by x-ray diffraction techniques, and investigate systematic variations in such orientation with changes in CVD parameters (e.g., deposition temperature)

3. Investigate feasibility of using dark-field transmission and replica electron microscopy methods to determine crystallographic orientation in selected samples.
4. Apply optical microscopy, scanning electron microscopy, and RED techniques to determination of surface topography and structure and internal grain structure of CVD Si films on glasses and ceramics.
5. Initiate study of modeling of polycrystalline Si films on various substrates, for purposes of making proper interpretation of electrical measurements.
6. Evaluate and apply spreading resistance method for obtaining profile of electrical properties (and thus impurity and/or defect concentrations) in polycrystalline Si films.
7. Attempt to measure minority carrier lifetime in CVD Si films on various substrates, using pulsed C-V method in MOS structures.
8. Investigate feasibility of using EBIC mode of SEM for evaluation of minority carrier transport properties in polycrystalline Si films.
9. Undertake comparison of van der Pauw and bridge methods for measurement of charge transport properties in CVD Si films.
10. Continue evaluation of laser etching method of defining Hall bridge patterns in Si film samples.

During the second quarter several of the above characterization procedures have been applied to many of the Si films prepared in the CVD experiments carried out in this period. The results of these investigations are summarized in the following sections.

2.5.1 Properties of CVD Si Films on Glass Substrates

A group of four undoped Si films deposited by SiH₄ pyrolysis in a He atmosphere on substrates of Corning Code 1715 glass (calcium aluminosilicate) was characterized for structural and electrical properties. The He flow rate was 6 lpm and the SiH₄ rate was 25 ccpm in the four depositions, carried out at temperatures of 858, 914, 955, and 1000°C. The four films are listed in Table 2-6.

Table 2-6. Properties of CVD Si Films Grown by
SiH₄ Pyrolysis in He on Corning Code 1715 Glass

DEPOS. TEMP. (°C)	AVERAGE FILM THICKNESS (μm)	DEPOSITION RATE (μm/min)	AVE. HORIZ. DIMENSION OF SURFACE FEATURES (μm)
858	5.9	0.6	0.9
914	14	1.4	3.5
955	16	1.0	4.0
1000	20	1.0	3.3

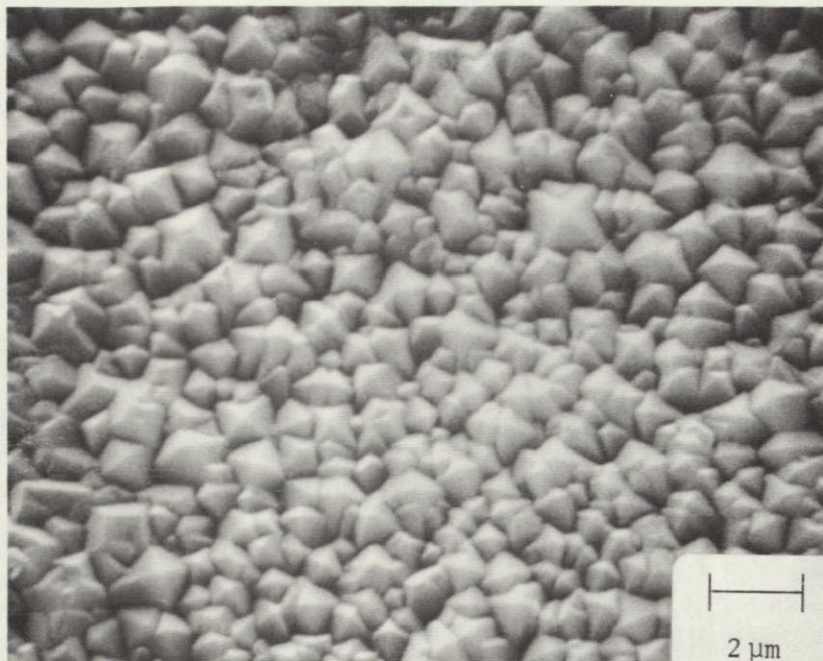
The film grown at $\sim 860^{\circ}\text{C}$ was observed to have a dark, somewhat granular appearance due to the microscopic faceting of the surface. Examination of the specimen by SEM revealed a surface of fairly regular approximately-tetrahedral features that appeared to be $\sim 0.9 \mu\text{m}$ in average dimension in a direction parallel to the film-substrate interface (see Table 2-6); the angular orientation of the facets was not determined. SEM photographs of the film surface at two different magnifications, one at normal incidence and one at a 45 deg viewing angle with the sample surface, are shown in Figure 2-22. The regular faceting of the surface features is clearly visible in the normal incidence view of Figure 2-22a. The oblique view in Figure 2-22b shows the steep sides of the largely tetrahedral features. This film has external characteristics quite similar to some of the Si films obtained earlier in the program on relatively fine-grained polycrystalline alumina substrates. It is striking that such characteristics have been obtained on an amorphous substrate.

Analysis of the x-ray diffraction line profiles for this film indicated a very strong preferred $\{100\}$ orientation, consistent with the external tetrahedral surface morphology observed in the SEM examination. There was also evidence of stronger $\{111\}$ orientation than is characteristic of random polycrystalline Si. The $\{110\}$ orientation did not appear to be detectable in this film.

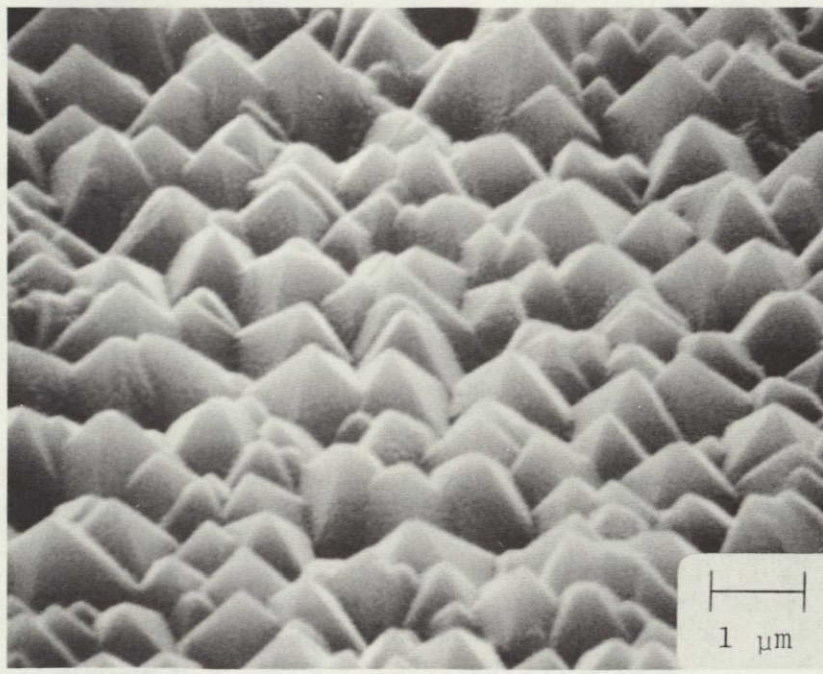
The other three films on 1715 glass were also examined. X-ray diffraction analysis of these films - in terms of the relative intensities of the (111) , (220) , (311) , and (400) lines - was carried out using both graphical analysis of the diffractometer traces and numerical results obtained from the new angle-mode programmer attachment for the diffractometer. The analyses clearly show a steady decrease in the amount of preferred $\{100\}$ orientation with increasing growth temperature, although even at 1000°C this orientation is more prevalent than in a randomly oriented polycrystalline Si sample. Conversely, the $\{110\}$ orientation, not preferred in the film grown at $\sim 860^{\circ}\text{C}$, increases in prevalence with increasing growth temperature to 955°C , and then decreases somewhat at 1000°C .

Similar evidence of a maximum in the degree of preferred $\{110\}$ orientation in this same general deposition temperature range and film thickness range was also observed by Kamins and Cass (Ref 4) for CVD Si polycrystalline films deposited on thermally oxidized Si wafers. The $\{111\}$ orientation, appearing as a preferred orientation in the film deposited at $\sim 860^{\circ}\text{C}$, also appeared to decrease steadily with increasing deposition temperature - a result different from that found by Kamins and Cass for Si on SiO_2 .

Examination of the same three specimens in the SEM showed surface features somewhat like those found on the film grown at $\sim 860^{\circ}\text{C}$. However, the average horizontal dimension of the regular surface features was found to be 3.5, 4.0, and $3.3 \mu\text{m}$ for the films deposited on 1715 glass at 914, 955, and 1000°C , respectively (see Table 2-6). It should be noted that the film grown at $\sim 860^{\circ}\text{C}$ was only about $6 \mu\text{m}$ thick, while the other three were two to three times as thick. If, as earlier evidence has indicated, individual grains tend to increase in horizontal dimension as the film thickness increases, then some of the difference between the observed surface-feature dimension for the 860°C film ($\sim 0.9 \mu\text{m}$) and that of the other three films ($3\text{-}4 \mu\text{m}$) could be attributed to the thickness difference. Cross-section examination of these samples will be undertaken to evaluate this possibility.



(a)



(b)

Figure 2-22. SEM Photographs of Surface of CVD Si Film Grown on Corning Code 1715 Glass by SiH₄ Pyrolysis in He at ~860°C.

a) View at Normal Incidence; b) View at 45 deg to Surface

The difference in the surface characteristics of the films deposited at the higher temperatures is shown by the SEM photographs of the 1000°C film in Figure 2-23. Considerably coarser surface features are evident, there are numerous tall bulbous projections, and faceting of the surface features is almost absent.

The two films deposited at the intermediate temperatures (914, 955°C) exhibited surface structures intermediate between those shown in Figures 2-22 and 2-23. Thus, the film deposited at 955°C resembled that deposited at 1000°C (Figure 2-23), while that grown at 914°C still exhibited some faceting, although not nearly as pronounced as that shown in Figure 2-22.

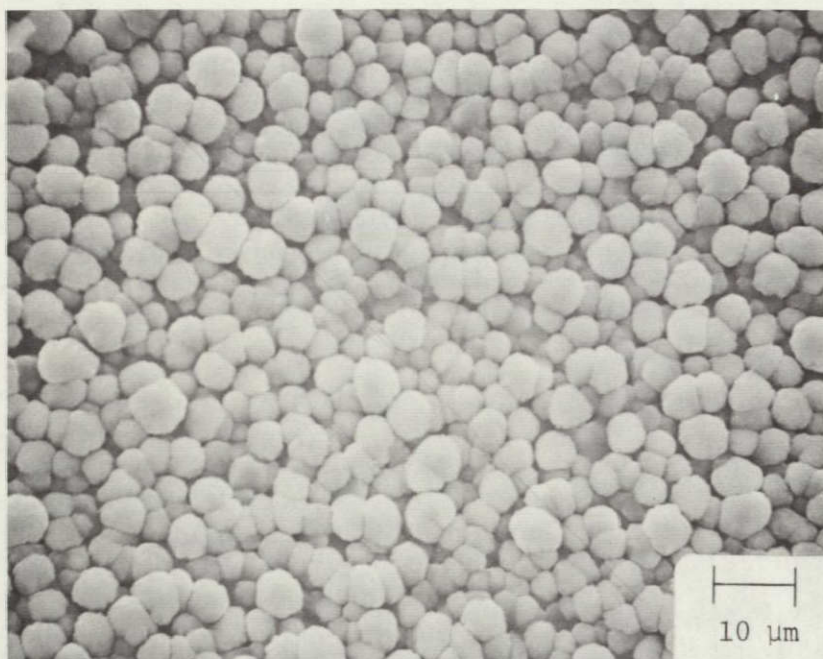
Electrical measurements were made on the four undoped Si films on Corning Code 1715 glass, using a Hall bridge pattern on all films and the van der Pauw method on all but the film grown at 860°C. The van der Pauw method was first used for electrical measurement; than a Hall bridge pattern was photolithographically etched into the Si film in the center of the region in which the van der Pauw measurements were made. Resistivity in all four was high, ranging monotonically from 2.8×10^5 ohm-cm in the film grown at ~860°C down to 8.1×10^4 ohm-cm in the film grown at 1000°C. All films were p type as grown, with measured carrier concentrations in the range from 5×10^{11} to $1 \times 10^{13} \text{ cm}^{-3}$. The films grown at the two intermediate temperatures (914 and 955°C) exhibited the highest carrier mobilities and the lowest carrier concentrations. Results of these measurements are given in Table 2-7.

Also included in the table are the results of electrical measurements on an undoped Si film deposited at ~860°C on Owens-Illinois glass GS211, a proprietary high-temperature glass of unspecified composition. The film was deposited in He carrier gas at a flow rate of 6 lpm with the SiH₄ flow rate 25 ccpm, resulting in an average thickness of ~35 μm. This undoped polycrystalline film was much more conducting than those on the Corning glass. A p-type carrier concentration $\geq 10^{15} \text{ cm}^{-3}$ indicates a fairly high density of structural defects or, more likely, a significant impurity content in the film - presumably from the glass.

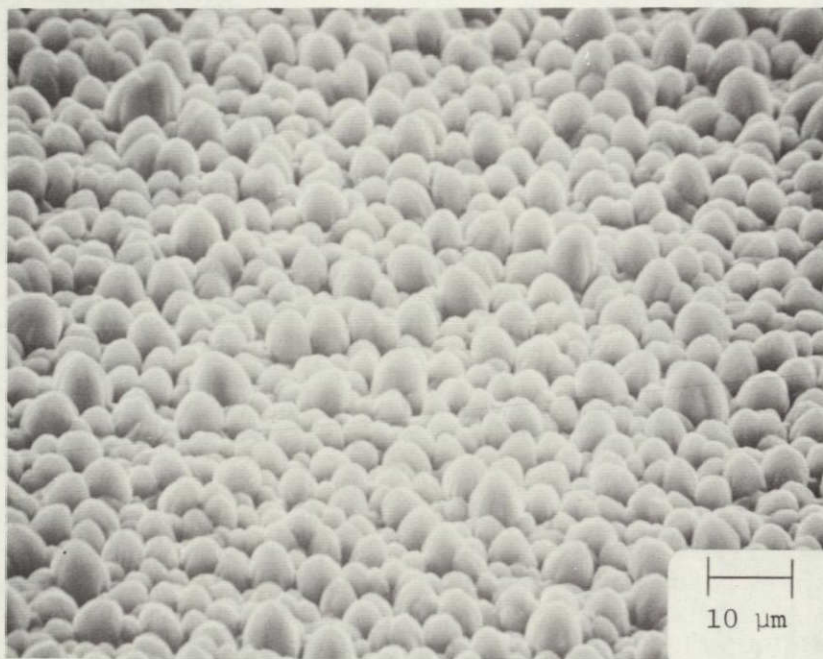
Table 2-7 also includes, as the last entry, the results of electrical measurements on a B-doped Si film deposited at 850°C on Corning Code 1715 glass. A high flow rate of B₂H₆-in-He was used in order to achieve a large doping concentration in the film (see Figure 2-21 and Section 2.3.3).

X-ray diffraction analysis of the film grown on GS211 indicated strong {110} preferred orientation, and the {100} orientation was stronger than in a random polycrystalline Si sample but not predominant.

Figure 2-24 shows SEM photographs of the surface of the film deposited on the GS211 glass. The deeply textured surface is seen to be more irregular than that found on the Si film deposited at the same temperature on the Corning Code 1715 glass (Figure 2-22). The surface features have an average horizontal dimension of about 4 μm, essentially the same as the surface features observed on the three thick Si films deposited on Corning Code 1715 glass at the higher temperatures, yet they resemble the tetrahedral morphology of Figure 2-22b. The large chunks of Si (or other material), referred to earlier, are quite visible in Figure 2-24a.



(a)



(b)

Figure 2-23. SEM Photographs of Surface of CVD Si Deposited on Corning Code 1715 Glass by SiH_4 Pyrolysis at 1000°C in He. (a) View at Normal Incidence; (b) View at 45 deg to Surface.

Table 2-7. Electrical Properties of CVD Si Films* Grown by SiH₄ Pyrolysis[†]
on Glass Substrates in He Carrier Gas^{††}

SUBSTRATE	DEPOS TEMP (°C)	AVE FILM THICKNESS (μm)	METHOD OF MEAS	RESISTIVITY (ohm-cm)	CARRIER CONC.* (cm ⁻³)	CARRIER MOBILITY (cm ² /V-sec)
Corning 1715 Glass	858	5.9	HB**	2.8 × 10 ⁵	1.1 × 10 ¹³	2.0
Corning 1715 Glass	914	14	vdP***	1.3 × 10 ⁵	5.8 × 10 ¹¹	82
			HB**	1.1 × 10 ⁵	5.0 × 10 ¹¹	111
Corning 1715 Glass	955	16	vdP***	1.0 × 10 ⁵	7.7 × 10 ¹¹	81
			HB**	4.5 × 10 ⁴	1.5 × 10 ¹²	95
Corning 1715 Glass	1000	20	vdP***	7.3 × 10 ⁴	1.1 × 10 ¹³	7.7
			HB**	8.1 × 10 ⁴	1.8 × 10 ¹²	43
Owens-Illinois GS211 Glass	861	35	vdP***	82.5	3.5 × 10 ¹⁶	2.2
			HB**	2 × 10 ³	1.0 × 10 ¹⁵	3.1
Corning 1715 Glass	850	70	vdP***	0.004 ^{xx}	4 × 10 ¹⁹ ^{xx}	36 ^{xx}
			FPP X	0.004 ^{xx}	—	—

* All films p type; all undoped except last entry

† SiH₄ flow rate 25 CCPM

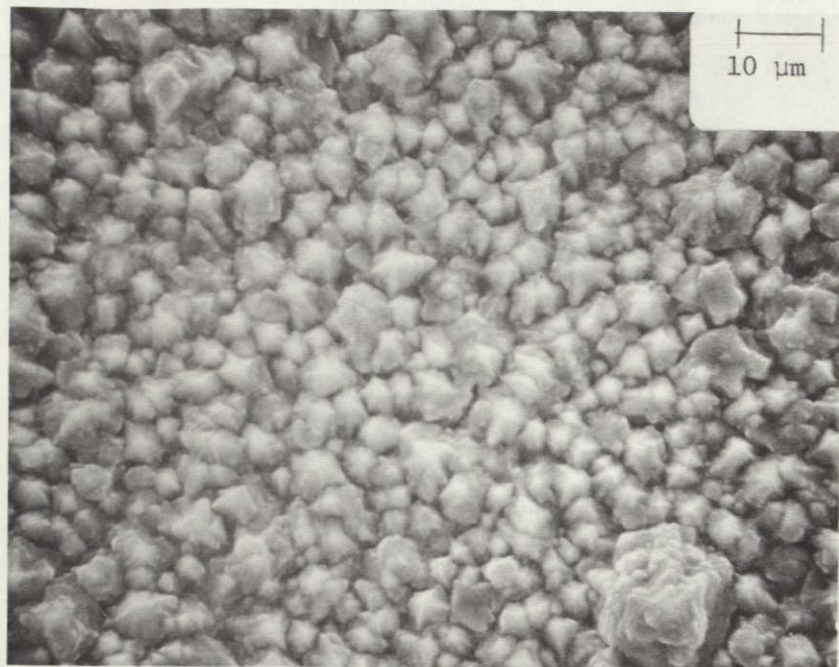
†† He flow rate 6 lpm

** HB = Hall bridge

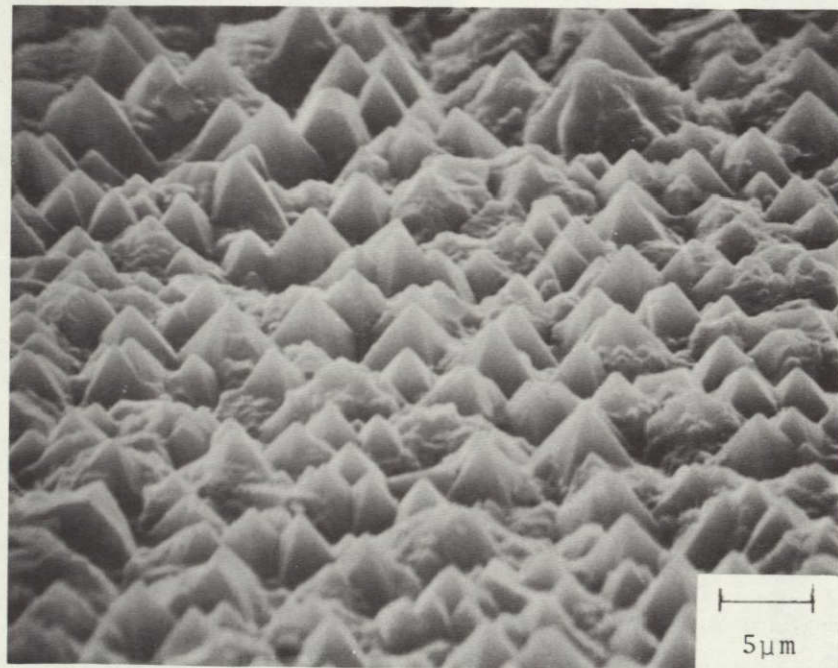
*** vdP = van der Pauw

X FPP = Four point probe

xx Film doped by addition of 500 CCPM of B₂H₆-in-He to reactant stream



(a)



(b)

Figure 2-24. SEM Photographs of Surface of Si Film Deposited on Owens-Illinois GS211 Glass by SiH_4 Pyrolysis at $\sim 860^\circ\text{C}$ in He. (a) View at Normal Incidence; (b) View at 45 deg to Surface

All Si-on-glass films discussed above have a general surface character similar to the rosette type of structure observed on Si films grown on polycrystalline as-fired alumina substrates and described in detail in Quarterly Report No. 1. Significantly different, however, is the greater degree of crystallographic faceting found in the films on glass and the larger angles made by these facets with respect to the nominal substrate surface plane. Analyses of other Si films on glass substrates are in progress.

2.5.2 Properties of CVD Si Films on Polycrystalline Alumina Substrates

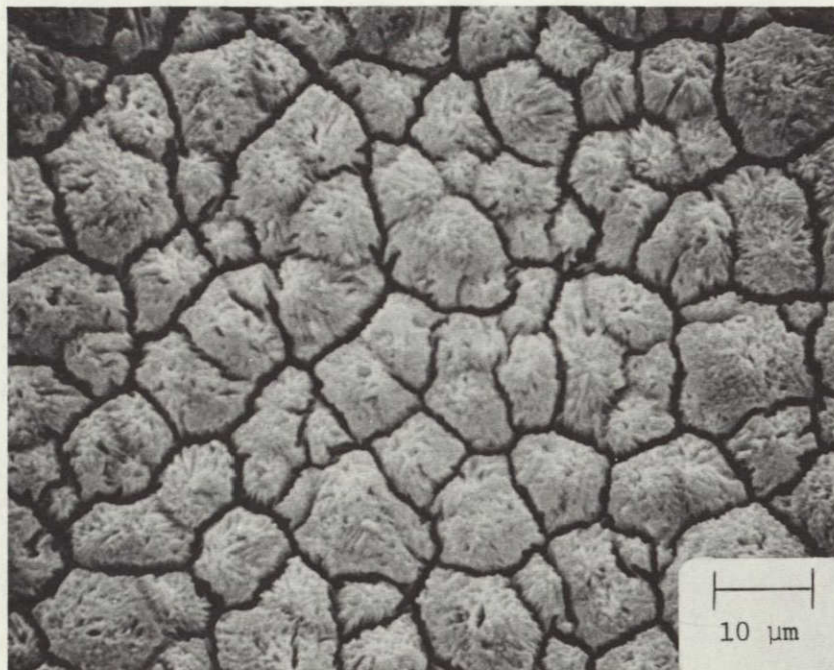
An undoped Si film sample grown early in the quarter on refired ASM805 alumina (3M Co.) at a temperature of $\sim 1030^{\circ}\text{C}$ in H_2 (4 lpm), with a SiH_4 flow rate of 25 cccpm to produce a film $\sim 45 \mu\text{m}$ thick in 15 min, exhibited a fairly good-looking typically-faceted surface with protrusions that were found, upon SEM examination, to have an average dimension of about $7 \mu\text{m}$ in a direction parallel to the film-substrate interface. This enhancement of the size of the surface features of a polycrystalline Si film grown on refired ASM805 (a typical surface-feature dimension for a film grown to the same thickness on normally-processed ASM805 is $< 5 \mu\text{m}$) provided considerable encouragement concerning the effects of enlarged substrate grain size on the average grain size in the Si film. X-ray diffraction analysis of this film showed a very strong {110} preferred orientation, similar to that observed in Si films grown on the normally processed ASM805 substrates but much more pronounced. No evidence of {100} orientation was found in the x-ray data.

As a result of additional processing of this sample in preparation for electrical measurements, some further information regarding grain size was obtained. Extensive etching with a modified Sirtl etch (used to produce Hall-effect bridge patterns defined by photomask techniques) produced deep trenches in the boundaries separating the three-dimensional rosette-like surface features that had been observed so clearly in SEM examination of this and other films deposited on polycrystalline alumina. The etching also resulted in some attack of the surfaces of the individual "mounds" or surface features. This is believed due to dislocations, stacking faults, or twin boundaries within the Si grains, with the etched trenches coinciding with true grain boundaries. That is, the external surface morphology appeared to accurately represent the size and shape of individual Si crystal grains in that portion of the film.

Figure 2-25 shows the surface of this Si film in the as-deposited condition as observed by SEM examination. The two photographs are at the same magnification; Figure 2-25a is for normal incidence and Figure 2-25b is made at a 45 deg viewing angle. The surface appearance is typical of the Si films that have been previously grown on ASM805 alumina.

Figure 2-26 shows the surface of the same Si film after the heavy etching described above, with the deep trenches around each mound clearly delineated in Figure 2-26a and the attack of the individual mounds shown distinctly in Figure 2-26b.

Efforts to define the grain boundaries in the interior of this Si layer by etching a vertical cross-section through the layer were less conclusive. Both fractured and lapped/polished sections exhibited prominent artifacts prior to etching. After etching, additional features — also believed to be artifacts — were delineated which obscured the grain boundary structure.

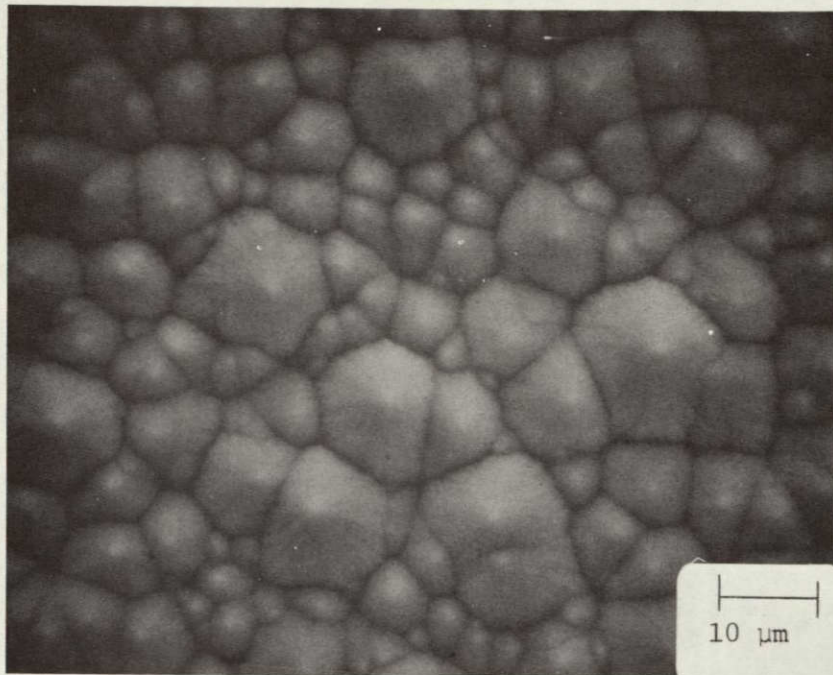


(a)

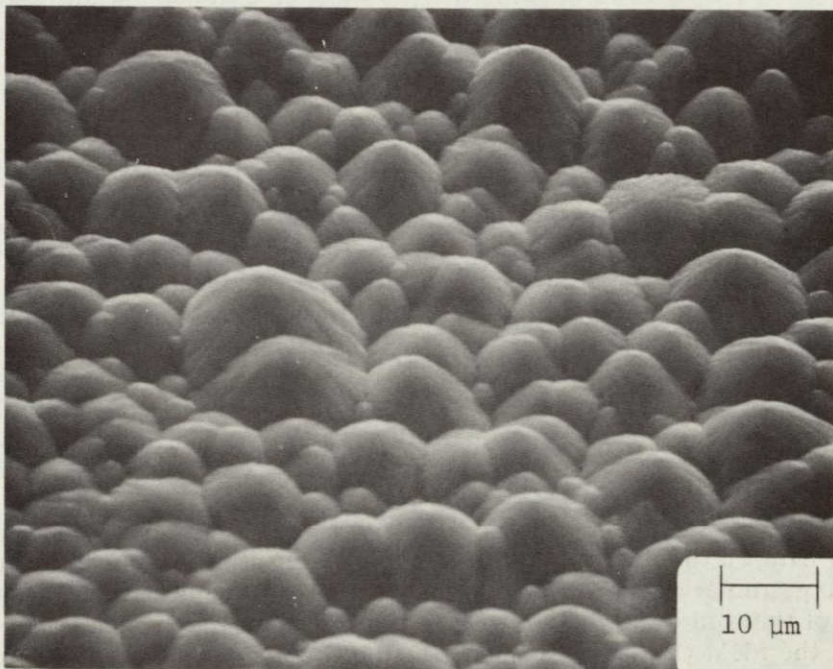


(b)

Figure 2-25. SEM Photographs of CVD Si Film on Refired ASM805 (a) at Normal Incidence and (b) at 45 deg to Sample Surface.



(a)



(b)

Figure 2-26. SEM Photographs of Film in Figure 2-25 after Extensive Etching in Modified Sirtl Etch.

Spreading resistance (SR) measurements were carried out on this undoped sample* to provide an indication of the uniformity of the electrical properties as a function of depth in the layer. The significance of the absolute values of resistance obtained with the two-point SR probe is subject to some question in polycrystalline materials. However, strong trends or any severe departures from a smooth continuous variation in resistivity as a function of depth into the layer — such as might be encountered with a major change in grain size in the interior — should be revealed by the SR profile, which is obtained by making measurements on a low-angle bevel extending through the entire layer.

The measurements, with appropriate corrections applied for film thickness, gave the data shown in Figure 2-27, which indicate very good uniformity as a function of depth into the layer. There is evidence of a gradual decrease in p-type carrier concentration as the film-substrate interface is approached; the approximate location of the interface for that portion of the sample measured is indicated by the vertical dashed line at $\sim 51 \mu\text{m}$ depth. The measurements were made on a ~ 5 -deg bevel, with a probe spacing of $30 \mu\text{m}$ and $10 \mu\text{m}$ between data points on the bevel. The ordinate scale of effective carrier concentration is arbitrary; the automatically printed data shown are converted from the measured SR probe resistance values by a computer program for single-crystal Si, so the resulting numbers are not valid for polycrystalline material. The trend of the data is the important thing in Figure 2-27.

Characterization of several of the undoped Si films grown on polished and unpolished (as-fired) Vistal alumina substrates from Coors was carried out during the quarter, although evaluation of some of the films is still in progress. As described in Section 2.3, Si films $\sim 18 \mu\text{m}$ thick were grown at $\sim 1025^\circ\text{C}$ simultaneously on (0112) polished sapphire, polished Vistal 4 (four firing cycles), and as-fired Vistal 4 substrates at an average deposition rate of $3 \mu\text{m}/\text{min}$.

The film on the polished polycrystalline alumina substrate exhibited very large highly-reflective regions, prominently visible to the unaided eye, which appeared almost certainly to be epitaxial upon inspection in the optical microscope (Figure 2-15). The larger regions were typically greater than $100 \mu\text{m}$ across, with crystallographically faceted surfaces characteristic of epitaxial Si of various nominal orientations, in each case replicating in size and shape the individual substrate grain on which it had grown (Figure 2-16). Among the large epitaxial "islands" were other heavily textured regions, some of which looked like the typical fine-grained polycrystalline Si surfaces seen in earlier deposits on polycrystalline randomly-oriented alumina substrates, and others of which may also have been epitaxial (or highly oriented) regions simply tilted in an orientation such that a very rough-textured surface resulted. The overall surface texture was three-dimensional, with some of the epitaxial islands appearing to have quite different thicknesses (Figure 2-16b).

The film on the unpolished (as-fired) Vistal alumina substrate also exhibited very large grains — of the same dimensions as observed on the polished substrate — but many of them did not appear to be epitaxial upon inspection in the optical microscope and the SEM (Figure 2-17). Although the average dimensions of the individual growth facets on the as-fired substrate are the same as those of the polished grains on the polished substrate, the crystallographic orientations in the two cases are quite different, as noted earlier. Thus, the structural characteristics of the Si layers in the two cases would be expected to be different, and this was, in fact, observed.

*Measurements made by Solecon Laboratories, Costa Mesa, CA.

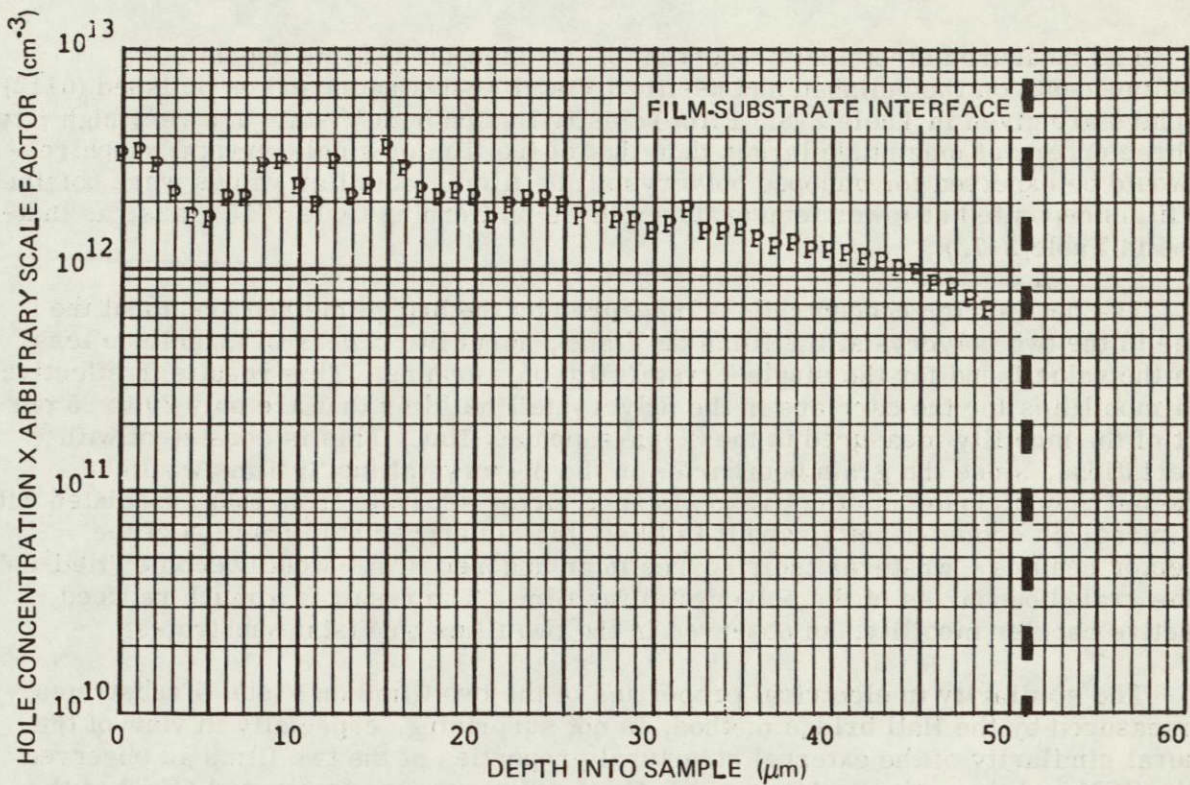


Figure 2-27. Hole Concentration (arbitrary scale factor) as Function of Depth in Si CVD Film of Figures 2-25 and 2-26, Measured by Spreading Resistance Method. (Bevel angle ~5 deg, probe spacing 30 μm , spacing between measurements 10 μm .)

X-ray diffraction analysis of the two films on Vistal 4 alumina showed strong {110} preferred orientation in both instances, although it was very much stronger in the film grown on the polished substrate. In addition, strong {100} preferred orientation was present in the film on the polished substrate, while this reflection in the other film was only slightly greater in intensity than what would be expected for a randomly-oriented polycrystalline film. Evidence of line broadening was found in the x-ray analyses, indicating average grain sizes $\sim 0.1 \mu\text{m}$, apparently in conflict with the external appearance of the films. However, it must be remembered that the numerous large epitaxial or near-epitaxial islands are evidently immersed in a sea of much smaller Si grains, so the smaller grain size obtained by x-ray analysis (which produces an average for essentially the entire Si film thickness) may not be as inaccurate as it seems at first glance. Further exploration of this point is in progress.

The question of the crystal structure and perfection of some of the individual grain regions in Si films deposited on the large-grained Vistal substrates will be examined in the next quarter by means of electron channeling patterns (ECP) obtained from the films. These patterns are typically used to obtain crystallographic orientation information on single crystals. The technique requires slight modification of the SEM now being used, and it also requires a relatively smooth surface on the sample being examined, as topographic information is superimposed on the ECP's. It may thus be necessary to polish the Si films to be investigated by this method.

The measured electrical properties of the undoped Si films deposited simultaneously on the polished and as-fired Vistal 4 substrates and on polished (0112) sapphire are given in Table 2-8. Film resistivities on both Vistals are very high — two to three orders of magnitude larger than that of the film on single-crystal sapphire — as would be expected for undoped polycrystalline films. (Similar values were obtained for films deposited at lower temperatures in He on Corning Code 1715 glass, as indicated in Table 2-7.)

The net carrier concentrations measured by the bridge method are about the same in the two polycrystalline films on Vistal, about two orders of magnitude less than the value found for the single-crystal film on sapphire. This results in effective Hall mobilities for the carriers in the polycrystalline films that are only 20 to 25 percent of the mobility measured in the Si-on-sapphire film. This is consistent with expectations, since the grain boundaries in the polycrystalline Si films would be expected to contribute an effective resistance factor separate from that associated with the intragrain doping density, and it is likely that an appreciable fraction of the acceptor centers — whatever their source in an undoped film — would become "tied-up" in the grain boundaries of the polycrystalline film. The result is a much reduced effective carrier mobility, as observed in the two films on Vistal substrates.

The similarity in electrical properties of the two films on Vistal 4 substrates, as measured by the Hall bridge method, is not surprising, especially in view of the general similarity of the external structural properties of the two films as observed in the SEM and the optical microscope. On the average, the integrated effect of the polycrystalline array comprising the film on the polished substrate might be expected to be very similar — electrically — to that of the different polycrystalline array comprising the film on the as-fired substrate. There is no explanation at present for the apparently inconsistent result obtained by the van der Pauw method for the film on the polished Vistal 4 substrate. It should be noted that the carrier concentration obtained for the undoped film on sapphire is consistent with the value ($\sim 4 \times 10^{14} \text{ cm}^{-3}$) previously determined as being representative of the background impurity doping level in the modified reactor system (see Section 2.3.4).

After the B doping procedures were established, several experiments were conducted in which doped Si films were deposited simultaneously on two or more alumina substrates. In one such experiment, a polished and an as-fired MRC Superstrate alumina substrate were used together with a polished (0112)-oriented sapphire for Si growth in H₂ (4 lpm) at 1025°C, with a SiH₄ flow rate of 10 ccpm. The flow rate of B₂H₆-in-He was 9.1 ccpm to provide a moderately high doping concentration (see Figure 2-21 and Section 2.3.3) in the 10^{17} - 10^{18} cm^{-3} range.

SEM analyses of the surfaces of the polycrystalline films on the two polycrystalline alumina substrates showed very little difference in the structural characteristics. Figure 2-28 shows SEM photographs of the Si film surface on the as-fired Superstrate. Figure 2-28a is made at normal incidence and Figure 2-28b is for a viewing angle of 45 deg with the substrate surface. The surface features are essentially identical to those observed on films grown on other Superstrate surfaces earlier in the program; relatively little crystallographic faceting is discernible.

Figure 2-29 shows similar SEM photographs for the doped Si film that was deposited simultaneously on a polished MRC Superstrate surface. Careful inspection indicates there may be slightly more faceting on the surface features of the film on the

Table 2-8. Electrical Properties of Undoped CVD Si Films Grown by SiH₄ Pyrolysis in H₂ at 1031°C
on Large-grain Vistal 4[†] Alumina and (0112) Sapphire Substrates

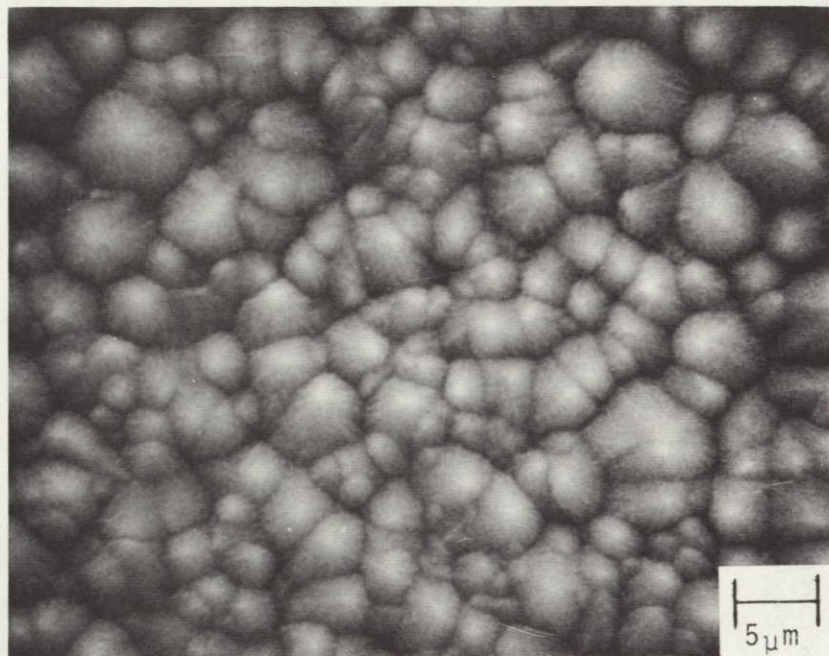
SAMPLE	FILM THICKNESS (μm)	METHOD OF MEAS.	RESISTANCE (ohm-cm)	CARRIER CONC.* (cm^{-3})	CARRIER MOBILITY ($\text{cm}^2/\text{V}\cdot\text{sec}$)
Vistal 4 (Polished)	17.9	vdP** HB***	2.4×10^4 2.4×10^5	8.6×10^{13} 1.0×10^{12}	3.0 26
Vistal 4 (As fired by mfr)	17.9	vdP** HB***	2.8×10^4 9.2×10^4	7.6×10^{12} 2.0×10^{12}	30 34
(0112) Sapphire (Polished)	17.3	HB***	1.6×10^2	2.8×10^{14}	144

[†]Vistal 4 subjected to four consecutive firings at >1800°C for 6 hr each

*Films are p type

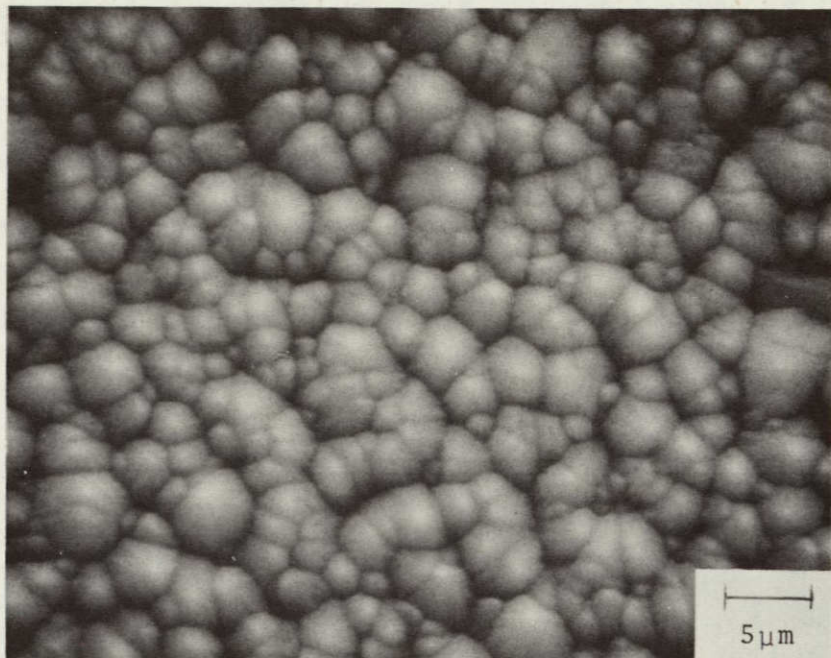
**vdP = van der Pauw

***HB = Hall bridge

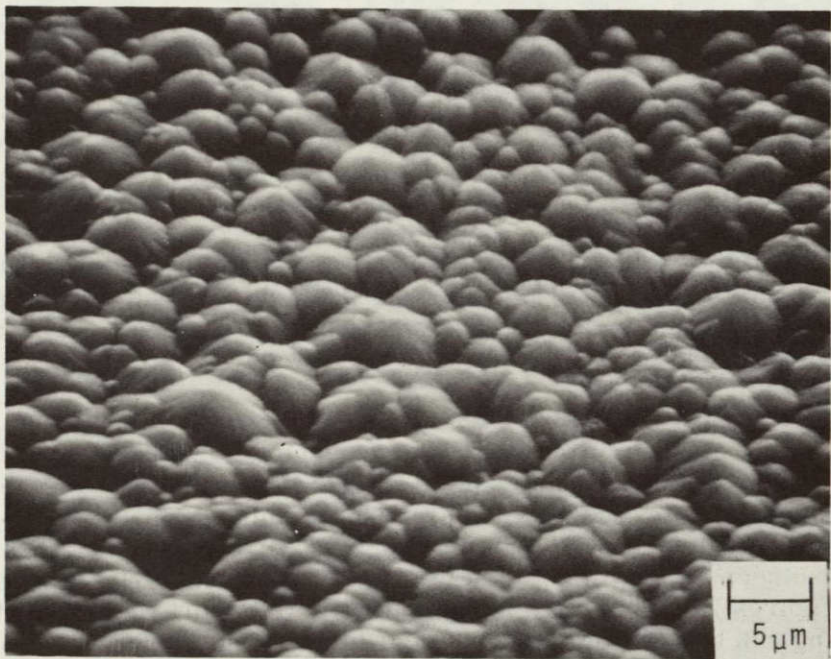


(b)

Figure 2-28. SEM Photographs of Surface of B-doped CVD Si Film Deposited by SiH₄ Pyrolysis in H₂ at 1025°C on As-fired Superstrate Alumina Substrate. a) Viewed at Normal Incidence; b) Viewed at 45 deg with Sample Surface.



(a)



(b)

Figure 2-29. SEM Photographs of Surface of B-doped CVD Si Film Deposited by SiH_4 Pyrolysis in H_2 at 1025°C on Polished Superstrate Alumina Substrate. a) Viewed at Normal Incidence; b) Viewed at 45 deg with Sample Surface. (Film deposited simultaneously with film of Figure 2-28.)

polished substrate, but the difference is almost insignificant. From the SEM examination it is found that the average horizontal dimension of the surface features on the doped film grown on the polished substrate is $\sim 2.8 \mu\text{m}$, while that for the film on the as-fired Superstrate is $\sim 3.0 \mu\text{m}$, again indicating little difference in the two cases.

X-ray diffraction analysis of the films on the two substrates indicated very strong $\{110\}$ preferred orientation in both films, although the relative line intensity was over twice as strong in the film on the polished substrate as in the other. There was also evidence of slight preferred orientation of the $\{100\}$ planes, again more so in the film on the polished substrate.

The results of electrical measurements on these films and on the film grown simultaneously on $(01\bar{1}2)$ -oriented sapphire are shown in Table 2-9. The bridge measurements on the epitaxial film on single-crystal sapphire indicate that the flow rate of B_2H_6 -in-He that was used produced a net carrier concentration of $\sim 10^{18} \text{ cm}^{-3}$; the observed Hall mobility in this film was $125 \text{ cm}^2/\text{V}\cdot\text{sec}$. The measurements on the two films on the polycrystalline substrates were made by the van der Pauw method, because the samples were subsequently to be sent to OCLI for solar cell fabrication and the entire sample area was to be preserved for that purpose. The resistivities of the polycrystalline Si films were nearly the same, and more than an order of magnitude larger than that of the companion film on sapphire. The measured carrier concentrations were nearly identical in the polycrystalline films, and about half of that in the single-crystal film. As a result, the effective Hall mobilities in the two films on MRC alumina were only about one-eighth that found in the film on sapphire.

The fact that the electrical properties as well as the structural properties are quite similar in these films raises some question as to the real value of the extra processing — that is, the mechanical polishing — invested in the one substrate. Since there was also little difference in the apparent surface roughness of the films on the polished and the as-fired substrates, even the presumed advantage of having a smoother film surface for subsequent device processing and contacting may not be valid for this particular substrate material.

Another experiment of the same type involved simultaneous deposition of Si by SiH_4 pyrolysis in H_2 ($4 \ell\text{pm}$) at 1033°C on substrates of polished MRC Superstrate, as-fired 3M ASM805, and single-crystal polished $(01\bar{1}2)$ sapphire. The SiH_4 flow rate was 10 CCPM and the B_2H_6 -in-He flow rate was 500 CCPM, to produce heavy B doping in the Si films.

SEM examination of the film surfaces produced the photographs shown in Figures 2-30 and 2-31. The former shows the surface of the film on the as-fired ASM805 alumina substrate, with a view at normal incidence in Figure 2-30a and at 30 deg with the film surface in Figure 2-30b. The surface features observed are very similar to those seen on Si films grown on this substrate material earlier in the program (cf Figures 2-17c, 2-18a, 2-19 in Quarterly Report No. 1). Little if any distinct faceting can be seen on the pyramidal features that comprise most of the surface (Figure 2-30b).

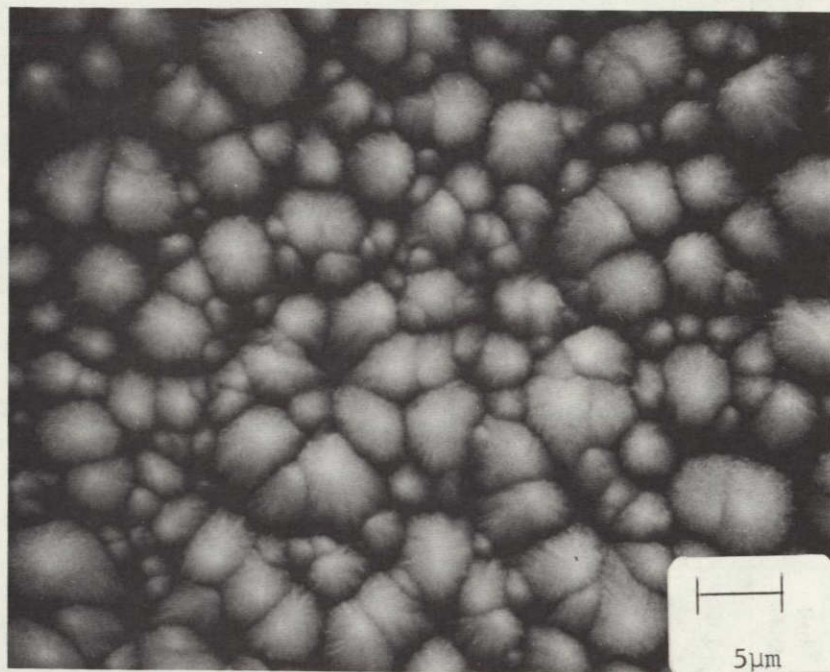
Figure 2-31 shows two views of the surface of the film on the polished MRC Superstrate alumina, at the same corresponding magnifications as those of Figure 2-30a and 2-30b. In both views there is some evidence of crystallographic faceting, as there is on the film of Figure 2-29, also deposited on polished Superstrate. The two film surfaces again appear to be quite similar, with perhaps slightly more evidence of

Table 2-9. Electrical Properties of B-doped CVD Si Films Deposited by SiH₄ Pyrolysis in H₂ (4 lpm) on Single-crystal and Polycrystalline Substrates of α Alumina (Al₂O₃)

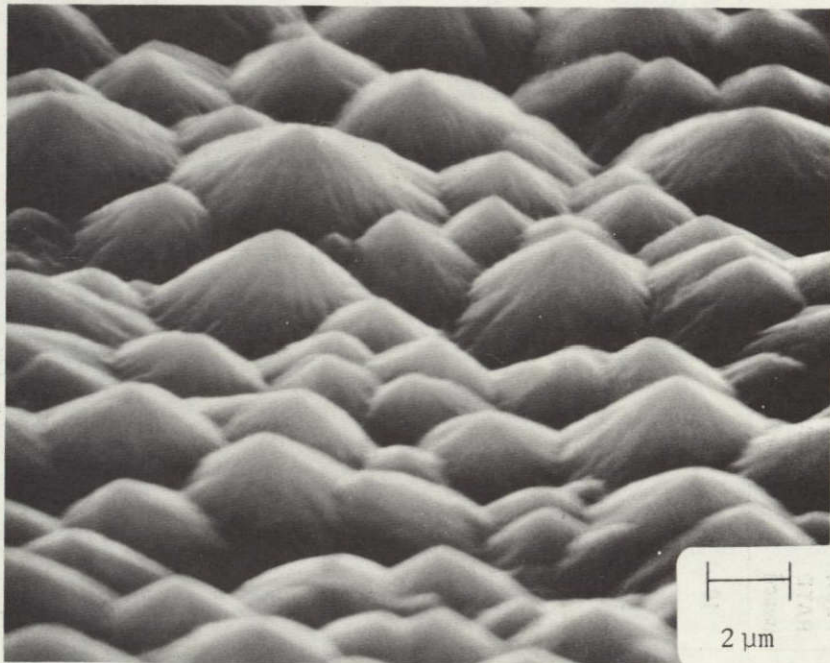
SUBSTRATE MATERIAL AND SURFACE CONDITION	SiH ₄ FLOW RATE (ccpm)	B ₂ H ₆ -IN-He FLOW RATE (ccpm)	DEPOS TEMP (°C)	APPROX FILM THICK (μ m)	RESISTIVITY (ohm-cm)		HOLE CONCENTRATION (cm ⁻³)		HALL MOBILITY (cm ² /V-sec)	
					van der Pauw	Hall Bridge	van der Pauw	Hall Bridge	van der Pauw	Hall Bridge
(0112) sapphire* (polished)	10	9.1	1025	19	0.061	0.052	1.0 x 10 ¹⁸	9.5 x 10 ¹⁷	102	125
MRC Superstrate alumina* (as fired)	10	9.1	1025	20	0.76	—	5.0 x 10 ¹⁷	—	16	—
MRC Superstrate alumina* (polished)	10	9.1	1025	20	0.86	—	4.8 x 10 ¹⁷	—	15	—
(0112) sapphire† (polished)	10	500	1033	25	0.0050	0.012	3.3 x 10 ¹⁹	1.7 x 10 ¹⁹	37	31
MRC Superstrate alumina† (polished)	10	500	1033	25	0.0094	—	2.0 x 10 ¹⁹	—	32	—
3M ASM805 Alumina† (as fired)	10	500	1033	25	0.0087	—	2.4 x 10 ¹⁹	—	30	—

*These substrates used for simultaneous growth of Si

†These substrates used for simultaneous growth of Si

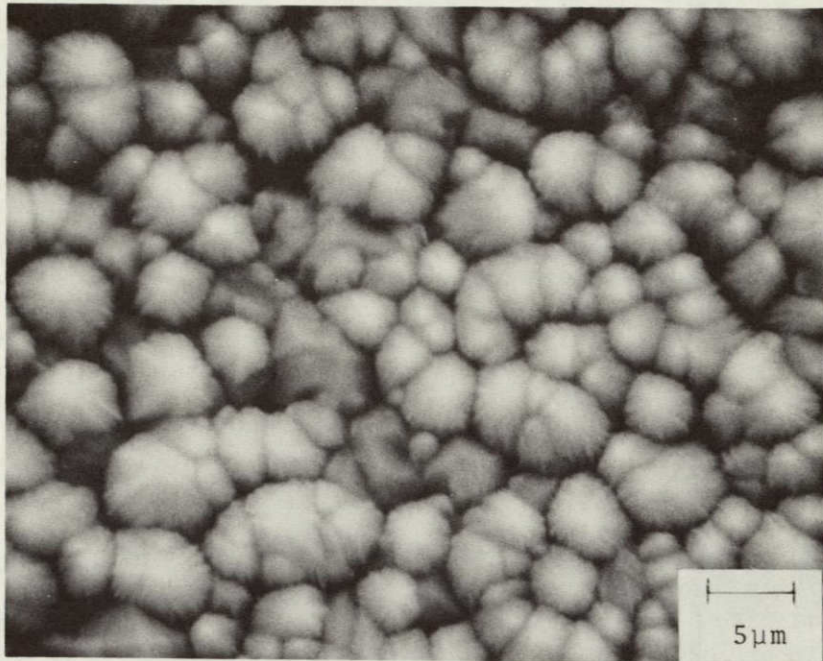


(a)

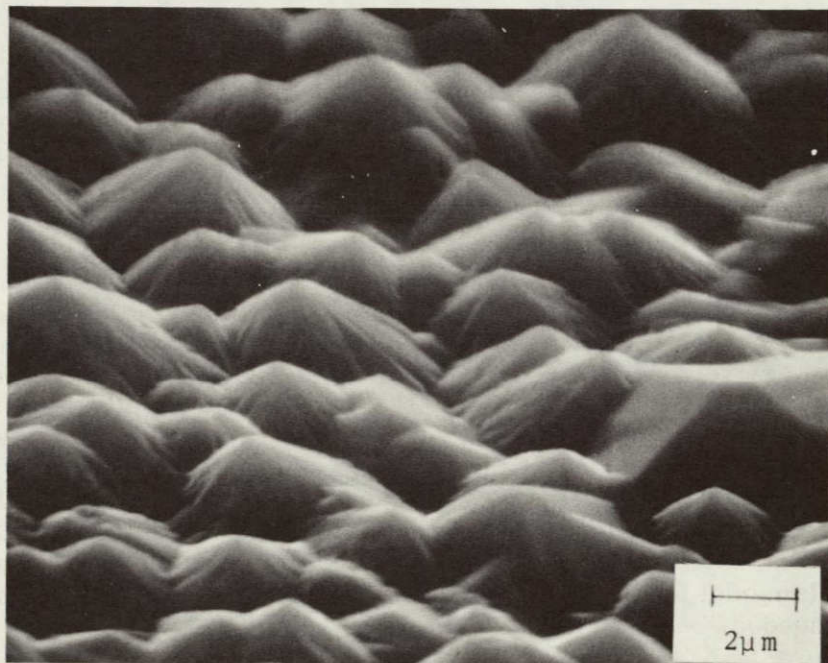


(b)

Figure 2-30. SEM Photographs of 25 μm -thick B-doped ($\sim 10^{20} \text{ cm}^{-3}$) Si Film on As-fired ASM805. (a) Normal to Sample surface; (b) 30 deg to Sample Surface.



(a)



(b)

Figure 2-31. SEM Photographs of 25 μm -thick B-doped ($\sim 10^{20} \text{ cm}^{-3}$) Si Film on Polished MRC Superstrate. (a) Normal to Sample Surface; (b) 30 deg to Sample Surface.

faceting on the film on the polished MRC substrate than on the other film. The average horizontal dimensions of the surface features observed in the SEM are $\sim 3.0 \mu\text{m}$ for the film on the as-fired ASM805 alumina and $\sim 3.4 \mu\text{m}$ for the film on polished Superstrate.

X-ray diffraction analysis of the two polycrystalline doped films showed very strong $\{110\}$ preferred orientation in the film on the polished Superstrate, as was the case in the experiment described above, although the effect is much greater in this experiment. As before, the $\{100\}$ planes also appeared as a preferred orientation in the film on the polished Superstrate.

The film on as-fired ASM805 also exhibited strong $\{110\}$ preferred orientation, but the $\{100\}$ planes were not detected at all. This result is similar to that found recently for undoped Si films deposited in H_2 on refired ASM805 at about the same temperature in a SiH_4 flow rate of 25 CCPM (Section 2.5.2) and, earlier in the program, on as-fired ASM805 at the same temperature and SiH_4 flow rate (see Quarterly Report No. 1, Section 2.3.5.2).

The surfaces of these Si films on the two aluminas are represented by the sections of profilometer traces shown in Figure 2-32. The trace in Figure 2-32a was obtained on the film on the polished MRC Superstrate, while that in Figure 2-32b is for the film on the as-fired ASM805 alumina. The vertical scale is the same in both instances. There is clearly less peak-to-valley excursion in the surface features of the film on the polished substrate (cf Figure 2-31) than for the film on the as-fired substrate (cf Figure 2-30).

Results of electrical measurements on the three films grown in this experiment are also given in Table 2-9. Because of the high concentration of diborane introduced into the reactant gas stream in this experiment (see table), the measured hole concentration in the epitaxial Si film grown on the single-crystal sapphire substrate was very high - about $2 \times 10^{19} \text{ cm}^{-3}$ as measured with the Hall bridge. The Hall mobility found for this film on sapphire was $31 \text{ cm}^2/\text{V}\cdot\text{sec}$, a reasonable value for Si on sapphire in the $10^{19}\text{--}10^{20} \text{ cm}^{-3}$ B doping range involved.

The characteristics of the films on the two polycrystalline aluminas were measured by the van der Pauw method; Hall bridge measurements are in progress, but the results were not available in time for use in this report. The resistivities of both films are similar and are somewhat larger than the resistivity of the Si film on sapphire. The net carrier concentration measured by the van der Pauw method in these films was about $2 \times 10^{19} \text{ cm}^{-3}$ in both cases, resulting in Hall mobilities of about $30 \text{ cm}^2/\text{V}\cdot\text{sec}$. The significance of the apparent inconsistencies in measured properties is not yet understood. The results of the measurements in progress with the Hall bridge may help to clarify this situation. Clearly, additional data are needed to provide a better measure of the extent of these effects, and theoretical studies relating to development of a suitable model for use in interpreting the electrical measurements on polycrystalline films are needed.

2.5.3 Comparison of Methods for Measuring Electrical Properties of CVD Si Films

Measurements of Si film resistivity, carrier concentration, and carrier mobility are made routinely on most of the film samples, utilizing either the van der Pauw method or the more accurate and conventional Hall-effect bridge method. The former method is particularly convenient as it permits measurements on a film sample of

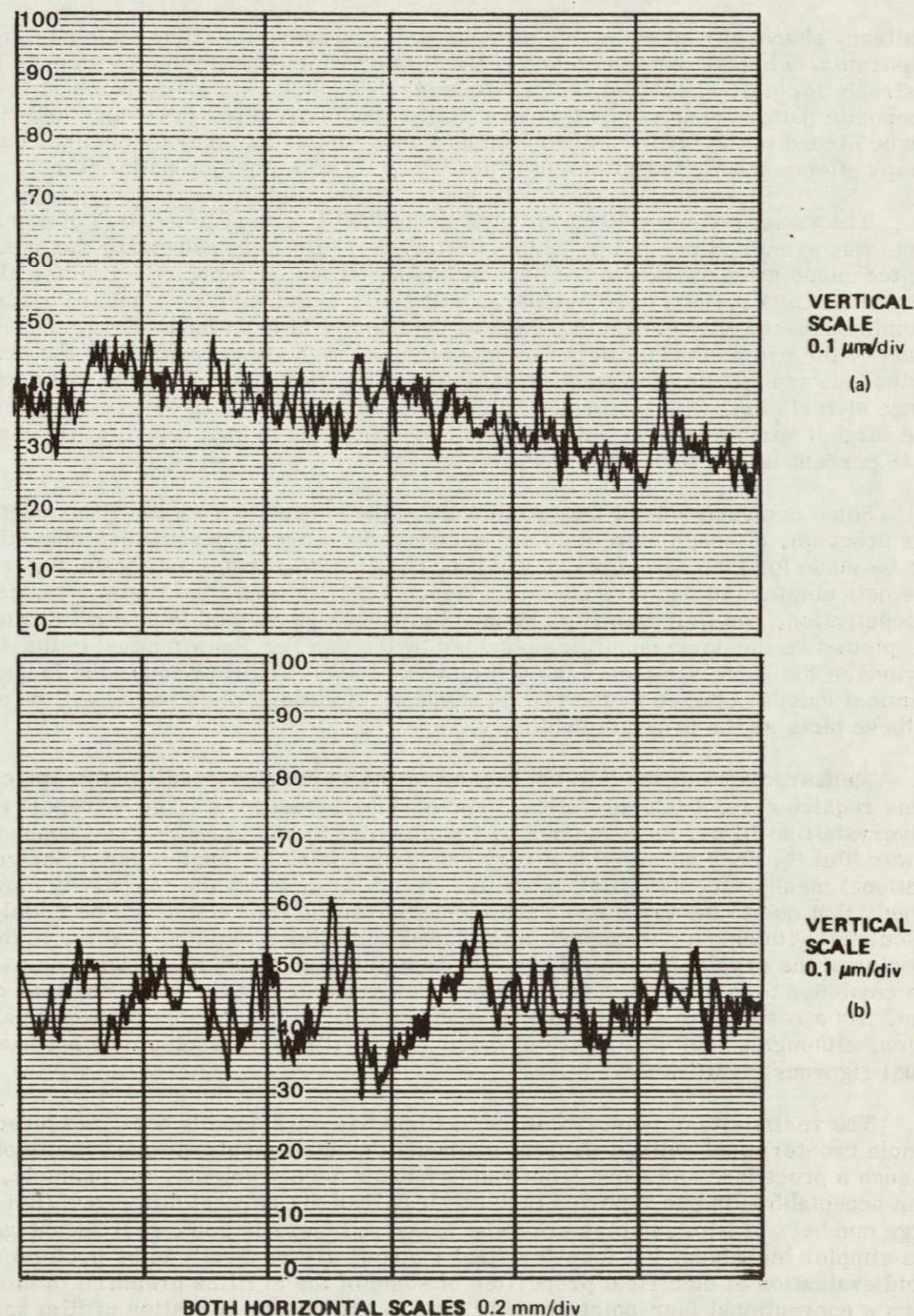


Figure 2-32. Dektak Profilometer Traces for Surfaces of B-doped CVD Si Films Grown at $\sim 1030^\circ\text{C}$ in H_2 by SiH_4 Pyrolysis, on Two Polycrystalline Alumina Substrates. (a) Polished MRC Superstrate; (b) As-fired 3M ASM805.

arbitrary shape without extensive processing. However, for films on insulating substrates, a bridge pattern etched in the film by photolithographic techniques is more desirable for Hall-effect and resistivity measurements. A major advantage is that a composite pattern consisting of several Hall bridges arranged in various orientations can be etched in the layer, using suitable masks; thus, data may be obtained on anisotropy effects and/or variations in film properties with position on the film.

The van der Pauw method for measuring the electrical properties of semiconductor films was examined in earlier studies at Rockwell (Ref 3) to determine the accuracy of the technique when applied to the evaluation of Si films on sapphire. Electrical data obtained by this method were compared with those found with the standard bridge-type samples subsequently etched into each of the films. In most cases the resistivity found by the two methods differed by most by less than six percent, with the bridge method always yielding the smaller value. The carrier concentrations had a wider range of variation, with the bridge value being an average of 12 percent smaller. The largest variation occurred in the Hall mobility; the bridge values were an average of 16 percent larger than those found by the van der Pauw technique.

Some comparisons of the two techniques have been made on Si films prepared in this program, although more data are needed before a good quantitative comparison can be made for the case of polycrystalline Si films on various substrate materials. The data obtained to date are shown in Figure 2-33, in which the resistivity, carrier concentration, and Hall mobility obtained by the bridge method in several samples are plotted vs the same quantities obtained by the van der Pauw method in the same regions of the same samples. In each plot the dashed line represents the locus of identical values obtained by the two techniques. Additional data points will be added to these plots as the program continues.

Measurements of the Hall coefficient to obtain carrier mobilities in polycrystalline films require careful interpretation. The barrier model for charge transport in polycrystalline films, as developed by Kamins (Ref 5) and later by Rai-Choudhury and Hower (Ref 6), does not provide a very good framework for application of the conventional measurements of Hall mobility. In a film in which the resistivity may be largely that due to the grain boundaries, the measured Hall effect will be mainly that associated with carrier transport in the lower resistivity regions, that is, in the interior of the crystal grains. Thus, the resistivity and Hall coefficient values that are combined to give carrier mobility may not really be for the same portions of the film. As a result, the calculated Hall mobility will be a somewhat artificial parameter which, although useful as a figure of merit for the film as a whole, may not have its usual rigorous significance.

The resistivity of polycrystalline Si films has occasionally been measured by simple two-terminal voltage-current methods; the agreement between results obtained by such a procedure and those from van der Pauw measurements, for example, has been acceptable--in one reported instance less than six percent difference (Ref 7). When large numbers of film samples are to be measured there is some real advantage to this simpler technique, but four-terminal methods are generally to be preferred. For rapid evaluation of electrical properties of some of the Si films prepared in this program a conventional four-point probe is used to provide an indication of film resistivity. In most instances to date it has been found that the four-point probe data have agreed closely with resistivity values obtained by the van der Pauw or the bridge methods.

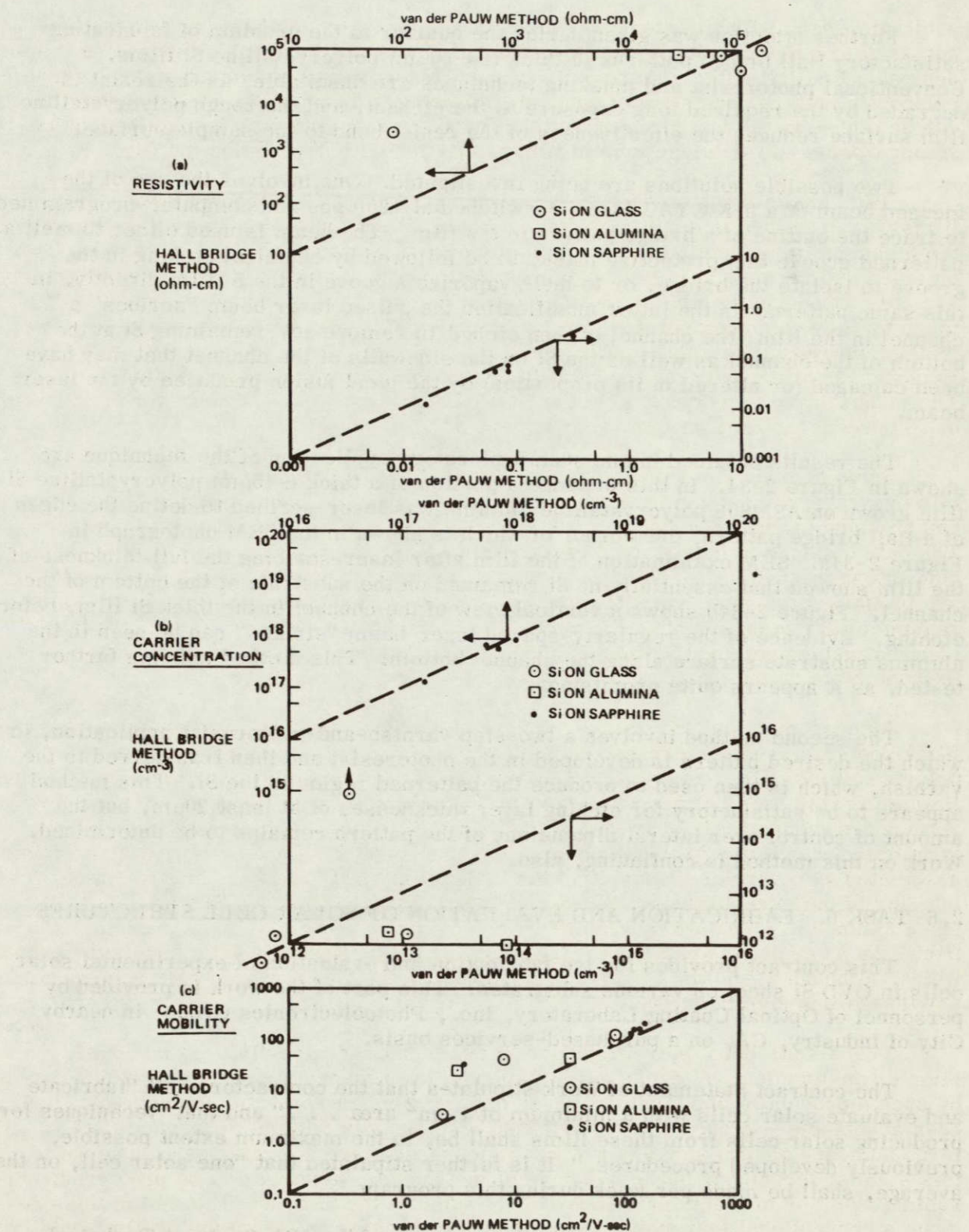


Figure 2-33. Comparison of Electrical Properties of CVD Si Films on Various Substrates as Determined by Hall Bridge and van der Pauw Methods. (a) Resistivity, (b) Carrier Concentration, (c) Hall Mobility

Further attention was given during the quarter to the problem of fabricating satisfactory Hall bridge patterns in thick ($20\text{-}50\mu\text{m}$) polycrystalline Si films. Conventional photoresist and masking techniques are unsuitable, as the resist is degraded by the required long exposure to the etchant, and the rough polycrystalline film surface reduces the effectiveness of the resist bond to the sample surface.

Two possible solutions are being investigated. One involves the use of the focused beam of a 5-Kw YAG laser Q-switched at 1200 pps and computer-programmed to trace the outline of a bridge pattern in the film. The beam is used either to melt a patterned groove in a protective mask, to be followed by chemical etching in the groove to isolate the bridge, or to melt/vaporize a groove in the Si film directly, in this same pattern. In the latter modification the pulsed laser beam "scribes" a channel in the film; the channel is then etched to remove any remaining Si at the bottom of the channel as well as the Si on the sidewalls of the channel that may have been damaged (or altered in its properties) by the local fusion produced by the laser beam.

The results obtained in one such exploratory application of the technique are shown in Figure 2-34. In this instance a portion of a thick ($\sim 45\mu\text{m}$) polycrystalline Si film grown on ASM805 polycrystalline alumina was laser-scribed to define the edges of a Hall bridge pattern, one corner of which is shown in the SEM photograph in Figure 2-34a. SEM examination of the film after laser-scribing the full thickness of the film showed that essentially no Si remained on the substrate at the bottom of the channel. Figure 2-34b shows a vertical view of the channel in the thick Si film, before etching. Evidence of the regularly-spaced laser-beam "strikes" can be seen in the alumina substrate surface along the channel bottom. This method is being further tested, as it appears quite promising.

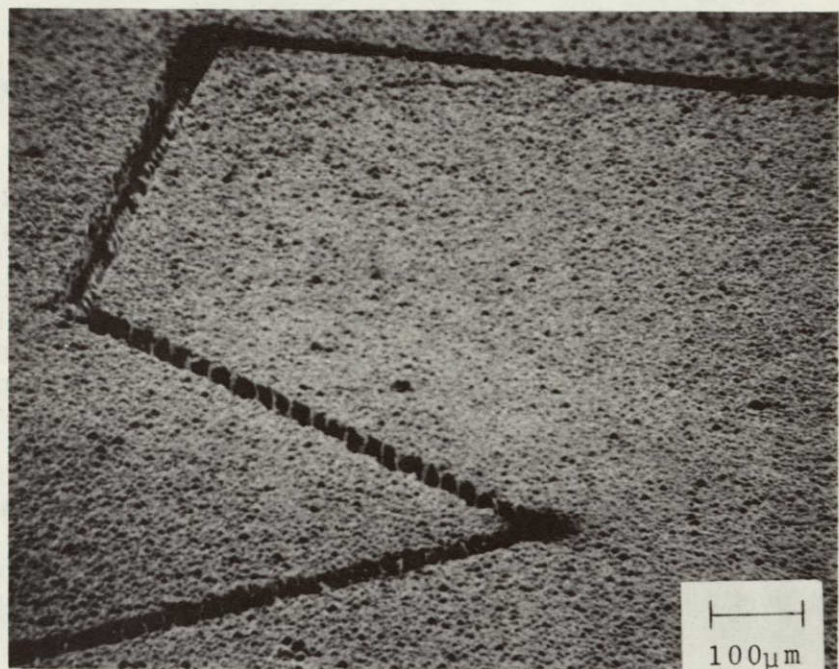
The second method involves a two-step varnish-and-photoresist application, in which the desired pattern is developed in the photoresist and then transferred to the varnish, which is then used to produce the patterned region in the Si. This method appears to be satisfactory for etching layer thicknesses of at least $20\mu\text{m}$, but the amount of control over lateral dimensions of the pattern remains to be determined. Work on this method is continuing, also.

2.6 TASK 6. FABRICATION AND EVALUATION OF SOLAR CELL STRUCTURES

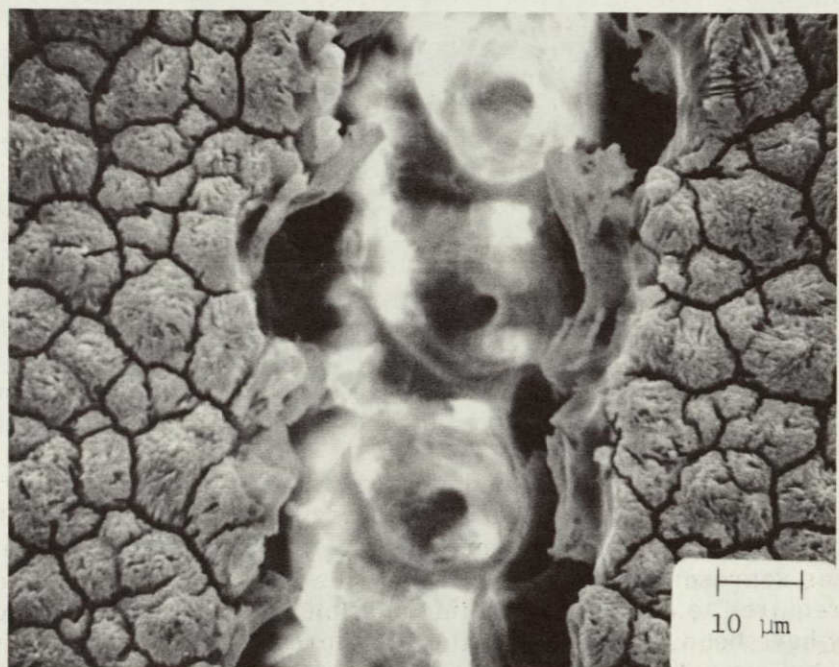
This contract provides for the fabrication and evaluation of experimental solar cells in CVD Si sheet on various substrates. This part of the work is provided by personnel of Optical Coating Laboratory, Inc., Photoelectronics Group, in nearby City of Industry, CA, on a purchased-services basis.

The contract Statement of Work stipulates that the contractor shall "fabricate and evaluate solar cells with a minimum of 1 cm^2 area . . ." and that "techniques for producing solar cells from these films shall be, to the maximum extent possible, previously developed procedures." It is further stipulated that "one solar cell, on the average, shall be made per week during this program."

With this requirement, and with the approval of the JPL Contract Technical Manager, an arrangement has been developed with OCLI that provides the necessary solar cell processing and evaluation work and that allows Rockwell personnel to concentrate on the Si CVD film nucleation and growth investigations involving various low-cost substrate materials.



(a)



(b)

Figure 2-34. SEM Photographs of Channel Produced in Si Film by Pulsed Laser Scribing. (a) Defining the Bridge Pattern; (b) Vertical View of Channel and Exposed Polycrystalline Alumina Substrate.

Eight samples were prepared and submitted to OCLI the first quarter. These eight samples, with the pertinent deposition parameters and film properties, are listed in Table 2-10.

Preliminary results obtained on the first four samples during the first quarter were not encouraging. Considerable difficulty was encountered in processing the samples at OCLI because they were quite thin ($\sim 3\mu\text{m}$, except for OCLI-4) and were undoped. Both OCLI-3 and -4 were found to be slightly n-type, whereas OCLI-1 and -2 had such high resistivity that they did not permit conductivity-type detection even with a very sensitive probe. On the strength of that evidence, however, all four samples were B-diffused (1050°C for 15 min) to attempt to form a p-n junction. Mesas were formed by etching, but no evidence of any rectification or photovoltage was found in the first evaluation.

As of the conclusion of the first quarter the plans for subsequent activities of this task included the following:

1. Meet with OCLI technical personnel, as needed, to discuss and correlate results obtained on CVD Si samples processed/evaluated to date
2. Prepare and submit additional samples of CVD Si sheet to OCLI for solar cell processing and evaluation, emphasizing films on fired polycrystalline alumina substrates and other high-temperature materials.

Early in the second quarter the processing of the first eight samples was completed. The first four samples had been heavily stained as a result of the B diffusion (extensive cleaning did not remove the stains). However, two sets of small mesas ($\sim 0.02 \text{ cm}^2$) were etched into the surfaces of all four samples, in two separate procedures using different etch rates in order to control properly the amount of material removed. No photovoltage was observed under illumination, with mechanical-contact probes on the mesa tops and on the remaining initial Si between mesas. A very high effective resistance (~ 1 megohm) was observed for the mesa structures.

Regions of the diffused layers left protected in forming the first two sets of small mesas were then etched to form relatively large-area mesas ($\sim 0.8 \text{ cm}^2$), and contacts were vacuum-deposited on the mesas and the exposed bottom region of the Si layer. Again no photovoltage was observed on probing the mesas under illumination.

It was concluded that the undoped nature of these thin layers precluded successful formation of a diffused junction that would exhibit a photovoltage. The effective diffusion rate of the common dopants (e.g., B and P) in Si of the varied structural properties represented in this set of samples is not known, so some experimentation will be required to establish such information. A separate layer-doping step should probably have been undertaken (using P) before the B diffusion for junction formation was carried out. The layer doping should involve a low-surface-concentration diffusion with a low-temperature long-time distribution of the diffusant, to attempt to achieve a fairly uniform low doping level throughout the layer.

Results on the second group of samples (OCLI-5, 6, 7, and 8) indicated that, at least on number 5 (Si $\sim 10\mu\text{m}$ thick on sapphire, grown at $\sim 1030^{\circ}\text{C}$), a photovoltaic effect was observed. Sample OCLI-5 as submitted to OCLI tested p type by thermal

Table 2-10. CVD Si Sheet Samples* Submitted to OCLI during First Quarter for Solar Cell Processing

Sample Designation	Substrate and (Thickness)	Observed Depos. Temp. (°C)	Carrier Gas and (Flow Rate)	SiH ₄ Flow Rate (ccpm)	Film Thickness (μm)	Average Growth Rate (μm/min)	Sample Dimensions (cm) (Approximate Area in cm ²)	Film Structure and/or Surface Texture
OCLI-1	(0112) Al ₂ O ₃ [†] (500 μm)	605	H ₂ (4 lpm)	10	3.5	~0.02	r ≈ 1.9** (3.6)	Poly; Random Orientation
OCLI-2	(0112) Al ₂ O ₃ [†] (500 μm)	860	H ₂ (4 lpm)	10	2.6	~0.5	r ≈ 1.9** (3.0)	Poly; Preferred {110} Oriented
OCLI-3	(0112) Al ₂ O ₃ [†] (500 μm)	1032	H ₂ (4 lpm)	5	3.0	~2.0	r ≈ 1.9** (2.5)	Epitaxial
OCLI-4	Multicrystalline Al ₂ O ₃ [†] (525 μm)	1025	H ₂ (4 lpm)	10	8.6	~1.7	2.2 x 1.9 (oval) (3.3)	Epitaxial in Separate Grains
OCLI-5	(0112) Al ₂ O ₃ [†] (500 μm)	1030	H ₂ (4 lpm)	5	10	~2.0	r ≈ 1.8** (2.5)	Epitaxial
OCLI-6	ASM805 Alumina (~640 μm)	1025	H ₂ (4 lpm)	25	20	~3.3	1.5 x 2.0 (3.0)	Poly; Preferred {110} Oriented; Directionally Reflective
OCLI-7	ASM805 Alumina (~640 μm)	1021	H ₂ (4 lpm)	10	24	~1.6	1.4 x 1.9 (2.7)	Poly; Preferred {110} Oriented; Directionally Reflective
OCLI-8	ASM805 Alumina (~640 μm)	1030	H ₂ (4 lpm)	25	40	~3.3	1.8 x 1.6 (2.9)	Poly; Preferred {110} Oriented; Directionally Reflective

* All Si films undoped.

† These substrates not subjected to high-temperature H₂ etch before deposition.

** These samples approximately 90 deg sector of circle of radius r cm.

probing, so a shallow n⁺ layer was formed by POCl_3 diffusion at 875°C for 20 min. Small mesas were formed on part of the diffused surface by masking and etching. Under illumination, and with mechanical-contact probes on the mesas and the lower region of the deposited layer, a photovoltage of ~200mV was obtained with a low photocurrent. Using a contactless rf method to measure the effective resistivity, a value of sheet resistance of ~100,000 ohms per square was obtained.

Larger mesas were formed on the remaining n⁺ diffused layer, and vacuum-deposited Al contacts were applied to the mesa tops and the exposed base-region p-type Si. Under tungsten-lamp illumination, with the diode reverse-biased to permit determination of the photocurrent, a current density of ~1.5ma/cm² and a photo-voltage of ~230mV were measured. It was estimated that a reduced internal resistance would permit a curve fill factor of ~0.5 and a conversion efficiency the order of 0.2 percent (determined by direct comparison with a conventional single-crystal cell) for a cell of the type formed here.

These first attempts to apply standard solar cell processing to some of the Si films again indicate that it may become necessary to develop and/or apply some specialized methods - for example, ion implantation doping instead of, or in addition to, diffusion doping for junction formation - to these polycrystalline films in order to get an adequate indication of their suitability for solar cell fabrication.

Another six samples of CVD Si sheet were submitted to OCLI during the second quarter. These samples are listed in Table 2-11, along with their deposition parameters and other pertinent properties. All of the Si films are B-doped, with measured active carrier concentrations in the range from 10^{17} to 10^{18} cm^{-3} . Four of the samples are CVD films on single-crystal (0112)-oriented sapphire substrates and thus are epitaxial; Hall mobilities for these films are in the range from 125 to $187 \text{ cm}^2/\text{V}\cdot\text{sec}$. The other two samples are polycrystalline CVD films grown on polycrystalline alumina (MRC Superstrate) substrates - one in the as-fired condition and one polished at Rockwell prior to its use as a substrate. The films on these two samples both exhibit strong {110} preferred orientation. All six Si films are in the thickness range 18-20 μm . All film surfaces are in the as-grown condition.

Processing has begun on all six samples. Because all samples were p-type, with measured carrier concentrations in a range reasonable for base region material for Si solar cells, a standard P diffusion was carried out to form the p-n junctions. Large mesas, covering nearly the entire sample area, were formed by etching to permit contact to the p-type base material below the junction.

Under W lamp illumination of approximately 100 mw/cm² intensity, the resulting photovoltaic junctions in samples OCLI-9, 10, 11, 12, 13, and 14 exhibited open-circuit photovoltages V_{oc} of 283, 355, 347, 278, 48, and 43 mV, respectively. For comparison, a randomly selected single-crystal Si 10 ohm-cm production-type cell (2x1 cm) produced V_{oc} of 510 mV in the same illumination. Although the data are quite preliminary, the variation in V_{oc} in the baseline Si sheet cells on sapphire perhaps can be correlated with the variation in the base material doping concentration (see Table 2-11). The greatly reduced V_{oc} values for the small-grained polycrystalline cells (OCLI-13 and -14), on MRC Superstrate alumina substrates, are undoubtedly related to factors such as the high reverse saturation current density in the junctions formed in polycrystalline material.

Table 2-11. B-doped CVD Si Sheet Samples Submitted to OCLI during Second Quarter for Solar Cell Processing and Measurement

SAMPLE NO.	SUBSTRATE MATERIAL AND THICKNESS (μm)	DEPOS. TEMP ($^{\circ}\text{C}$)	CARRIER GAS AND FLOW RATE (lpm)	SiH ₄ FLOW RATE (ccpm)	DOPANT GAS* FLOW RATE (ccpm)	FILM THICKNESS (μm)	AVE. GROWTH RATE ($\mu\text{m}/\text{min}$)	FILM RESISTIVITY ($\text{ohm}\cdot\text{cm}$)	HOLE CONCENTRATION (cm^{-3})	HALL MOBILITY ($\text{cm}^2/\text{V}\cdot\text{sec}$)	SAMPLE DIMENSIONS (cm) AND APPROX AREA (cm^2)	FILM STRUCTURE AND/OR SURFACE TEXTURE
OCLI-9	(0112) Al ₂ O ₃ 375	1022	H ₂ 4	10	0.91	18	1.8	0.26†	1.3 $\times 10^{17}$ †	187†	1.0 x 1.1 1.1	Epitaxial
OCLI-10	(0112) Al ₂ O ₃ 300	1025	H ₂ 4	10	9.1	18	1.8	0.070†	6.1 $\times 10^{17}$ †	145†	1.15 x 1.0 1.15	Epitaxial
OCLI-11	(0112) Al ₂ O ₃ 300	1023	H ₂ 4	10	9.1	20	1.9	0.063†	6.8 $\times 10^{17}$ †	146†	1.0 x 0.9 0.9	Epitaxial
OCLI-12	(0112) Al ₂ O ₃ 300	1025	H ₂ 4	10	9.1	19	1.9	0.052†	9.5 $\times 10^{17}$ †	125†	1.0 x 0.95 0.95	Epitaxial
OCLI-13	MRC Superstrate alumina (as fired) 700	1025	H ₂ 4	10	9.1	20	2.0	0.76**	5.0 $\times 10^{17}$ **	16**	1.3 x 1.2 1.6	Poly; preferred {110} oriented
OCLI-14	MRC Superstrate alumina (polished) 675	1025	H ₂ 4	10	9.1	20	2.0	0.86**	4.8 $\times 10^{17}$ **	15**	1.4 x 1.4 2.0	Poly; preferred {110} oriented

*Films B-doped from B₂H₆-in-He (46 ppm)

†Measured by Hall bridge method

**Measured by van der Pauw method

Simple interdigitated contacts were applied to the top of the large mesa on two of the cells (OCLI-10 and -13), and preliminary indications of response in an AMO solar simulator were obtained, without any control of cell temperature during exposure. Under these very non-rigorous conditions the comparison production cell (nominal 10 percent efficiency) generated about 13 mw/cm^2 of calculated load power, while OCLI-10 and -13 generated approximately 0.9 mw/cm^2 and $6 \times 10^{-3} \text{ mw/cm}^2$, respectively, under the same conditions. No reflection-loss correction was made for the two uncoated film-type cells in these results; with such a correction, OCLI-10 would exhibit an efficiency of about 1 percent.

All six of the cells in the last group are being further processed and evaluated, but only these preliminary results are available now. The cells fabricated in the polycrystalline material are obviously suffering from several expected shortcomings. However, it is anticipated that the complete results acquired from this group of samples, together with similar results to be obtained from additional polycrystalline sheet samples to be processed during the next quarter, will provide good indication of probable trends of cell characteristics with variations in controllable Si film properties.

3. CONCLUSIONS AND RECOMMENDATIONS

The modification of the CVD reactor system has been completed. Except for minor changes that will be made from time to time throughout the remainder of the contract work and for routine maintenance and repairs that will occur on a continuing basis, it is anticipated that no major further activity concerned with modification and test of the CVD reactor system will take place.

The response of most of the glass and ceramic manufacturers contacted relative to solving the substrate problem has continued to be excellent. Several specially-prepared materials have been supplied, in addition to a variety of commercially-available materials, for evaluation as potential low-cost substrates. Several glasses capable of withstanding high temperatures (at least 850°C) have been received, and results with these amorphous substrates during the second quarter have been encouraging. Si growth on Corning Code 1715 glass has produced films exhibiting either a {100} preferred orientation or a {110} preferred orientation, depending upon the deposition temperature. Encouraging results have also been obtained for films grown on glasses supplied by Owens-Illinois (GS211 and GS213). However, the glasses examined to date do not tolerate a H₂ atmosphere; an inert atmosphere such as He appears to be a requirement for depositing Si on these glasses at high temperature, i.e., ≥850°C. It may be that substrates unstable in H₂ could first be covered by a Si film deposited in He followed by further Si growth in a H₂ atmosphere, in order to improve film thickness uniformity and reaction efficiency.

The results obtained for CVD Si growth on fired polycrystalline ceramics - especially alumina - have also been encouraging. Aluminas with enlarged grains resulting from special supplementary firing procedures beyond those used in the normal commercial processing have been found to be quite promising for growth of Si films with enhanced grain sizes. Films with grain dimensions as large as 200 µm have been prepared.

Unfortunately, however, the polycrystalline aluminas all have a surface topography that is not conducive to smooth Si layer growth by CVD. Differences in the properties of Si films grown on mechanically-polished polycrystalline ceramic substrates and those grown on the as-fired surfaces are being compared. Profilometry measurements indicate a 5-fold improvement in surface roughness for an 18 µm-thick Si film grown on a polished large-grained alumina (Vistal) when compared with a film grown simultaneously on an as-fired substrate. Any improvement in film properties or in surface topography resulting from use of polished substrates must be weighed against the added cost of the additional processing step (i.e., the polishing).

Several planned variants on the normal deposition of Si films by SiH₄ pyrolysis are to be investigated, for the purpose of influencing the early stages of growth of the Si films and thus the ultimate properties of the resulting sheet material. The use of HCl in the SiH₄ gas stream, to attack smaller crystallites and thus allow larger ones to survive and grow more rapidly, is being examined. The use of a two-step deposition process, such as one employing SiH₄ and one of the silicon halides to accomplish essentially the same thing, will be examined in subsequent studies during the third quarter.

P-type doping of the Si films has been initiated, using B₂H₆-in-He as the source of B doping. Films were grown first on single-crystal Si and sapphire substrates for baseline data and then on various polycrystalline substrates. The properties of the doped polycrystalline and single-crystal films are now being compared. Principal

measurements are being made using the van der Pauw and Hall-bridge techniques, and occasionally the spreading-resistance method.

In addition, optical microscopy, scanning electron microscopy, x-ray diffractometry, x-ray topography, and other analytical methods are being used for film characterization and will be continued. It has become increasingly important to correlate substrate properties with film properties, so further improvements in speed of sample analysis will be needed. Because of the complex physical structure and the mechanisms of charge transport in the polycrystalline Si films, the nature of the measurements made and the interpretation of the results of the measurements must be given careful consideration. When the properties of the Si films have improved sufficiently, additional evaluation techniques--such as Schottky-barrier methods for determination of impurity distributions, EBIC-mode analysis with the SEM to investigate properties of individual crystal grains and the intervening grain boundaries, and surface photovoltage measurements to obtain effective minority carrier diffusion length values--will be applied to give more complete understanding of the Si sheet properties.

The results obtained to date in applying standard Si solar cell processing to the CVD sheet samples have clearly indicated the importance of using films properly doped during growth for the cell fabrication. The observed differences in results with epitaxial Si on sapphire (for baseline data) and polycrystalline Si on non-single-crystal substrates have again emphasized that methods other than diffusion doping for junction formation - such as sequential impurity doping during film growth or ion implantation doping - may have to be invoked with these polycrystalline Si films to exploit fully their potential for low-cost large-area solar cell fabrication. It is again recommended that this possibility be given consideration in the near future, depending upon further results to be obtained at OCLI with other samples of CVD Si films, even though initial program plans did not place a high priority on such specialized process development.

4. PLANS FOR THE THIRD QUARTER

The planned work for the next quarter will follow the Updated Technical Program Plan given in Appendix B of this report. Summarized by task, the planned work is as follows:

TASK 1.

The work of this task was completed during the second quarter.

TASK 2

1. Continue experimental evaluation and screening of candidate substrate materials by structural analyses and by Si CVD experiments, with major emphasis on glasses made available by Owens-Illinois and Corning and on large-grained aluminas provided by Coors.
2. Continue interactions with potential suppliers of substrate materials, and plan second trip to visit substrate suppliers.
3. Compare properties of as-fired and mechanically-polished alumina substrates of various purities from several suppliers, and compare properties of CVD Si grown on both types.
4. Continue to investigate effects of various substrate surface treatments, including metal deposits, on resulting film properties.

TASK 3

1. Continue studies to identify preferred substrate materials and CVD parameters.
2. Continue investigation of effects of dopant impurities on Si film growth phenomena and on Si film properties.
3. Continue $\text{SiH}_4\text{-HCl}$ growth rate studies in H_2 as a function of gas composition and deposition temperature and apply results to development of two-step growth process.
4. Investigate effects of in-situ and post-growth annealing on Si film properties.
5. Initiate experiments with partial-coverage deposits of Si on selected substrate(s) to examine incubation phenomena and film nucleation processes.

TASK 4.

1. Prepare samples of relatively thick (20–50 μm) doped p-type Si films on substrates of polycrystalline alumina for evaluation of film properties and for delivery to OCLI for solar cell processing.

TASK 5.

1. Continue analyses of Si film and substrate structural properties by surface profilometry, x-ray diffraction, reflection-electron diffraction, and scanning electron microscopy techniques.
2. Continue application of x-ray diffraction methods for determination of preferred orientation and grain size in polycrystalline substrates and in CVD Si films on various substrates, and investigate systematic variations in these properties with changes in deposition temperature and other CVD parameters.
3. Investigate applicability of x-ray topographic methods, dark-field transmission and replica electron microscopy methods, and electron channeling pattern studies (in SEM) or orientation determination in selected polycrystalline Si film samples.
4. Extend theoretical studies to develop model to be used in interpreting charge transport measurements in polycrystalline Si films.
5. Continue use of spreading resistance measurements to determine carrier concentration profiles and locate structural inhomogeneities in polycrystalline Si films on various substrates.
6. Investigate methods for measurement of minority carrier diffusion lengths/lifetimes in CVD Si films - including pulsed C-V method in MOS structures, EBIC-mode analysis of barriers in SEM, photoconductive decay.
7. Continue development of pulsed-laser scribing method for defining Hall bridge patterns in thick polycrystalline Si films on non-conducting substrates.

TASK 6..

1. Prepare and submit additional samples of CVD Si sheet to OCLI for solar cell processing and evaluation, emphasizing doped films on glass substrates and on polycrystalline alumina substrates.

5. NEW TECHNOLOGY

No reportable items of new technology have been identified during the conduct of the second quarter of work on this contract, which is the period covered by this report.

6. REFERENCES

1. H. M. Manasevit, Arnold Miller, F. L. Morritz, and D. H. Forbes, AIME Meeting, Chicago, Oct. 1966.
2. J. Bloem, *J. Crystal Growth* 18, 70 (1973)
3. R. P. Ruth, A. J. Hughes, J. L. Kenty, H. M. Manasevit, D. Medellin, A. C. Thorsen, Y. T. Chan, C. R. Viswanathan, and M. A. Ring, "Fundamental Studies of Semiconductor Heteroepitaxy," Final Report, August 1973, ARPA Order No. 1585, Contract DAAH01-70-C-1311. (Prepared by Rockwell International, Electronics Group, Research and Technology Division, Anaheim, CA, for USAMICOM, Redstone Arsenal, AL).
4. T. I. Kamins and T. R. Cass, *Thin Solid Films* 16, 147 (1973).
5. T. I. Kamins, *J. Appl. Phys.* 42, 4357 (1971).
6. P. Rai-Choudhury and P. L. Hower, *J. Electrochem. Soc.* 120, 1761 (1973); originally given as Paper 240, Fall Meeting of The Electrochemical Society, Miami Beach, October 1972.
7. J. D. Joseph and T. I. Kamins, *Solid-St. Electron.* 15, 355 (1972).

PRECEDING PAGE BLANK NOT FILMED

APPENDIX A. MANPOWER AND FUNDING EXPENDITURES

This report covers the second quarter of the contract, through the sixth month. Through the fifth month of the contract (that is, through May 29, 1976) a cumulative total of 2302 engineering and support manhours and a cumulative total of \$76,026 (excluding fee) were expended.

For the sixth month of the contract (May 30 through July 3, 1976) a total of 610 engineering and support manhours and a total of \$19,379 (excluding fee) were expended in the first four weeks - that is, through June 26, 1976.

The cumulative manpower expenditure total through June 26, 1976, is thus 2912 manhours, and the cumulative cost total (excluding fee and commitments) through that date is \$95,405.

PRECEDING PAGE BLANK NOT FILMED.

APPENDIX B. UPDATED TECHNICAL PROGRAM PLAN

The Initial Technical Program Plan was approved by the JPL Technical Manager on February 4, 1976.

An Updated Technical Program Plan, revised to show changes in the date of completion of reactor modifications and the date of the design review for Task 1, was included in the Monthly Technical Progress Report for April, 1976. That revised plan was approved by the JPL Technical Manager on May 17, 1976.

A further updating of the plan, showing a suggested change in schedule for Technical Goal No. 4 of Task 5, was proposed in the Monthly Technical Progress Report for May, 1976. Although this change has not yet been approved by the JPL Technical Manager, the plan included in this report shows that suggested change.

It also shows the actual manpower and funding expenditures through June 26, 1976, as given in Appendix A.

**CHEMICAL VAPOR DEPOSITION GROWTH
SILICON SHEET GROWTH DEVELOPMENT**

JPL CONTRACT NO. 954372

**TASK 2: LARGE AREA SILICON SHEET
JPL/ERDA LOW COST SILICON SOLAR ARRAY PROJECT**

UPDATED TECHNICAL PROGRAM PLAN

(Note: Numbered technical goals are listed at end of each task)

TASK/ACTIVITY	1976												1977					
	J	F	M	A	M	J	J	A	S	O	N	D	J	F	M	A	M	J
1. MODIFICATION AND TEST OF EXISTING CVD REACTOR SYSTEM																		
A. PREPARE REACTOR SYSTEM FOR INITIAL CVD EXPERIMENTS																		
B. DESIGN REACTOR SYSTEM MODIFICATIONS																		
C. INSTALL NEW REACTOR SYSTEM COMPONENTS AND CONTROLS																		
D. TEST MODIFIED CVD REACTOR SYSTEM																		
E. DEFINE AND DOCUMENT STANDARD OPERATING PROCEDURE FOR REACTOR SYSTEM																		
1. Complete required modification of CVD reactor system																		
2. Conduct required Design and Performance Review																		
2. IDENTIFICATION/DEVELOPMENT OF SUITABLE SUBSTRATE MATERIALS																		
A. IDENTIFY AVAILABLE CANDIDATE MATERIALS																		
B. CONDUCT CVD EXPERIMENTS TO SCREEN AVAILABLE CANDIDATE MATERIALS																		
C. VISIT SUBSTRATE SUPPLIERS TO ARRANGE PREPARATION OF SPECIAL MATERIALS																		
D. CONDUCT CVD EXPERIMENTS ON SPECIAL SUBSTRATE MATERIALS																		
E. EVALUATE COMPOSITE SUBSTRATE STRUCTURES																		
F. INVESTIGATE EFFECTS OF SUBSTRATE SURFACE TREATMENTS ON Si PROPERTIES																		
1. Identify most promising available material(s) using conventional Si CVD growth techniques																		
2. Initiate experiments on deposition of metals for Si nucleation																		
3. Identify most promising special substrate material(s)																		
4. Specify preferred substrate surface treatment																		
5. Identify preferred configuration(s) of most promising substrate material(s)																		
3. EXPERIMENTAL INVESTIGATION OF Si CVD PROCESS PARAMETERS																		
A. CONDUCT EXPERIMENTS TO IDENTIFY PREFERRED PARAMETERS FOR CANDIDATE SUBSTRATE MATERIALS																		
B. INVESTIGATE 2-STEP DEPOSITION PROCESS FOR CANDIDATE SUBSTRATE MATERIALS																		
C. STUDY EFFECTS OF <u>IN SITU</u> AND POST-GROWTH ANNEALING ON Si PROPERTIES																		
D. ESTABLISH DOPING PARAMETERS FOR Si ON VARIOUS SUBSTRATES																		
E. DETERMINE EFFECTS OF DOPANTS ON Si GROWTH PHENOMENA																		
1. Decision regarding application of 2 step process																		
2. Identify preferred parameters for p type doping of CVD Si sheet																		
3. Select acceptor doping impurity most favorable to Si sheet growth																		
4. Identify preferred carrier gas for Si CVD growth process																		
5. Identify preferred <u>in situ</u> annealing procedure																		
6. Specify details of 2-step process for improved Si sheet growth																		
7. Define preferred CVD growth parameters for candidate substrate materials																		
8. Identify preferred parameters for n-type doping of CVD Si sheet																		
9. Determine/characterize effects of annealing procedures																		
4. PREPARATION OF Si SHEET SAMPLES																		
A. PREPARE SAMPLES FOR MATERIAL CHARACTERIZATION STUDIES																		
B. PREPARE SAMPLES FOR POST-GROWTH PROCESSING																		
C. PREPARE SAMPLES FOR SOLAR-CELL FABRICATION																		

ORIGINAL PAGE IS
OF POOR QUALITY.

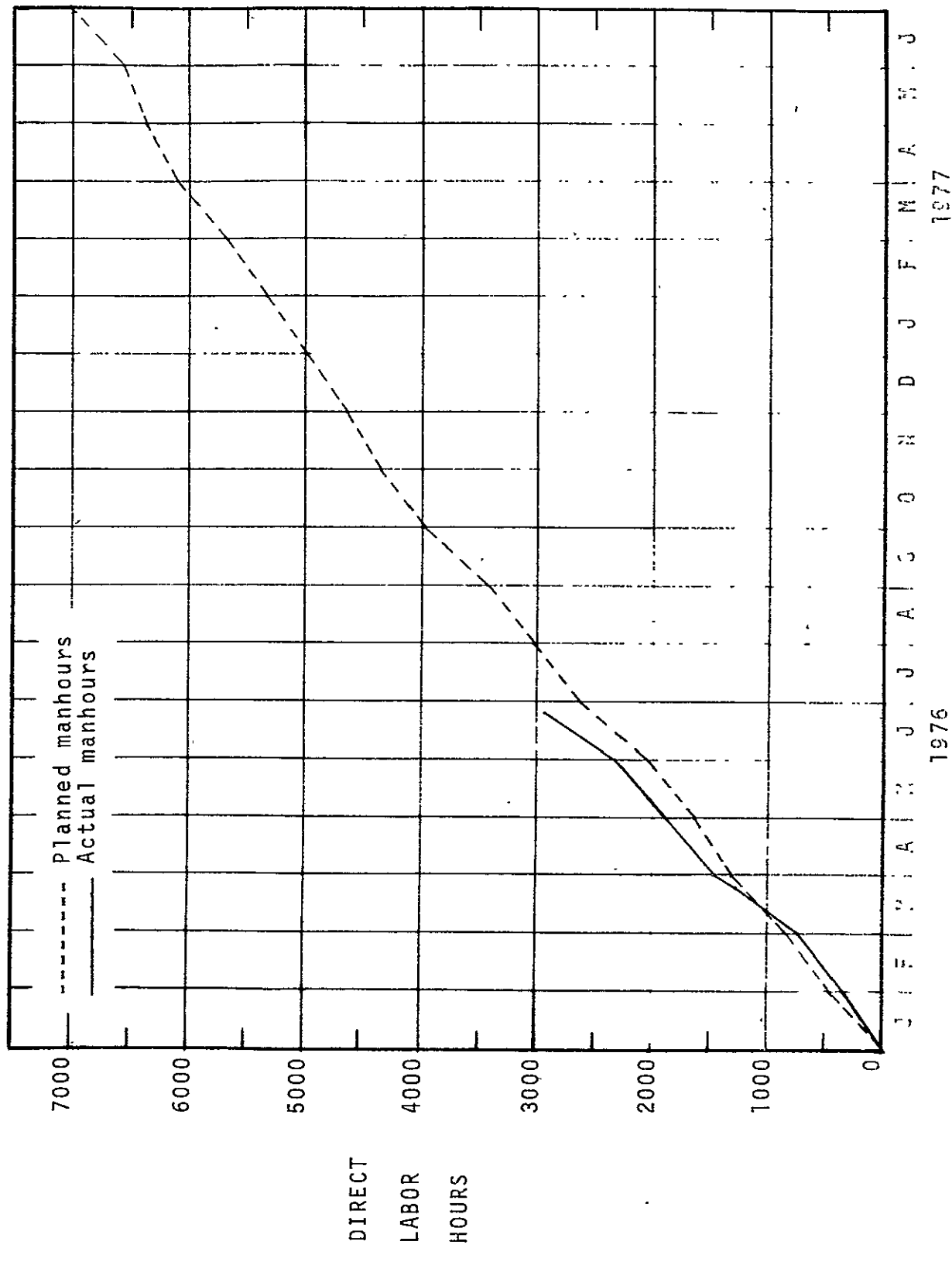
TASK/ACTIVITY	1976												1977					
	J	F	M	A	M	J	J	A	S	O	N	D	J	F	M	A	M	J
5. EVALUATION OF Si SHEET MATERIAL PROPERTIES																		
A. APPLY X-RAY, SEM & OPTICAL TECH. FOR GRAIN SIZE DETERMINATION	1		3				8											
B. USE X RAY AND ELECTRON MICROSCOPE METHODS FOR ORIENTATION DETERMINATION	2				6			10										
C. DEVELOP/ADAPT MODEL FOR INTERPRETING CHARGE TRANSPORT MEASUREMENTS													11					
D. MEASURE ELECTRICAL PROPERTIES USING CHARGE TRANSPORT AND STORAGE, SEM, AND OPTICAL METHODS							5	7	4	9								
E. DETERMINE IMPURITY CONTENT AND OTHER PROPERTIES BY SUITABLE METHODS																		
1. Obtain x-ray linewidth standards for grain size in polycrystalline Si																		
2. Establish detailed procedures for determining preferred orientations by x-ray methods																		
3. Establish details of x-ray methods to be used for grain size determination																		
4. Determine suitability/reliability of van der Pauw method for electrical properties																		
5. Complete apparatus (or vendor arrangements) for spreading resistance measurements																		
6. Determine applicability of dark-field transmission and replica electron microscopy methods for orientation determination in selected samples																		
7. Complete apparatus/procedure for determining minority carrier diffusion lengths by SEM and/or barrier photocurrent methods																		
8. Determine suitability of SEM techniques for grain size determination																		
9. Establish suitability of C-V-t measurements for determining minority carrier lifetimes																		
10. Determine suitability of SEM electron channeling method for grain orientation determination																		
11. Complete definition of model																		
6. FABRICATION AND EVALUATION OF SOLAR CELL STRUCTURES																		
A. ESTABLISH DETAILS OF OCLI SAMPLE PROCESSING AND EVALUATION MEASUREMENTS	1																	
B. SUBMIT EPITAXIAL Si-ON Al ₂ O ₃ SAMPLES FOR PROCESS AND MATERIAL BASELINE DATA																		
C. SUBMIT SELECTED SAMPLES FOR CELL FABRICATION AND EVALUATION AND CORRELATE RESULTS WITH CVD EXPERIMENTS																		
1. Issue purchase order to OCLI for solar cell processing using CVD Si sheet samples																		
TECHNICAL DOCUMENTATION																		
A. PROGRAM PLAN AND UPDATE	▼	▼	▼	▼	▼	▼	▼	▼	▼	▼	▼	▼	▼	▼	▼	▼	▼	▼
B. MONTHLY TECHNICAL PROGRESS REPORT	▼	▼	▼	▼	▼	▼	▼	▼	▼	▼	▼	▼	▼	▼	▼	▼	▼	▼
C. QUARTERLY REPORT																		
D. INTERIM SUMMARY REPORT																		
E. ANNUAL REPORT																		
F. DRAFT FINAL REPORT																		
G. FINAL TECHNICAL REPORT																		
H. LABORATORY OPERATIONS NOTEBOOK																		
TECHNICAL MEETINGS																		
A. TASK INTEGRATION SESSIONS	▼							▼										
B. PROGRAM REVIEW MEETINGS	▼							▼										
C. WORKSHOP	▼							▼										

ORIGINAL PAGE IS
OF POOR QUALITY

CHEMICAL VAPOR DEPOSITION GROWTH
SILICON SHEET GROWTH DEVELOPMENT

JPL CONTRACT NO. 954372

TASK 2: LARGE AREA SILICON SHEET
JPL/ERDA LOW COST SILICON SOLAR ARRAY PROJECT



PROGRESS LABOR SUMMARY

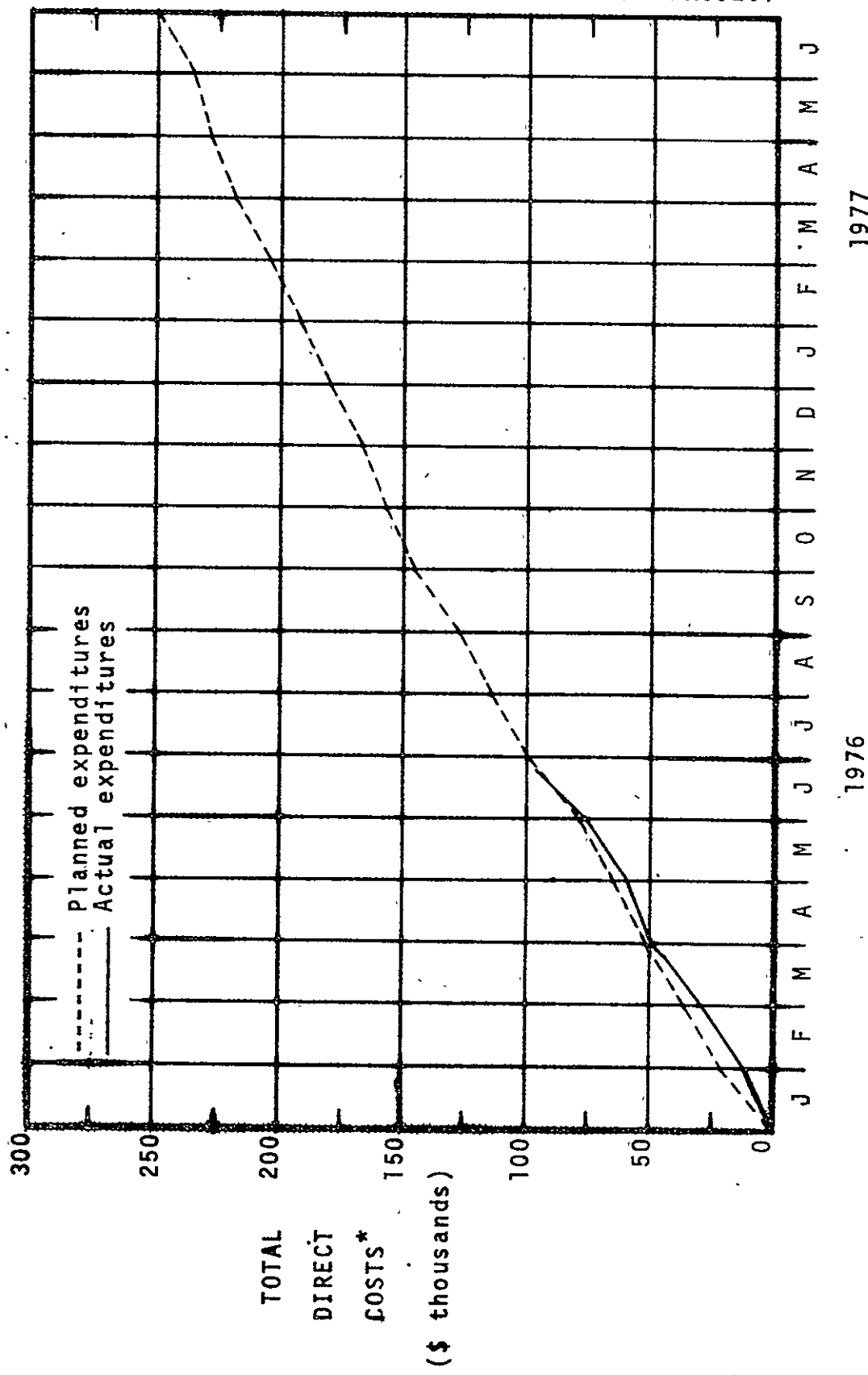
1976

1977

CHEMICAL VAPOR DEPOSITION GROWTH
SILICON SHEET GROWTH DEVELOPMENT

JPL CONTRACT NO. 954372

TASK 2: LARGE AREA SILICON SHEET
JPL/ERDA LOW COST SILICON SOLAR ARRAY PROJECT



PROGRAM COST SUMMARY

*excluding fee